

ANNALS OF THE NEW YORK
ACADEMY OF SCIENCES

VOLUME 125, ART.

FORMS OF WATER II

Conference
JOSEPH F. SAUNDERS, Chairman

AUT

H. J. BERENDSEN, T. G. OWE BER
CLIFFORD, J. D. DAVIES, G. F. D
FENICHEL, H. FERNANDEZ-MORAN, H
E. H. GRANT, R. I. N. GREAVES, G.
S. B. HOROWITZ, R. S. KIBLER, A. LE
MACKENSIE, N. V. B. MARSDEN, P. M
M. D. PERSIDSKY, B. A. PETHICA,
SAKAIKA, J. F. SAUNDERS, H. A. SCH

THE NEW YORK ACA

(Founded

BOARD OF

J. JOSEPH LYNCH, S.

HILARY KOPROWSKI *Class of 1963*

W. STUART THOMPSON EDMUND J. *Class of 1963*

HENRY C. BRECK LEON S. *Class of 1963*

GORDON Y. BILLARD FREDERIC *Class of 1963*

EMERSON DAY, P. J. JOSEPH LYNCH, CHARLES W. MUS EUNICE THOMAS M.

SCIENTIFIC C

EMERSON D. JACOB FELE

J. J. BURNS, *Vice-President*

ANDRES FERRARI

Recording Secretary

Elected 1963

RHODES W. FAIRBRIDGE

1963

ALBERT S. GORDON

1964

N. HENRY MOSS

1965

EUNICE THOMAS M.

SECTION OF BIOLOGICAL

GABRIEL G. NAHAS, *Chairman*

DIVISION OF A

JEROME BRIGGS, *Chairman* ANNEM

ANNALS OF THE NEW YORK ACADEMY OF SCIENCES

VOLUME 125, ART. 2 PAGES 249-772

Editor

HAROLD E. WHIPPLE

October 13, 1965

Managing Editor

HURD HUTCHINS

FORMS OF WATER IN BIOLOGIC SYSTEMS*

Conference Cochairmen

JOSEPH F. SAUNDERS and JOHN E. FLYNN

CONTENTS

Introductory Remarks. <i>By JOSEPH F. SAUNDERS.</i>	251
The Effect of Solutes on the Structure of Water and its Implications for Protein Structure. <i>By HAROLD A. SCHERAGA</i>	253
Hydrophobic Hydration and the Effect of Hydrogen Bonding Solutes on the Structure of Water. <i>By FELIX FRANKS</i>	277
Diffusional Specificity in Water. <i>By I. ROBERT FENICHEL AND SAMUEL B. HOROWITZ</i>	290
Bonds in Water and Aqueous Solutions. <i>By T. G. OWE BERG</i>	298
The Formation of Ice at Water-Solid Interfaces. <i>By P. R. CAMP</i>	317
Electrical Properties of Bound Water. <i>By H. P. SCHWAN</i>	344
The Effect of Various Biologic Compounds on Proton Conductivity and Activation Energy in Ice. <i>By F. HEINMETS</i>	355
Hydration Structure of Fibrous Macromolecules. <i>By H. J. C. BERENDSEN AND C. MIGCHELSSEN</i>	365
Ion Incorporation and Activation Energies of Conduction in Ice. <i>By GERARDO WOLFGANG GROSS</i>	380
Mechanism of the Electrical Conductivity in Ice. <i>By C. JACCARD</i>	390
The Physical State of Water in Living Cell and Model Systems. <i>By GILBERT NING LING</i>	401
The Structure of Water Neighboring Proteins, Peptides and Amino Acids as Deduced from Dielectric Measurements. <i>By EDWARD H. GRANT</i>	418
Solute Behavior in Tightly Cross-Linked Dextran Gels. <i>By N. V. B. MARSDEN</i>	428
N.M.R. and Raman Properties of Water in Colloidal Systems. <i>By J. CLIFFORD, B. A. PETHICA, W. A. SENIOR</i>	458

*This series of papers is the result of a conference entitled *Forms of Water in Biologic Systems*, held by The New York Academy of Sciences on October 5, 6, 7 and 8, 1964. *Order No G-729 (33-20-001)*.

The Effects on Biologic Systems of Higher-Order Phase Transitions in Water. By WALTER DROST-HANSEN.....	471
Phase Transitions Encountered in the Rapid Freezing of Aqueous Solutions. By B. J. LUYET.....	502
Factors Affecting the Mechanism of Transformation of Ice Into Water Vapor in the Freeze-Drying Process. By ALAN P. MACKENZIE.....	522
Separate Effects of Freezing, Thawing and Drying Living Cells. By R.I.N. GREAVES AND J. D. DAVIES.....	548
Transport Properties of Water. By ALEXANDER LEAP.....	559
Diffusion and the Transport of Organic Nonelectrolytes in Cells. By SAMUEL B. HOROWITZ AND I. ROBERT FENICHEL.....	572
The Hydrate Microcrystal Theory of Anesthesia. By J. F. CATCHPOOL.....	595
A Proposed Water-Protein Interaction and Its Application to the Structure of the Tobacco Mosaic Virus Particle. By DONALD T. WARNER.....	605
Intracellular Water Structure and Mechanisms of Cellular Transport. By OSCAR HECHTER.....	625
Rapid Freezing and Thawing of Blood. By R. R. SAKAIDA, G. F. DOEBBLER, R. S. KIBLER, A. P. RINFRET.....	647
The Role of Cell Membranes in the Freezing of Yeast and Other Single Cells. By PETER MAZUR.....	658
New Approaches in Measuring the Linear Rate of Ice Crystallization in Water and Aqueous Solutions. By MAXIM D. PERSIKSKY AND VICTOR RICHARDS.....	677
Enzyme Patterns of Tumors Demonstrated Histochemically in Cryostat Sections. By P. J. MELNICK.....	689
Chemical and Morphologic Changes in the Prostate Following Extreme Cooling. By MAURICE J. GONDER, WARD A. SOANES, VERNON SMITH.....	716
Summation and General Discussion.....	730
H. S. FRANK.....	730
H. FERNÁNDEZ-MORÁN.....	739
GENERAL.....	754

Copyright, 1965, by The New York Academy of Sciences.

*All rights reserved. Except for brief quotations by reviewers, reproduction of this
publication in whole or in part by any means whatever is strictly prohibited without
written permission from the publisher.*

INTRODUCTORY REMARKS

Joseph F. Saunders

*Bioscience Programs Division,
National Aeronautics and Space Administration,
Washington, D.C.*

We are deeply grateful to The New York Academy of Sciences, the National Aeronautics and Space Administration and the Office of Naval Research for sponsoring this worthy conference.

Our program is one that we consider to be the interdisciplinary type, including basic and applied studies of the complexity of water in its various forms. At first, we thought of devoting this meeting to the field of cryobiology. Later, however, we decided that we should not limit the scope of the conference to the study of water as ice, but to extend our discussion to the physicochemical and biologic parameters governing the role of water in living systems. We hoped for a meeting of biologists, chemists, physicists, clinicians and engineers so that the exchange of views and ideas would shed more light on the complexity of water.

Most of us consider water as a homogeneous fluid with definite physical properties subject to variation or alteration as a function of temperature and pressure. We know that water is indispensable for the maintenance of normal metabolic activity. We appreciate, too, that disturbances occur in water metabolism with and without consistent alterations in other metabolic processes. For instance, in many diseased states, there is an imbalance in water metabolism without any significant disturbance in electrolyte metabolism. On the other hand, during the rapid freezing of biologic systems such as erythrocytes, water is transformed into ice with simultaneous dehydration and concentration of electrolytes in the tissue.

Many cryobiologists believe that the manner of freezing of living systems is irrelevant, so long as a protective substance is added to the medium. There are still those who assume that, because of their structure, many substances act as water or as substitutes for water during freezing and lyophilization. Perhaps this conference may tend to illuminate such concepts.

With the advent of numerous new physicochemical techniques, we find that water is not the simple, homogeneous substance we once assumed it to be. Depending on its environment or substrate, if you will, such properties of water as total energy, ionic mobility, viscosity, dielectric behavior and position among molecular fluids are subject to obvious as well as subtle changes. We often wonder how microorganisms can survive at -70°C. and lower, perhaps. Is there a "built in" protective mechanism against damage from ice formation?

Why is it possible to preserve blood indefinitely at temperatures as low as those provided by cryogenic gases? Certainly rapid freezing to avoid massive destruction by ice formation is not the only answer.

What is the source of water or mechanism(s) by which an organism obtains water from a hydrocarbon environment?

How does water contribute to the molecular architecture of living systems not only in adult form, but in embryonic form? Water must be the medium upon which unique cellular morphology is dependent. Perhaps it is water that is the directing or orienting force in the morphogenic development of tissue specificity, membrane structure and function, and biochemical functionality.

Cellular transport, oxygen transfer in respiratory pigments, photosynthesis and every other process we can think of depend upon water. Yet, the fundamental mechanisms by which water regulates life processes continue to be evasive so as to handicap us in our quest for understanding life.

We hope that this conference will serve to clarify and elucidate at least a few of the problems associated with the ubiquitous water molecule.

We believe that experimental data will be presented to confirm some of the theoretical values established for some of the parameters of water behavior. Finally, we wish that the papers will engender broad discussion of problems, and new ideas which result in new and significant avenues of approach to our understanding of the structure and function of water in living systems.

THE EFFECT OF SOLUTES WATER AND ITS IM- PROTEIN STI

Harold A. S

*Department of
Cornell University*

The properties of aqueous solutions are determined by the interaction of water with the dissolved solute. In order to understand the physical treatment of such systems it is necessary to know the nature of the influence of the solute and solvent on each other. A fruitful discussion of the properties of aqueous solutions can be based on a basis for the formulation of appropriate interaction parameters. This has been presented by Frank and Wen.^{1,2}

It is necessary to distinguish between two types of interactions between solute and solvent. These have been discussed both types of systems. However, from the present point of view, most of the recent progress in the study of aqueous solutions of nonpolar solutes. Therefore, we will consider here the properties of aqueous solutions of polar solutes. We will consider here the properties of aqueous solutions of polar solutes.

tially a story of the various forms in which this hydrogen bonding was envisaged as existing; the modern view, emphasizing extensive hydrogen bonding, was initiated by Bernal and Fowler.⁶ Two recent surveys of theories of water structure have been presented elsewhere.^{7,8} From these considerations,⁷ the "flickering cluster" concept proposed by Frank and Wen^{1,2} was selected and used by Nemethy and Scheraga^{1,9} as a basis to develop theories of liquid H₂O and D₂O.

Frank and Wen^{1,2} have argued that the formation of a hydrogen-bonded dimer of two H₂O molecules makes it easier to form additional hydrogen bonds with other H₂O molecules because of the contribution (to the partially covalent hydrogen bond) of a resonant form having a partial charge separation. In other words, the formation of hydrogen bonds in the liquid is a cooperative phenomenon, i.e. the bonds are not made and broken singly but several at a time, thus producing short-lived "clusters" of highly hydrogen-bonded regions surrounded by nonhydrogen-bonded molecules. These clusters may be expected to be compact and nearly spherical in shape. On

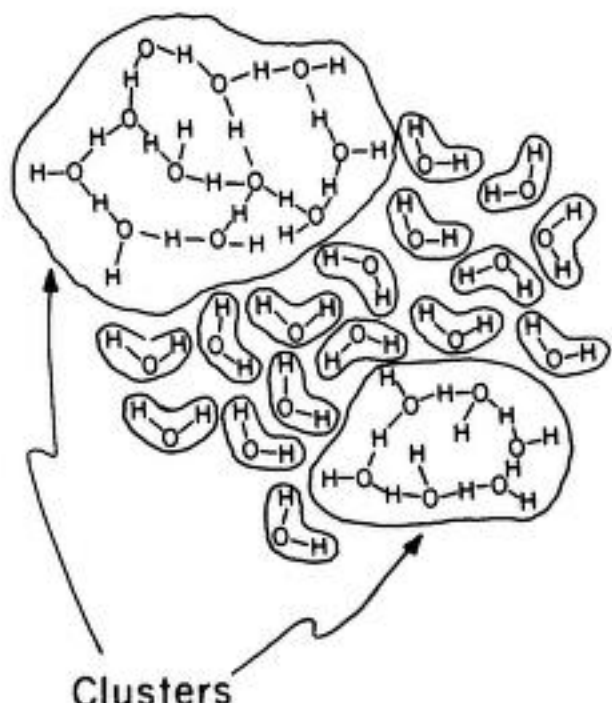


FIGURE 1. Schematic representation of liquid water, showing hydrogen-bonded clusters and unbonded molecules. The molecules in the interior of the clusters are tetracoordinated, but not drawn as such in this two-dimensional diagram (Nemethy & Scheraga¹).

the basis of the Frank-Wen assumptions, no appreciable amount of small aggregates (dimers, trimers, etc.) will exist — only clusters and monomers. The model is represented in FIGURE 1. While there is probably a distribution of cluster sizes, the theory was developed on the assumption that all clusters are of uniform size, equal to the mean size, which varies with temperature.

Even though there are only two main structures, free molecules and clusters, the individual molecules may be distributed among five classes, depending on the number of hydrogen bonds in which they are involved. The monomeric species constitute one class, and there are four more classes of species in the cluster; inside the cluster there are tetrabonded species, while on the surface of the cluster there are tri-, di-, and monobonded species. An energy level can be assigned to each species, depending on the number of its hydrogen bonds, as shown in FIGURE 2. The ground state is occupied by tetracoordinated species; as hydrogen bonds are broken the upper states become populated. The state labeled "vapor" lies much higher on the energy scale and does not play a role in a theory of the liquid. Even though the "unbonded" molecules (i.e. the monomeric species) do

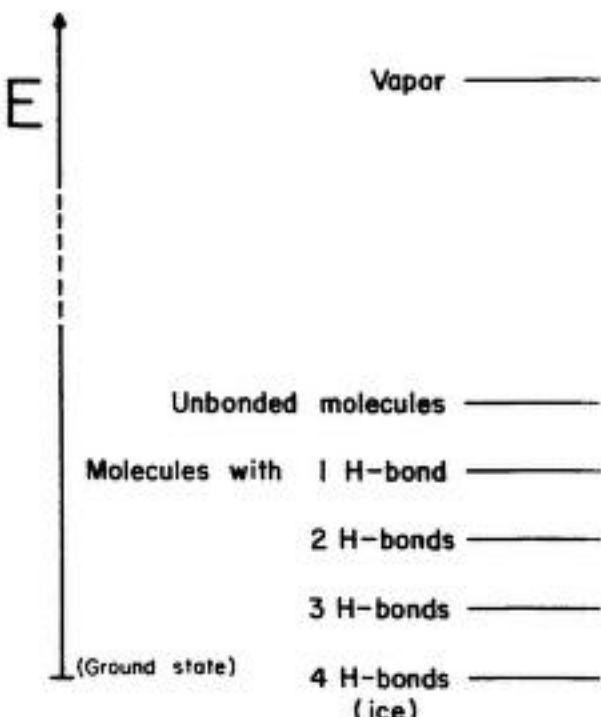


FIGURE 2. Schematic representation of energy levels for H_2O molecules in liquid water (Nemethy & Scheraga²).

not participate in hydrogen bonding, they are still close enough in the liquid (unlike those in the vapor) to interact by dipole forces.

In order to completely define the state of the system, the populations of the various energy levels must be computed. For this purpose, it is necessary to specify the spacings of the levels. Consider first the difference in energy between the ground state (level 4) and that corresponding to the unbonded molecules (level u). In order to bring a molecule from level 4 to level u, four hydrogen bonds must be broken; but a molecule in level u has approximately eight neighbors⁷ with which it interacts by dipole forces. Therefore, the separation between these two levels is the difference in the energy to break four hydrogen bonds and the dipole interaction energy with eight neighbors. This net energy was taken as an empirical parameter in the theory, obtained by fitting the resulting equations to experimental data for the thermodynamic properties of liquid water; the resulting value was a reasonable one, on the basis of current estimates of hydrogen bond energies and dipole interaction energies. In addition, a second parameter, the "free volume" for the translational motion of unbonded molecules, was introduced; it too was found to be a reasonable one, on the basis of known values of the free volume of many substances. The distance between levels 4 and u was divided up equally in order to obtain the location of levels 1, 2 and 3.

The populations of the various levels are not independent. For example, for a cluster containing a given number of molecules, the number on the surface is not independent of the number inside, i.e. there is a correlation between the number on the surface and the number inside, a kind of surface-to-volume ratio. These cluster correlations were put in the form of empirical equations (relating the mole fractions of the various species), obtained by building models of various sized clusters and counting the number of each species. With these cluster correlations and the Boltzmann principle, it was possible to write the partition function for the system, and evaluate it in order to calculate the populations of the levels and the thermodynamic parameters of the system. The internal motions of each species were represented by Einstein oscillator functions, using frequencies from infrared and Raman spectra.

The first result which emerged from the calculation is the cluster size. These data are shown in TABLE 1 and FIGURE 3 and provide a quantitative description for the model shown in FIGURE 1. The original papers^{7,8} may be consulted for the other parameters describing the clusters (e.g. the mole fractions of the various species). From recent infrared spectroscopic studies, Buijs and Choppin¹⁰ obtained structural parameters for liquid H₂O, with values which appear to be similar to the theoretical ones.⁷ The cluster sizes given in TABLE 1 are also compatible with data on the viscosity of water^{11,12} and on the conductivity of aqueous solutions of electrolytes.¹³

Scheraga: Effect

TABLE
TEMPERATURE-DEPENDENCE^{7,8} OF CLUSTER
 x_n , OF NONHYDROGEN-BONDED MOLE

t, °C.	n_{cl}	
	H_2O	D_2O
0	91	—
4	—	117
10	72	97
20	57	72
30	47	56
40	38	44
50	32	35
60	28	29

It is of interest to compare D_2O and H_2O . The following factors are probably applicable to both systems; the only difference is in the magnitude of the effect: (1) the hydrogen bond energy, (2) the vibrational frequencies, (3) the moments of inertia. The hydrogen bond energy is about 10% higher for D_2O than for H_2O , and the vibrational frequencies are about 10% lower.

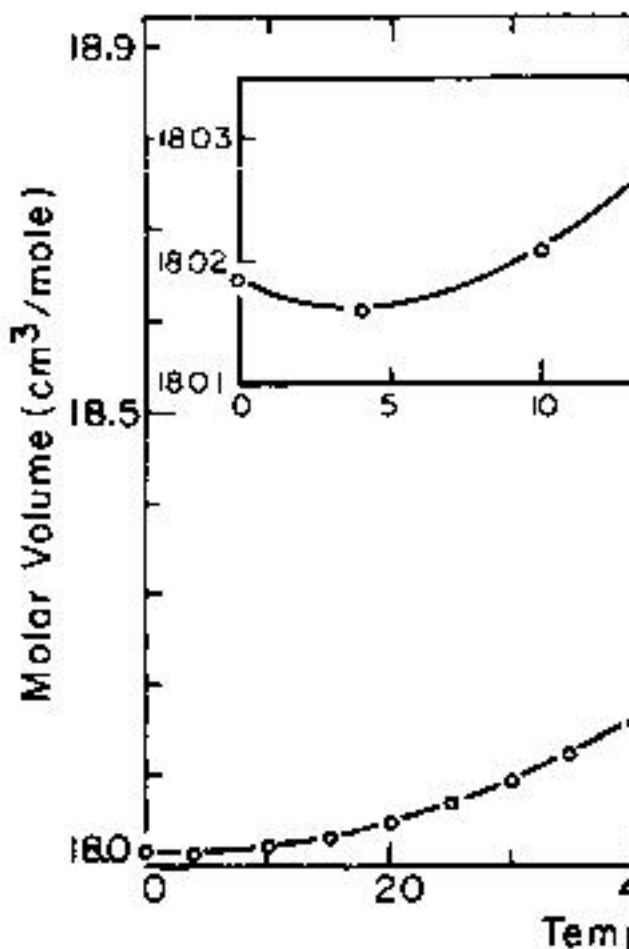


FIGURE 4. Comparison of calculated molar volume of H_2O as function of temperature. The agreement is within three per cent at lower temperatures. (Nemethy & S-

tropy of liquid H_2O agree with each other to within less than three per cent. For liquid water the agreement is within one per cent. The calculated temperature dependence of the entropy of

Scheraga: Effect

FIGURES are enlargements at low temperature, it is seen that tonically with temperature. If we ignore the effect of n_{cl} with temperature, i.e., if we assume that the clusters disappear at high temperatures, then a liquid consisting of clusters and normal unbonded liquids should show a monotonic rise in V with increasing temperature. However, recognizing that n_{cl} decreases with increasing temperature (See TABLE 1), it can be seen that the molecules are removed from the open spaces between the centers of the clusters and packed more densely in the unbonded liquid; this procedure increases the volume with increasing temperature. This increase, together with the normal thermal expansion of the unbonded liquid gives rise to the curves shown at 4°C. and 11.2°C. for H₂O and D₂O. In FIGURE 4, the curves of FIGURES 4 and 5, one need only subtract the coefficients of thermal expansion for the clusters.

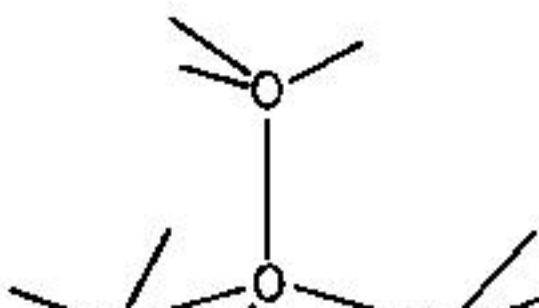
For the clusters, the coefficient of expansion (for H₂O and D₂O), extrapolated into the liquid phase of the unbonded liquid, an empirical equation (with the same supplemental data as H₂O and D₂O) was obtained:

carbon solutions, the changes in there is a very large negative excess ideal mixing; this leads to a large solubility because of the dominance of

Frank and Evans¹³ proposed that these terms are due to the ordering of the water molecules. While pure water contains "flickering" fluctuations, a carbon solution is even more highly ordered. If this explanation is accepted, the solubility of carbon in water is understandable. However, before accepting the explanation, two questions must be answered: (1) *why* does the dissolved carbon cause ordering of the water, and (2) *why* is there a decrease in volume?

In order to answer these two questions, we must first consider the structures shown in FIGURE 6. When a near-spherical

A



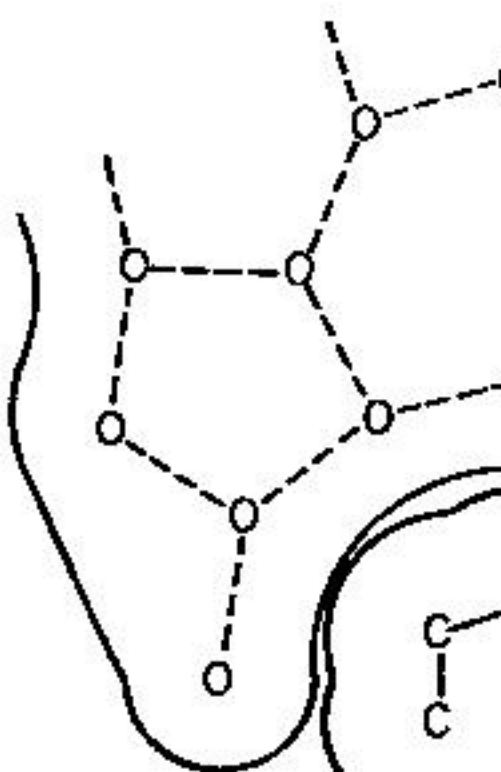
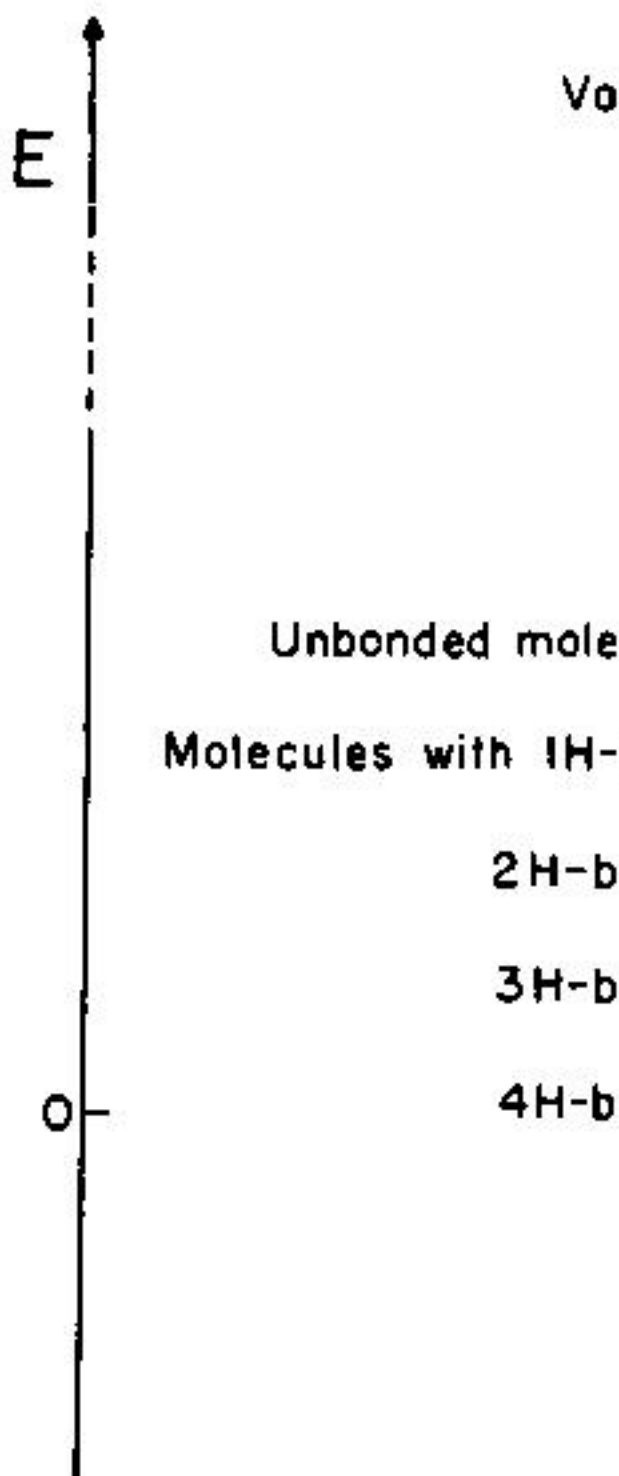


FIGURE 7. Schematic cross-section of a hydrocarbon solute molecule, indicating the solute. The O-H...O hydrogen bond heavy lines correspond to the surfaces and radii of the molecules involved (Nemethy et al., 1968).

affect its energy (FIGURE 6B). Since water molecules can take part in four carbon molecule as a fifth neighbor; in come pentacoordinated. The cluster, in



Scheraga: Effect

when hydrocarbon molecules are transposed into water.

The concept of a partial cage derived from the structures of hydrates of the rare gases and of ice structures there are large polyhedral cages (as in ordinary ice) formed by tetra-hydrogen-bonded water molecules ranging in diameter from 5.2 to 6.3 Å. A hydrocarbon molecule which effectively increases the number of the water molecules in the wall of the cage excludes the solute molecules in neighboring cages from the structure, since a given water molecule can bind one solute molecule. However, in dilute solutions the solute molecules do not approach each other close enough to exert appreciable interaction. Therefore, partial cages, rather than complete cages, are encountered, i.e., one obtains the partial cage without the partial cage being itself part of a larger cage.

The calculation of the populations of the various species in the partial cages was carried out as in the case of pure water, employing the statistical mechanical equations and the Boltzmann principle. It was thus possible to calculate the mole fractions of the various hydrogen-bonded species in the first layer around a hydrocarbon molecule and to determine the ice-likeness upon introduction of a hydrocarbon molecule.

bons which are in good agreement ature range of 0° to 70°C. Estima were also obtained. The dependence hydrocarbon size arises directly from carbon molecule, the greater will be first layer around it having their

Recent experimental data¹⁶ indicate containing hydrocarbons are similar. However, the theory of the solubility has been completed.¹⁷

With the good agreement between thermodynamic parameters for hydrocarbons, confidence in the model, and proceeded to study hydrocarbons in solution, i.e., the hy-

Formation of

The interaction of hydrocarbons is known to arise simply from the van der Waals interaction of molecules.¹⁸ However, Kauzmann¹⁹ has shown that changes in the structure of water molecules play an important role in the formation of hydrocarbon aggregates. It was later shown²¹ that the contraction between two hydrocarbon molecules

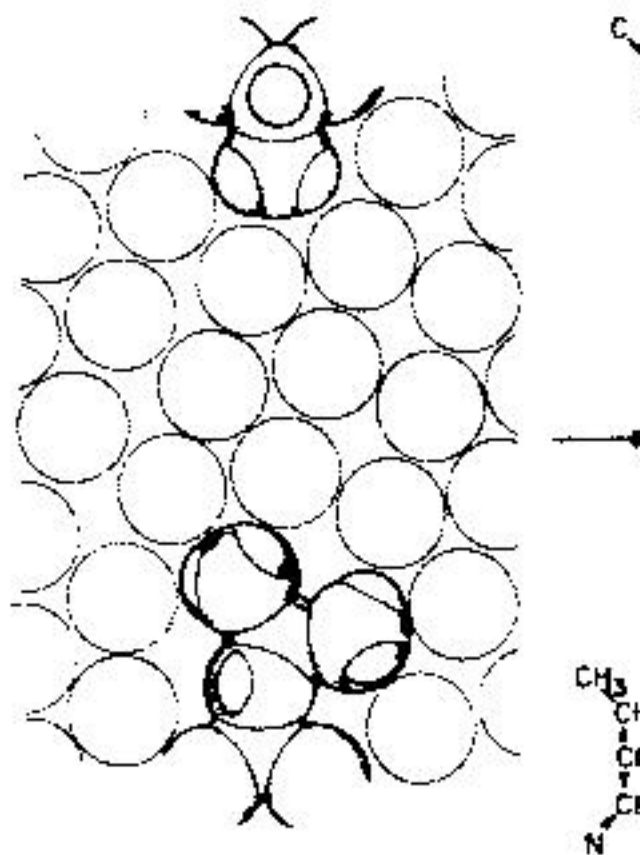


FIGURE 10. Schematic representation of the interaction between two isolated side chains (alanine) through an approach of the two side chains such that the number of nearest water neighbors is less than the maximum obtainable for the system. It is shown only schematically, without indicating the bonded networks (Nemethy & Scheraga²¹).

carried out for all possible pairs of s

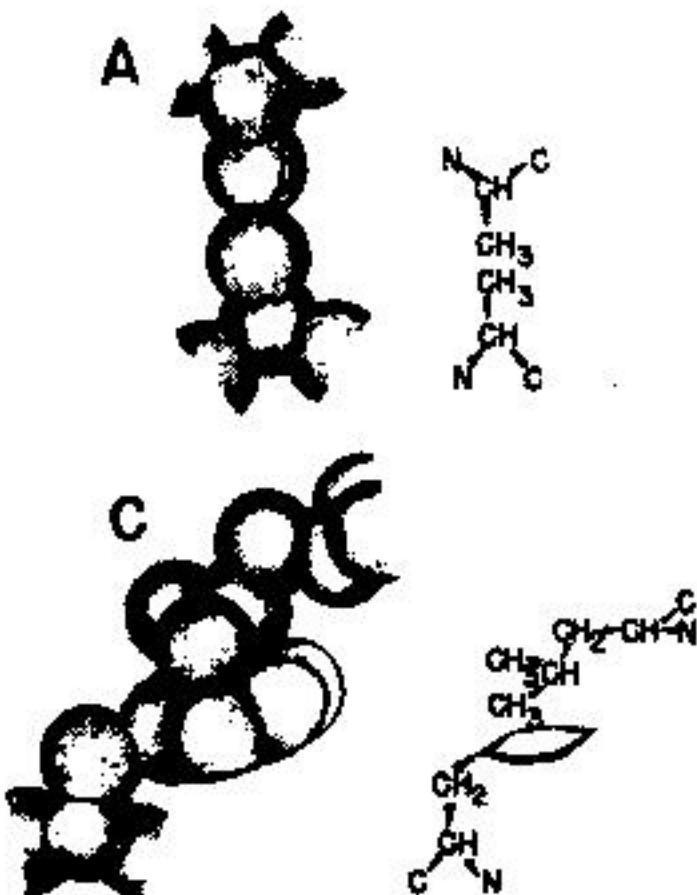


FIGURE 11. Illustrative examples of solvated side chains. The hydrogens are omitted but with the van der Waals radii reduced. The structural formulas to the right show the arrangement of the atoms. A, alanine-leucine-isoleucine bond (maximum solvent exposure); D, phenylalanine-leucine bond (maximum strength); E, phenylalanine-alanine bond (intermediate).

Scheraga: Effect

Experimental Verification of

It is worthwhile to consider next some of the theoretical calculations. In water or in polar resin, cross-linked polystyrene, polar groups form a hydrophobic bond between the nonpolar resin.²² Subtracting the energy of the nonpolar resin, it is possible to obtain the higher homologues, it is possible to obtain thermodynamic parameters for hydrophobic bonds between the nonpolar groups involved. These are shown in Table I. There is very good agreement between the calculated values.

Urea was found to decrease the binding energy of carboxylic acid,²³ i.e., presumably urea reduces the hydrophobic bonds.

TABLE I
THERMODYNAMIC PARAMETERS²³ FOR HYDROPHOBIC BONDS BETWEEN THE NONPOLAR PARTS OF CARBOXYLIC ACIDS

R groups of acid	Experimental	
	ΔF°	ΔH°
CH ₃	-1.2	-1.0
CH ₂ Cl	-0.8	-0.6
CH ₂ Br	-0.7	-0.5
CH ₂ Cl ₂	-0.6	-0.4
CH ₂ Br ₂	-0.5	-0.3
CH ₂ ClBr	-0.4	-0.2
CH ₂ Cl ₂ Br	-0.3	-0.1
CH ₂ Cl ₂ Br ₂	-0.2	-0.05

it probably has the following struc-
mation between the R groups, in a

R—

R—

Subtracting the thermodynamic
for the higher homologues eliminat-
bond and yields data for pair intera-
given in TABLE 4, where they are com-
puted on two different bases). The data
support for the validity of the theory of
hydrophobic bonds.

As another example, we cite the
the lowering of the transition tem-

Scheraga: Effect

TABLE I
LOWERING OF THE TRANSITION TEMPERATURE BY ONE MOLE PER LITER OF ALCOHOL IN 0.1 MOLAR SOLUTIONS OF RIBONUCLEASE

Alcohol	Lowering, °C.
Experimental	Calculated
CH ₃ OH	1.0
CH ₃ CH ₂ OH	3.0
CH ₃ CH ₂ CH ₂ OH	7.0
CH ₃ CH ₂ CH ₂ CH ₂ OH	13.0

of ribonuclease caused by alcohols of increasing chain length. These calculations were based on the assumption that the alcohol binds to a similar nonpolar site of the denatured protein, thus favoring denaturation. The binding constants and theoretical values²¹ of the hydrophobic interaction are given in TABLE 5. Again, the excellent agreement between calculated and experimental values is striking.

volume decrease accompanying the
Here again, the device of subtracting
homologous series, in order to obtain
group, was used. The agreement between
is fairly good, especially at the higher
concentrations.

Of course, the volume change associated with hydrophobic bonds will have the opposite effect. Volume decreases in association with the formation of hydrophobic bonds and increases in dissociation with the formation may be involved.

In summary, it appears that we now have a reasonable experimental basis for predicting the steric hindrance of various nonpolar side-chains. In the next section we shall explore some of the implications of these hydrophobic bonds.

Some Implications

As with other noncovalent interactions, the hydrophobic bond is affected by various conformations of polypeptides. The hydrophobic bond between two nearby residues in a protein molecule has a definite structure²¹ (see FIGURE 12). In the case of the α -helix of alanine, the β -methyl group of an adjacent residue is in close proximity to the α -carbon atom of the same residue.

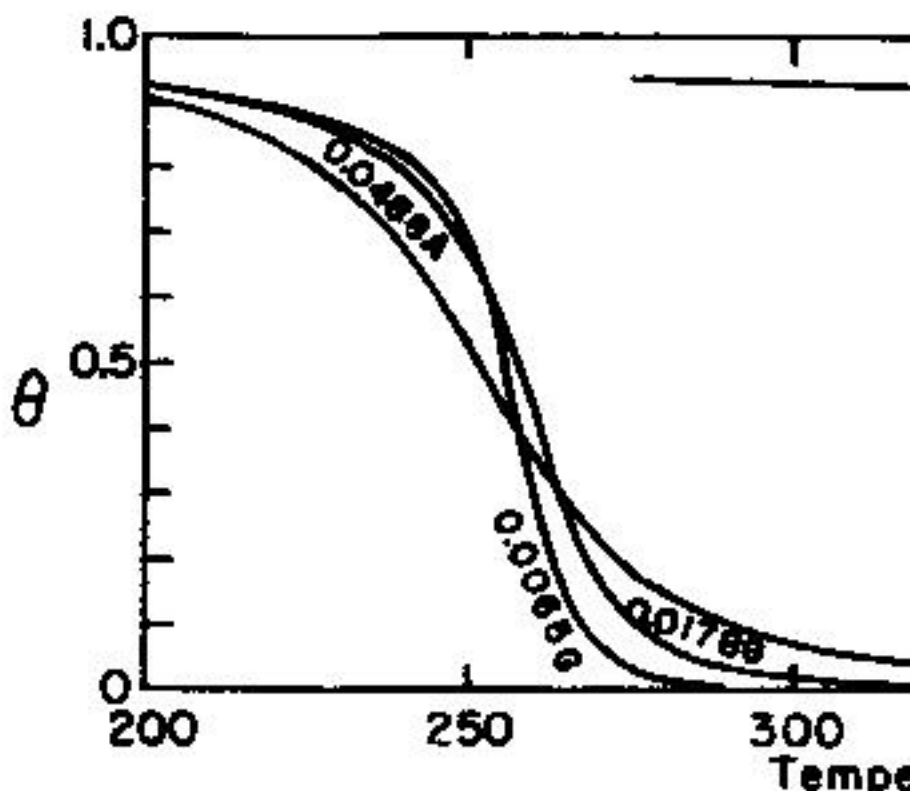
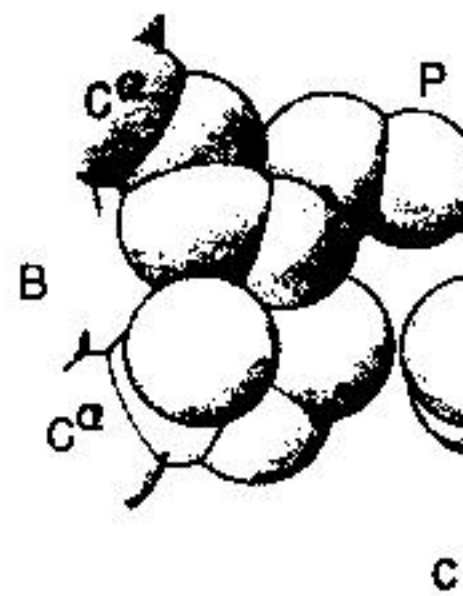
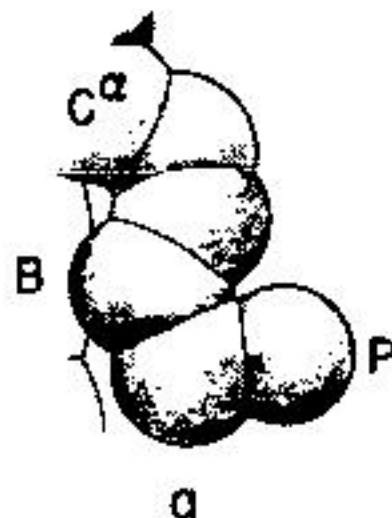


FIGURE 13. Computed curves for a helix content θ versus temperature T for poly-L-alanine (A) containing different values of the enthalpy of formation of the amide hydrogen bond (ΔH_{am}) (Bixon *et al.*³⁶).

with the α -CH group on the $(i+3)$ residue of the α -helix.²¹ The effect of this hydrogen bond on the α -helix can be seen by comparing calculated curves for polyglycine and poly-L-alanine (FIGURE 13).



Scheraga: Effect

tropy²⁹ (also characteristic of hydrophobic association) and such association are the protein of tobacco mosaic virus. These are in contrast to the associations of proteins accompanied by a decrease in enthalpy, which are due to intermolecular hydrogen bonds.

Summary

On the basis of a recent theory of water-solute interactions we understand the effect of nonpolar solutes on the ionization equilibria of acids and bases. Although no quantitative theory for the effect of ions and polar molecules on the ionization equilibria of acids and bases has been developed, but current work³ on this problem may be mentioned. As a consequence of the theory of aqueous ionization equilibria, the possibility of theoretical thermodynamic parameters for the interactions between nonpolar groups in proteins and other biological macromolecules has been established. Theoretical data have recently been verified by a number of investigations. As a result, it is possible to calculate, on a quantitative basis, the contribution of hydrophobic interactions to the reactivity of proteins.

Note Added

Recently,³ progress has been made in the use of deuterium oxide and D₂O and in obtaining a theory of the

Z_{\max} is then a function of the energies E_i .

In evaluating Z_{\max} it is assumed for each f_i are equal and the three equal, and that the frequencies for ones for H_2O by the appropriate treatment of H_2O and D_2O there are levels as variables.

The assignment of the frequencies the translational and librational frequencies be assigned with confidence (210) between 650 and 800 cm^{-1} for the between 650 and 800 is not too critical other frequencies is that they be normal species.

From the work of Buijs and Cope in energy between the levels for the is about 2.7 kcal/mole. Therefore the between 2.5 and 3.0 kcal/mole and the three levels may be varied but not the highest levels. The same energy We then have 8 frequencies and 4 degrees

Scheraga: Effect

bond from forming. We treat the position variables. In region 2 there are five such

With this model, we have been able to obtain data for the alkali halides at infinite dilution.

References

1. H. S. FRANK & W. Y. WEN. 1957. J. Phys. Chem. 61: 1025.
2. H. S. FRANK. 1958. Proc. Roy. Soc. (London) A 243: 161.
3. J. H. GRIFFITH & H. A. SCHERAGA. 1960. J. Phys. Chem. 64: 1025.
4. W. KAUFMANN. 1959. Adv. Protein Chem. 14: 1.
5. W. H. BARNES. 1929. Proc. Roy. Soc. (London) A 100: 100.
6. J. D. BERNAL & R. H. FOWLER. 1933. J. Phys. Chem. 37: 749.
7. G. NEMETHY & H. A. SCHERAGA. 1960. J. Phys. Chem. 64: 1025.
8. J. L. KAVENAU. 1964. Water and Solvents. Holden-Day Inc., San Francisco, Calif.
9. G. NEMETHY & H. A. SCHERAGA. 1960. J. Phys. Chem. 64: 1025.
10. K. BUIJS & G. R. CHOPPIN. 1963. J. Phys. Chem. 67: 1025.
11. A. A. MILLER. 1963. J. Chem. Phys. 38: 1025.
12. R. A. HORNE & R. A. COURANT. 1964. J. Phys. Chem. 68: 1025.
13. H. S. FRANK & M. W. EVANS. 1945. J. Phys. Chem. 49: 1025.
14. G. NEMETHY & H. A. SCHERAGA. 1960. J. Phys. Chem. 64: 1025.
15. M. v. STACKELBERG *et al.* 1954. Z. Elektrochem. 58: 130.
16. G. C. KRESHECK, H. SCHNEIDER & H. A. SCHERAGA. 1960. J. Phys. Chem. 64: 1025.
17. G. NEMETHY & H. A. SCHERAGA. 1960. J. Phys. Chem. 64: 1025.
18. K. U. LINDEMSTRÖM - LANG. 1952. Proc. Roy. Soc. (London) A 210: 1025.

37. J. C. KENDREW. 1962. Brookhaven
38. I. Z. STEINBERG & H. A. SCHERAG
39. W. L. PETICOLAS. 1962. *J. Chem.*
40. J. M. STURTEVANT, M. LASKOWSK
1955. *J. Am. Chem. Soc.* 77: 616

HYDROPHOBIC HYDRATION HYDROGEN BONDING STRUCTURE OF LIQUIDS

Felix FR

*Department of Chemistry,
Institute of Technology,
Bradford, England*

Investigations into the thermodynamics of the noble gases and of hydrocarbons have led to a better understanding of the structure of liquid water. Various attempts have been made to interpret the properties of hydrocarbons from aqueous solution by means of models. Liquid water is regarded as a molecular model in which each molecule is capable of forming tetrahedrally-oriented hydrogen bonds, and the properties of the species, the properties of which are not yet fully understood, are explained by the gas hydrate type model put forward by J. D. Bernal and R. F. H. Allmand. The quasicrystalline structure proposed by G. Nemethy and H. A. Scheraga, on the basis of the distribution of ice-like clusters dispersed in water, is also discussed.

T

**PARTIAL MOLAR ENTHALPIES AND
DILUTION OF HYDROCARBONS AND A
ENTROPIES OF DISSO**

Solute	Solution*		Hyd
	ΔH_2 kcal.	ΔS_2 e. u.	
CH ₄	3.2	32	
C ₂ H ₆	4.1	35	
C ₃ H ₈	5.8	41	1
n-C ₄ H ₁₀	6.1	42	
iso-C ₄ H ₁₀	5.4	40	

Franks: Hydrophobicity

has two unshared electron pairs. Thus the water mixtures must in some degree also mutually incompatible types of association comparing the solution properties of monohydric alcohols and sugars. As the number of molecules increases, so the anomalies observed become more marked, and sugar solutions, although showing extremely complex behavior shown by the

In a study of the physical properties of dilute aqueous concentration regions would appear to consist of alcohol molecule molecules dispersed throughout the volume of liquid water, either by being incorporated into the water molecule without changing this a great deal, or by forming small, non-polar, three-dimensional clusters. On the other hand, in concentrated solutions the available evidence favors the view that the alcohol molecules form aggregates and water-centered associations.

The present discussion is confined almost entirely to the case of monohydric aliphatic alcohols, and in particular to such mixtures it is shown that the observed anomalies can be explained in terms of an interstitial model similar to that proposed for organic solutions.^{1,4}

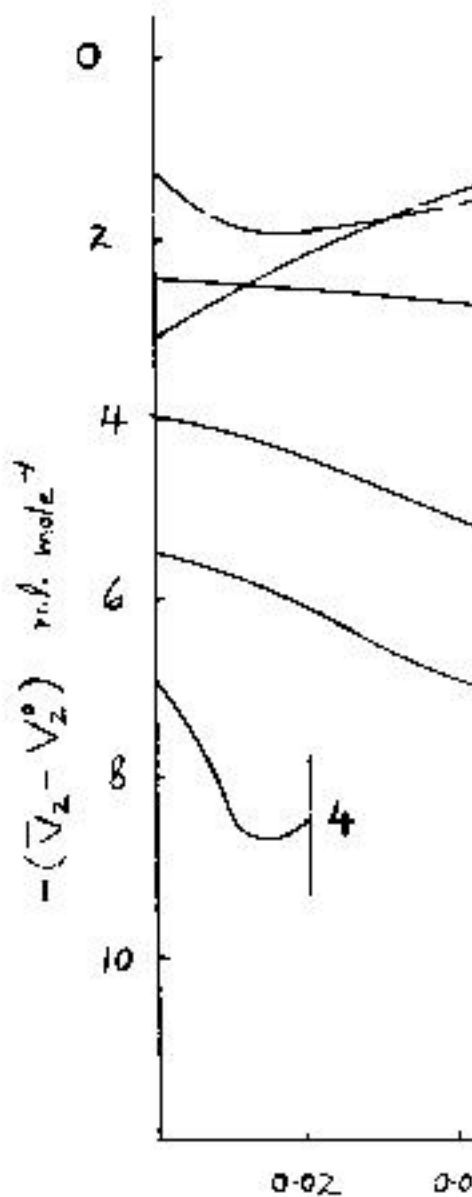


FIGURE 1. Partial molar volumes:
 (3) n-PrOH, (4) n-BuOH, (5) ethyl

Franks: Hydrophobicity

(3) the concentration at which (\bar{V}_2)_{min} occurs. This value depends on the size and shape of the molecule. For example, the minimum \bar{V}_2 of 2-methyl propanol-1 and 2-methyl propanoic acid occur at the same concentration, about 1.5 mol/liter, but the minimum \bar{V}_2 of 2-methyl propanoic acid is at a higher concentration than that of 2-methyl propanol-1. The low solubility of 2-methyl propanoic acid makes it impossible to ascertain the exact value of \bar{V}_2 .

FIGURE 2 shows that it is likely to be negative for all alcohols. Negative partial molar volumes appear to be a general phenomenon and have also been reported for electrolytes containing polar groups, such as the tetraalkyl ammonium salts and their fates,¹⁴ and as is the case with the alcohols, the magnitude of the increase in the number of carbon atoms in the molecule. In the interstitial solution model, i.e., the conformational changes in water molecules around solute sites in a water quasilattice. Although no hydrates of alcohols are known and have been reported for alcohols, Jeffrey and his colleagues,¹⁵ the analogy between alcohols and alkanes has been pushed too far. Methane, ethane, propane, and n-butane form hydrates (see TABLE 1), but no hydrate of iso-butane. Qualitative differences can be observed between the hydrates of n-butane and iso-butane or of n-butane and 2-methylpropane.

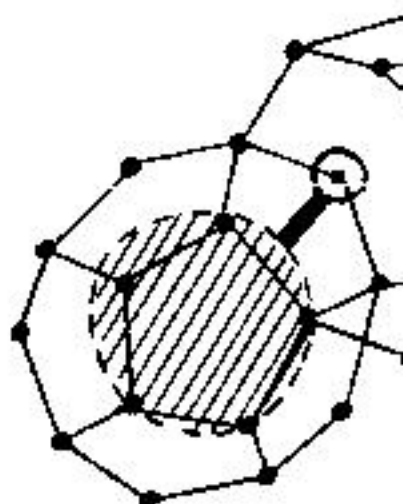


FIGURE 3. The alcohol molecule occupies a hexagonal cavity in the framework and hydrogen bonded in the same manner as the water molecule to the oxygen atom; the inability of the alcohol molecule to form hydrogen bonds gives rise to a structural hole indicated by the open circle.

bonds are stronger than water-water bonds, and the base strength increases as does the base strength of the solvent. It is also known that the alcohol oxygen atom is active in forming hydrogen bonds and can account for the observed results. For example, it has been found that the findings that ethylene oxide forms a complex with water in which the molecule is not hydrogen bonded to the water molecule, but is hydrogen bonded to an inert gas.¹⁸ This result would appear to indicate that the lack of miscibility with water arises from the fact that the alcohol molecule is not able to form hydrogen bonds with the water molecule.

Franks: Hydrophobic

$$V_1^*(T) = a +$$

and $V_2^*(T) = a' -$

If there is a structural contribution involving a zero volume of mixing,

$$\Delta T_{\text{observed}} = \Delta T_{\text{ideal}}$$

For most solutes $\Delta T_{\text{observed}}$ is negative. $\Delta T_{\text{observed}}$ at low concentrations is positive of the alkyl group; FIGURE 4 shows ΔT and tert-butanol. The maximum effect is in the $\bar{V}_2(x_2)$ curve.

As a good approximation, ΔT can be expressed in terms of the excess molar expansibility ϕ_E by the relationship

$$\frac{\Delta T}{m} = -\phi_E \left(\frac{\partial^2 V}{\partial T^2} \right)_p$$

where $\phi_E = (\partial \phi_v / \partial T)_p$, and m is the molal concentration ($x_2 < 0.03$) where ΔT is positive, aqueous alcohols exhibit negative expansibilities. This is in contrast to water, although it has been pointed out that ϕ_E is small and increases rather suddenly above the inflection in the $\bar{V}_2(x_2)$ curve occurs.²¹

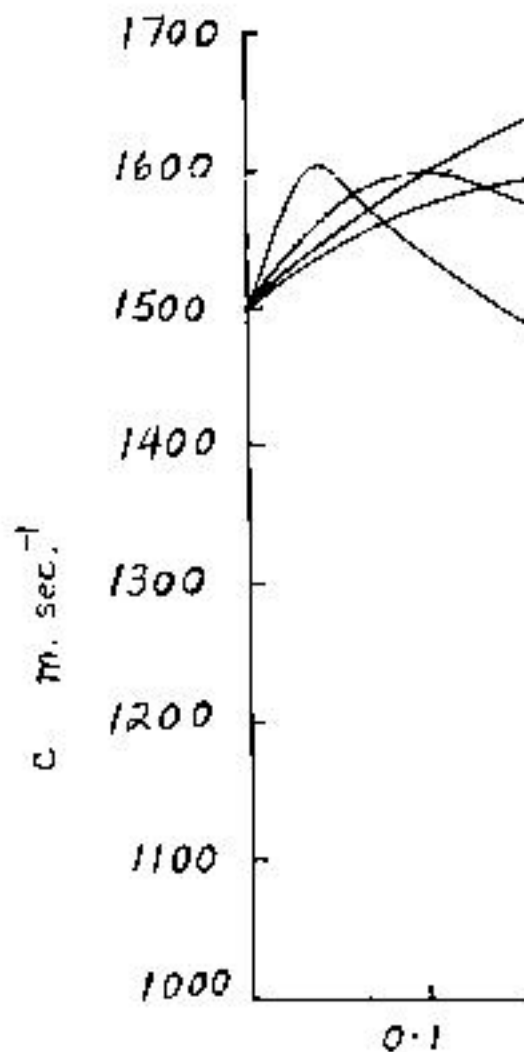


FIGURE 5. The velocity of sound
n-PrOH, and (4) ethylene glycol. (A)

conveniently obtained from a stud

Franks: Hydrophobic

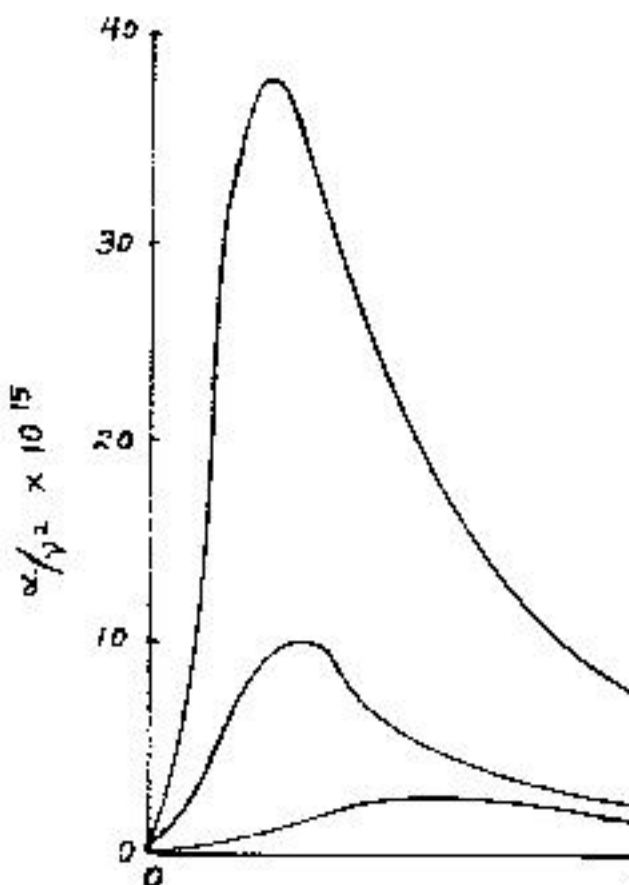
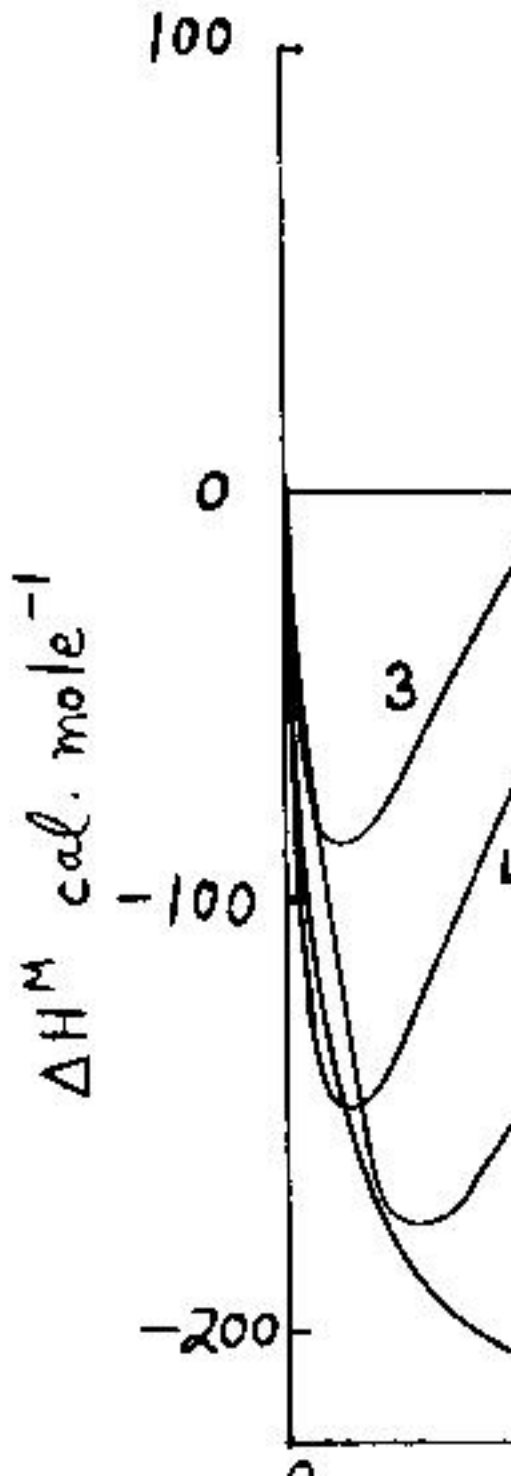


FIGURE 6. The ultrasound absorption coefficients for the pure alcohols and for dilute aqueous solutions of the alcohols: (1) EtOH, (2) n-PrOH, (3) tert.-BuOH.

the existence of structural entities which are not found in pure water. Such additional structures may have an interstitial nature of the solution and may be formed by hydrogen bonds formed between alcohol



Franks: Hydrophobic

with water, capable of forming hydrogen bonds, which would destroy the peculiar structure of water.

Finally the behavior of water-alcohol mixtures should be considered: in spite of Raoult's Law implying strong interactions, the mixtures show deviations from Raoult's Law, because of the nature of mixing. Most experimental determinations of such mixtures have been based on the use of a method which is unsuitable for the present purpose, namely a very comprehensive investigation of freezing points, enthalpies of mixing, and vapor pressures of solutions of the C₁-C₄ alcohols, has revealed deviations from Raoult's Law,²⁷ a hypothesis advanced by F. Franks and D. J. G. Davies²⁸ to account for the observed deviations in the tensions of very dilute solutions of alcohols. An example of this type of behavior; it is seen that the Raoult's Law activity coefficient of water, f_1 , decreases

tration. The corresponding solute activity, a_2 , therefore is greater than that predicted by Henry's Law. Eventually the $a_2(x_2)$ curve cuts the Henry's Law reference line, and as x_2 increases further, the behavior normally associated with water-alcohol mixtures is observed.

In this connection it is of interest to note that the behavior shown in FIGURE 8 should give rise to a lower consolute temperature (LCT). Although for the aliphatic alcohols the LCT would lie below the freezing point of the mixture, at low temperatures the solubilities of n-, iso-, and sec-butyl alcohols do indeed have negative temperature coefficients, and LCT's as high as 45° have been reported for water-glycol ether mixtures.²⁹

Spectroscopic Properties

Paradoxically, spectroscopic methods have not so far yielded much information about the nature of the hydrogen bonds and structural properties of water-alcohol mixtures. The infrared and Raman spectra are extremely complex, and at the time of writing the interpretation of such spectra for liquid water is still very much under discussion. In recent years several independent proton magnetic resonance (PMR) studies have led to mutually contradicting results, possibly because of the presence of small amounts of acidic impurities. W. G. Paterson and H. Spedding, as the result of an extensive study of proton exchange rates, found that the lifetime of a proton in a given position increases in the order MeOH < EtOH < PrOH < n-BuOH < iso-BuOH < iso-PrOH < sec.-BuOH < tert.-BuOH,³⁰ thus underlining the acid-base nature of the hydrogen bond.

Finally of great interest is a recent study of the effect of alkyl groups on the water proton shift.³¹ The observed shift of -0.02 p.p.m. per CH₂ group at first sight indicates that hydrocarbon groups cause a net breaking of hydrogen bonds in water. However, this conclusion is based on the frequently made assumption that the hydrogen bond is of a purely electrostatic nature. The PMR results are quite consistent with other experimental observations on water-hydrocarbon and water-alcohol systems, if a covalent contribution to hydrogen bonding is invoked.³² The association shift in the direction of a higher field could thus arise from an additional polarization of the hydrogen bond in the proximity of an interstitial (i.e. nonbonded) hydrocarbon group; this effect might be considered as the origin of the "icebergs," first postulated by H. S. Frank and M. W. Evans to account for the thermodynamic properties of aqueous solutions of nonelectrolytes,³³ and employed by later workers in the development of structural models for liquid water.^{1,2,4}

References

1. FRANK, H. S. & A. S. QUIST. 1961. J. Chem. Phys. 34: 601.
2. NEMETHY, G. & H. A. SCHERAGA. 1962. J. Chem. Phys. 36: 3382; 3401.
3. CLIFFORD, J. & B. A. PETHICA. 1964. Trans. Faraday Soc. 60: 1483.

4. FRANK, H. S. & F. FRANKS. In preparation.
5. ZACHARIASEN, W. H. 1935. J. Chem. Phys. 3: 158.
6. BERMAN, N. S. & J. J. MCKETTA. 1962. J. Phys. Chem. 66: 1444.
7. BROWN, A. C. & D. J. G. IVES. 1962. J. Chem. Soc. : 1608.
8. PRIGGIGNE, I. R. DEFAY. 1954. *Chemical Thermodynamics*, Longmans Green & Co., London, England. P. 11 ff.
9. MITCHELL, A. G. & W. F. K. WYNNE-JONES. 1953. Disc. Faraday Soc. 15: 161.
10. FRANKS F. 1964. Unpublished results.
11. ALEXANDER, D. M. 1959. J. Chem. Eng. Data 4: 252.
12. MASTERTON, W. L. 1954. J. Chem. Phys. 22: 1830.
13. WEN, W. Y. & S. SAITO. 1964. J. Phys. Chem. 68: 2639.
14. FRANKS, F. & H. T. SMITH. 1964. J. Phys. Chem. 68: 3581.
15. McMULLAN, R. K. & G. A. JEFFREY. 1959. J. Chem. Phys. 31: 1231.
16. BUTLER, J. A. V., D. W. THOMSON & W. H. MACLENNAN. 1933. J. Chem. Soc. : 674.
17. PATERSON, W. G. & H. SPEDDING. 1963. Canad. J. Chem. 41: 714; 2472; 2477.
18. JEFFREY, G. A. 1964. Private communication.
19. WADA, G. & S. UMEDA. 1962. Bull. Chem. Soc. Japan 35: 646.
20. FRANK, H. S. Unpublished work.
21. FRANKS, F. & H. H. JOHNSON. 1962. Trans. Faraday Soc. 58: 656.
22. BURTON, C. J. 1948. J. Acoust. Soc. Am. 20: 186.
23. GIACOMINI, A. 1942. Acta Pontif. Acad. Sci. 6: 87.
24. HALL, L. 1948. Phys. Rev. 73: 775.
25. SCHNEIDER, W. G. 1959. Colloque Internat. Centre Nat. Recherche Sci. (Paris). 77: 529.
26. GLEW, D. N. 1962. Nature 195: 698.
27. KNIGHT, J. 1961. Ph.D. Thesis. Princeton University, Princeton, N. J.
28. FRANKS, F. & D. J. G. IVES. 1960. J. Chem. Soc. : 741.
29. LANDOLT - BOERNSTEIN. 1960. *Zahlenwerte und Funktionen*. 2: 406. Springer, Berlin, Germany.
30. FRANK, H. S. & W. Y. WEN. 1957. Disc. Faraday Soc. 24: 133.
31. FRANK, H. S. & M. W. EVANS. 1945. J. Chem. Phys. 13: 507.

DIFFUSIONAL SPECIFICITY IN WATER*

I. Robert Fenichel and Samuel B. Horowitz

Laboratory of Cellular Biophysics, Albert Einstein Medical Center,
Philadelphia, Pa.

The usual starting point in discussions of diffusion in very dilute aqueous solutions is the Stokes-Einstein equation

$$D_{12} = \frac{kT}{6\pi\eta_1 r_2} \quad (1)$$

where η_1 is the solvent viscosity, r_2 the radius of the diffusing solute, and D_{12} its diffusion coefficient, or the more general Sutherland equation¹

$$D_{12} = \frac{kT}{6\pi\eta_1 r_2} \frac{1 + 3\eta_1/\beta_{12}r_2}{1 + 2\eta_1/\beta_{12}r_2} \quad (2)$$

where β_{12} is a coefficient of sliding friction.

Despite the limitations inherent in the derivation of these equations, they provide a fair description of diffusion of a large number of solutes in water. Quite good correlations of this data have been obtained by several equations of similar form, such as that of Wilke and Chang.²

$$D_{12} = \text{const} \frac{T}{\eta_1 V_{12}^{1/3}} \quad (3)$$

where V_{12} is the solute molar volume.

It is not commonly realized that the success of these equations is, in the light of current ideas of the equilibrium properties of liquid water, anomalous. The striking feature in Equations 1-3 is that, among different solutes, D_{12} depends on size only. In the derivation of Equation 1 for large solutes, this dependence is natural, since it is assumed that a large solute will carry an immobilized water shell, with shear occurring only between water molecules. In the case of small solutes, no shell exists,³ and a dependence of D_{12} on size alone implies that water-solute interactions are independent of the chemical composition of the solute. Both theory and experiment⁴ show that, even in the gaseous state, such independence is to be expected only if solvent and solute molecules behave like hard, perfectly elastic spheres. There is overwhelming evidence, from studies of the equilibrium properties of water and aqueous solutions, that a description in terms of a hard sphere model is inadequate. Strong, highly directional attractive forces — hydrogen bonds — exist in water, and solutes differ in their ability to form H-bonds with water molecules. One would

*This work was supported in part by National Science Foundation Research Grant GB 1794 and by Public Health Service Research Grant GM 11070 from the Division of General Medical Sciences.

expect this variation to be reflected in D_{12} . Why, then, do Equations 1 and 3 fit the data for water so well?

An answer to this question is suggested by a comparative study of diffusion in parallel solvent systems, one containing water, and the other, formamide. In this study the self-diffusion coefficients, at very low concentration, of a variety of solutes were determined in swollen dextran gels containing about 80 per cent formamide or water. Details of technique and tabulations of experimental data have been presented elsewhere.⁵ Comparison of the data in water-swollen gels with that available in liquid water showed the effect of the dextran matrix to be a constant factor independent of solute species:

$$D_{12} = 0.65 D_{11, \text{pure}} \quad (4)$$

The same will be assumed for the formamide gels. The data, corrected for this factor, may then be considered in terms of a frictional coefficient f_{12} , given by

$$D_{12} = \frac{kT}{f_{12}\eta_1 r_2} \quad (5)$$

where η_1 is taken as the viscosity of pure formamide or water.

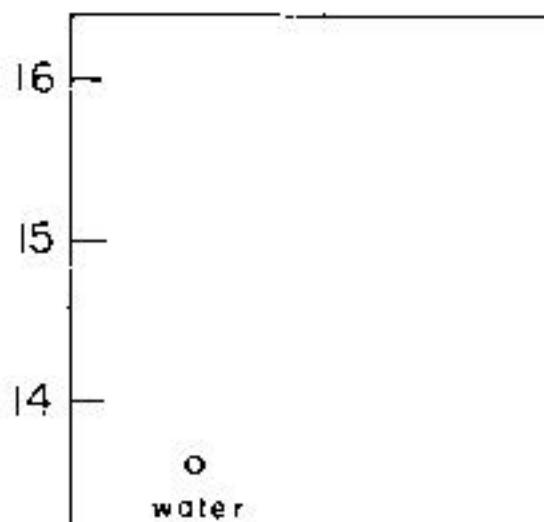
The frictional coefficient f_{12} as defined by Equation 5 incorporates the contributions to the overall frictional resistance not described by the solvent viscosity, η_1 , and the reciprocal first-power dependence on solute radius, r_2 . Experimentally, f_{12} is found to vary, and this is expected on theoretical grounds.

A number of studies have shown that, as the size of the diffusing molecule relative to that of the solvent increases, the value of f_{12} increases.^{6,7} For very large solutes, f_{12} has a value of about 6π ; in self-diffusion in the pure liquid, in which the equation

$$D_1 = \frac{kT}{f_{11}\eta_1 r_1} \quad (6)$$

replaces Equation 5, the value of f_{11} is approximately 4π , the Sutherland value for $\beta = 0$; for solutes smaller than the solvent a smaller value yet is observed.⁸ The origin of this variation with size is suggested by kinetic theory, in which molecular collisions and therefore transport coefficients are dependent upon molecular cross-sections, r_1^2 , rather than radius, r_1 . Also, the larger r_2 relative to r_1 (the molecular radius of the solvent), the greater the probability of multibody collisions; this also will make f_{12} an increasing function of r_2 . The dimensions of D require that r_2 enters as an inverse first power in Equation 5; the additional dependence of f_{12} on r_2 must therefore be in terms of a reduced radius. The constancy of f_{11} observed in the self diffusion of pure liquids, over a wide range of values of r_1 , supports the idea that the appropriate reduced radius is r_2/r_1 .

The coefficient f_{12} also reflects and solvent molecules which are d The solvent viscosity, η_1 , is intr assumption that the unit process are the same in diffusion and visco tially correct for self diffusion in of f_{11} .^{3,4} In the diffusion of solutes f_{12} will reflect differences between interactions, reduced, in part, to Equation 5. The stronger the solut solvent interactions, the larger w r_2/r_1 should, therefore, reflect bo



Fenichel & Horowitz:

and the specific variation due to the character of the solvent.

In FIGURE 1, data for diffusion of 1% dextran gels are presented as f_{12} , calculated from Equation 6, as a function of r_2/r_1 . Values of molar volumes at 20°C., V_0 , using the

$$r = \frac{1}{2} \left(\frac{V_0}{N_A} \right)^{1/3}$$

where N_A is Avogadro's number.*

The striking feature of FIGURE 1 is the nature of the diffusing solute. At any given value of r_2/r_1 , the greater the H-bonding ability of the solute, the greater the strength¹⁰ of H-bonding groups. Acetone, which has no H-bonding acceptors which are unable to donate, has the smallest values of f_{12} . The alcohols have the largest alcohol studied (1-pentanol) has the largest values of f_{12} . Only the solutes able to form strong H-bonds — water, urea, thiourea, and glycerol — have f_{12} values near unity.

A general increase in f_{12} with r_2/r_1 can be seen most clearly among the alcohols, water, urea, thiourea, glycerol. How-

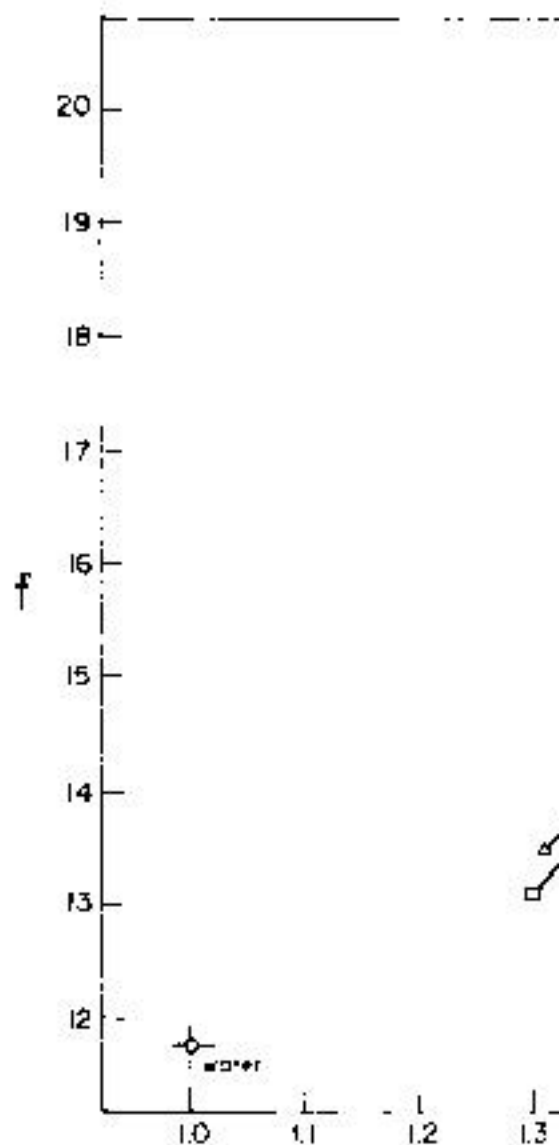


FIGURE 2. Frictional coefficients, f , versus the ratio of r_2/r_1 . The values of r_2/r_1 for the various alcohols are as in FIGURE 1.

Fenichel & Horowitz:

tures. Secondly, a close correlation can be found between the entropy of vaporization of the solute and the interaction parameter, which strongly reflects iceberg formation.

Because of the influence of iceberg formation on the interaction parameters, it is of interest to consider how the interactions depend on contributions from both H-bonding and non-H-bonding sites. A reciprocal relation, however, exists between the number of H-bonding groups and the number of non-H-bonding groups of equal size, the more H-bonding groups there are, the fewer non-H-bonding groups there are, vice versa. Because of this reciprocal relation, the interaction parameters are not small even though the interactions strengths are.

The solute interactions in water can be compared by reference to the comparison of FIGURES 1 and 2. The solutes common to both systems, the alcohols, are shifted upward relative to f_{11} , in general, in the same direction. This shift is consistent with the role of icebergs in the formation of the solvation shell. The shift is not the same among all of the alcohols, however. The ether is shifted more than the ester and ketone. These shifts are consistent with the data on ΔS_v of Frank and Evans. The alcohols with the largest van der Waals radius, the alcohols are better icebergs than the ester and ketone. The positions of the alcohols, then, reflect both the better H-bonding interactions, as indicated from the formamide data, and their better solvation, as indicated by the shifts in the equilibrium data.

process. Attention is merely shifted of the principal problems in the traditional approach to liquid theory, the "gas" model being more readily adaptable to fluid theory than the "lattice". $D\eta \propto kT/r$ is derivable from the former, while the latter, on the other hand, lattice theories more naturally lead to the conclusion that viscosity, fluidity and diffusion are activated processes with exponential temperature dependence.

The problem, then, is two-sided. On the one hand, the Stokes-Einstein behavior of water is typical of a solid-like medium, the Stokes-Einstein behavior being typical of a liquid-like medium. Since the work of Bernal and Fowler, it has been known that water has liquid water as having, in greater or lesser degree, some of the structural features of a solid-like medium. The extent of structural order in water is related to the integrity of the structure of the hydrogen bonds. As solid-like it must be, so as to permit the formation of a network of hydrogen bonds. Descriptions may, to some extent, be given of the behavior of water molecules in terms of a liquid-state model, they nonetheless exhibit differences in the behavior of water molecules under different conditions. For example, in the "frozen" state, the viscosity of water is

Fenichel & Horowitz:

ionic hydration in salt solutions. An enthalpy by "two-state" ideas of the structuring, perhaps on the order of kT , can produce transport properties. The extent to which this scopically depends upon the stability of solvation, relative to those in pure water. The strength of the interaction, but by the component. Moreover, (using again the such interactions, the clusters becomescopic transport behavior would tend to the "gas-like" extreme. Inertial stabilizat like" behavior, are in fact seen in systems which are, in a sense, a large-scale a system.

1. SUTHERLAND, G. B. B. M. 1905. Phil. M.
2. WILKE, C. R. & P. CHANG. 1955. Am.
3. DULLIEN, F. A. L. 1963. Trans. Farada
4. HIRSCHFELDER, J. O., C. F. CURTISS
of Gases and Liquids. J. Wiley & S
5. HOROWITZ, S. B. & I. R. FENICHEL. 1
6. LONGSWORTH, L. G. 1955. In Electrical
T. Shedlovsky, Ed. : 225. J. Wiley
7. POLSON, A. 1950. J. Phys. Colloid Chem.
8. HIMMELBLAU, D. M. 1964. Chem. Rev.
9. HORN, E. 1964. *Advances in Colloid and*

BONDS IN WATER AND

T. G.

T. G. Owe Berg, In

Intr

The molecules in liquid as well as gaseous water, are held together by bonds. The bond strength, as measured by the heat of vaporization per mole for liquid water and 12 kcal./mole from a difference in the electronic energy, is about 100 kcal./mole as compared to gaseous water and 10 kcal./mole which may amount to two or three times as much. These bonds are generally referred to as hydrogen bonds.

In aqueous solutions, the bonds between water molecules are broken and the heat of water vaporization is released. It appears that the solute may affect the breaking of the bonds by changing the electronic energy. There are some solutes which combine chemically with water to form new species. Thus, SO_3 gives H_2SO_4 with the loss of a molecule of water.

It follows from this example and many others that aqueous solutions are strongly affected by the presence of solutes.

Owe Berg: Bond

on the basis of the constituent properties can be determined empirically only, e.g. The treatment of these properties in empirical, although, of course, the structures should agree among themselves and with properties as well as with general laws.

The Structure of

The coalescence of two water drops through the formation of intermolecular bonds. A study of the coalescence process may intermolecular bonds in water. Such a

Two drops were mounted on thin platinum wires. A voltage was applied between the wires and the assembly was photographed by high speed photography. FIGURE 1 shows two typical frames. In one frame the contact surface is flattened as a result of pressure. In the other frame, a narrow

LIGHT
CAMERA

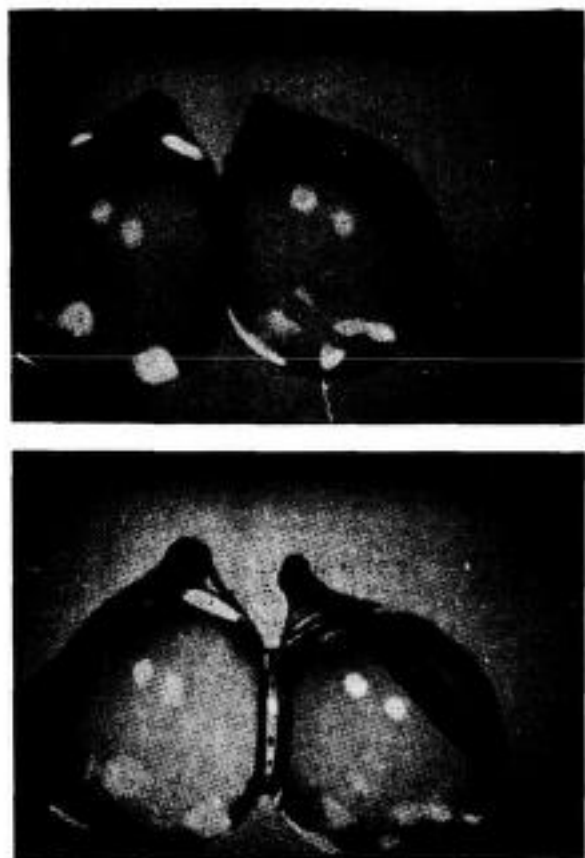
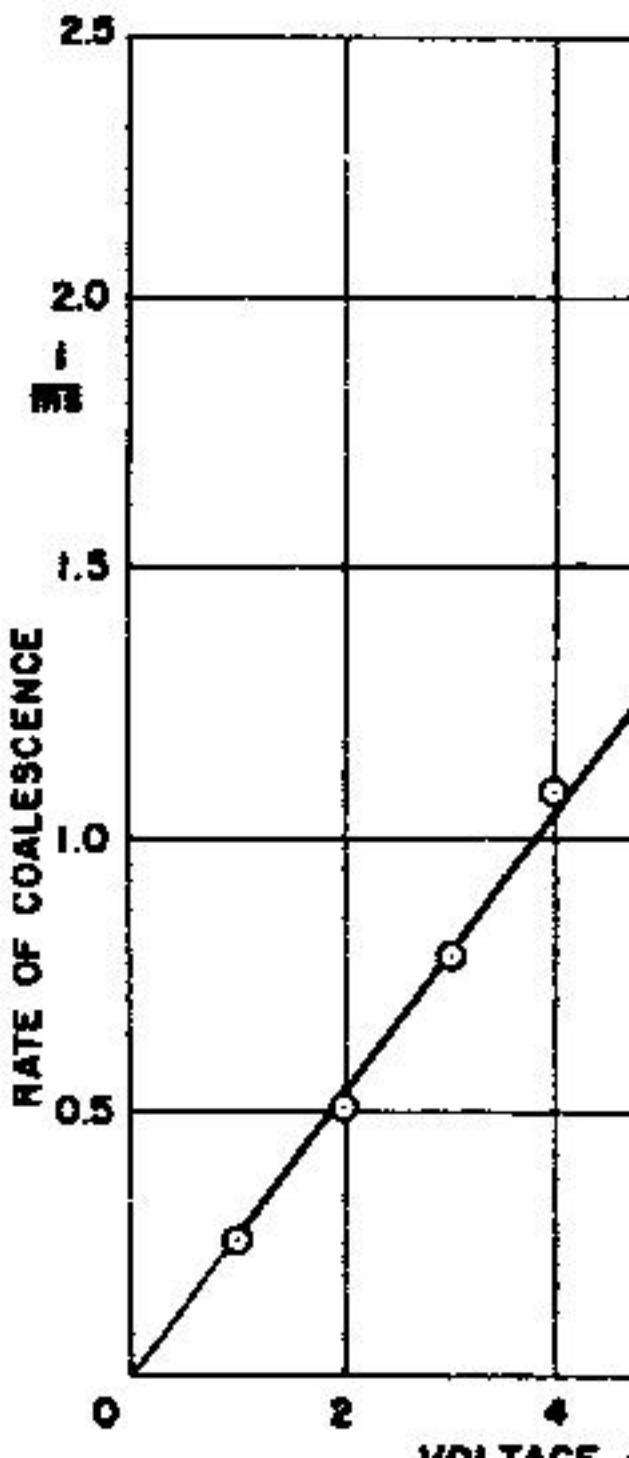


FIGURE 2. Flattening of drops and appearance of lens in coalescence.

face. This lens widens in later frames. The appearance of the lens is indication of coalescence.

The time delay t , of the order of 0.1 to 1 ms. in our experiments, between contact and coalescence was measured at various voltages V , between 1 and 10 volts. The product tV was found to be a constant as shown in FIGURE 3. Repeating the experiment with various alcohols instead of water, it was found that the product $tV \sqrt{\epsilon - 1}$ is the same constant for all these liquids, ϵ denoting the dielectric constant of the liquid. The time delay t depends thus upon the product of the induced dipole moment $\mu = \sqrt{\epsilon - 1}$ of the bond and the applied electric field. Hence, coalescence is effected by the orientation of bond dipoles in the direction of the electric field across the interface. A similar case is encountered in electrolytic conduction, discussed later. In this case, transport of electricity is effected by charge transfer along intermolecular bonds, rate-determining being the

Owe Berg: Bo



been determined by x-ray diffraction, the H₂O molecule being surrounded by four H₂O molecules being located at the vertices of a regular tetrahedron.

There is x-ray evidence to the effect that each water molecule is bonded to four in liquid water too.¹⁷ The small difference in coordination number in liquid water is thus five. Let us consider aggregates of five H₂O molecules, where each molecule is bonded to four others, although they are relatively far from one another. This model permits us to calculate the entropy of vaporization.

The entropy of vaporization is the difference between the entropy of liquid and gaseous water. This difference is due to the permutations of 10 hydrogen atoms among the 10 positions of two hydrogen atoms of five individual molecules.

$$\Delta S = \frac{1}{5} R \ln$$

This compares very well with the experimental value.

The entropy of fusion is also readily calculated by this same model. In liquid water, a molecule A is bonded to four molecules B, at the vertices of a regular tetrahedron. The molecules B are bonded to one another at the centers of the faces of the tetrahedron.

Owe Berg: Bond

mined by the structure and is, indeed, a function of the structure.

It is clear that this bonding in liquid water is characterized by considerable bond strain as compared to the solid state. The measure of this strain energy is the heat of fusion.

Electrical Conduction

Electrical conduction in aqueous solutions may be considered as the propagation of an electronic wave through the solvent. This mechanism, which seems to be the most probable, was proposed by von Grotthuss⁹ in 1806. In this mechanism the conduction process may conceivably be one among the various mechanisms of bond stretching in the direction of the applied field. It is the rate-determining step in the propagation of the oriented bond. An analysis of the mechanism leads to the following expression for the rate-determining step:

If c is the number of effective bonds per unit volume, n the number of dipoles oriented in the direction of the field, and ϵ the activation energy,

$$c \frac{\mu E}{3 kT} e^{-\epsilon/kT}$$

where ϵ denotes the activation energy, μ the dipole moment, k the Boltzmann constant, T the absolute temperature, and e the charge transferred, the current density J is given by

are the same for these various solutes and also for all concentrations of the solutions. Hence, the rate-determining step is the orientation of a free H₂O molecule in the liquid.

The process may be studied in further detail by an analysis of the entropy ΔS . Taking the equivalent conductivity

$$\Delta = \frac{\kappa}{c} \quad (8)$$

formula (6) gives

$$\ln \frac{\Delta}{\Delta_\infty} = \frac{\Delta S}{R} - \frac{\Delta S_\infty}{R} - \frac{\Delta S'}{R} \quad (9)$$

the subscript ∞ denoting infinite dilution. Plots of $\ln \Delta/\Delta_\infty$ against the mole fraction of solute are straight lines for all aqueous solutions for which data are available. The linear plot holds for NaCl solutions in the

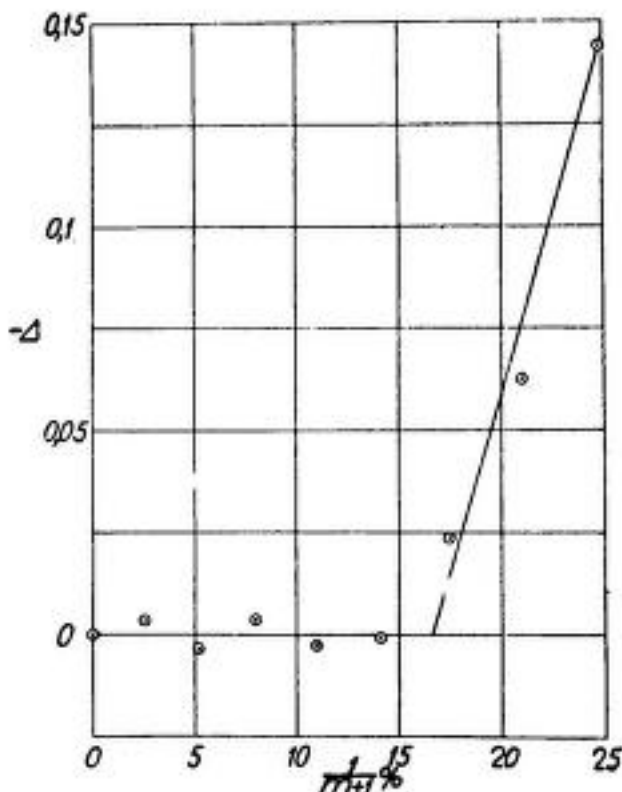


FIGURE 4. The plot of $\ln \Delta$ against the mole fraction $\frac{1}{m+1}$ of solute is a straight line. The deviation Δ is plotted against $\frac{1}{m+1}$ for HCl at 15° on the data of Kohlrausch.¹¹

Owe Berg: Bon

entire range of solubility, for HCl solutions up to 10 N solutions. FIGURE the straight line for HCl and HClO₄ of solute.

For HCl and HNO₃ solutions, which fore convenient to treat in this short

$$\text{HCl: } \ln \frac{\Delta}{\Delta_\infty} = 0.0001$$

$$\text{HNO}_3: \ln \frac{\Delta}{\Delta_\infty} = -0.04$$

In these formulae, m denotes the number of solute.

Let us consider an H₂O molecule that and that has all its bonds with its four these neighbor molecules is a solute molecule. The probability that the fraction the solute molecule is 1/4; the probability H₂O molecule is 3/4. The probability both these events is 1/4 × 3/4 = 3/16.

or, per H atom

$$\Delta S_o = \frac{1}{2} R \ln$$

The data give $\Delta S_o = R \ln 0.42^{10}$

$$\Delta S'$$

when N is the number of H_2O molecules.

This number is N = 10 for HCl and 12 for HNO_3 . Using these values and ΔS_o from formula (1)

$$HCl: \ln \frac{\Delta}{\Delta_x} = -0.42$$

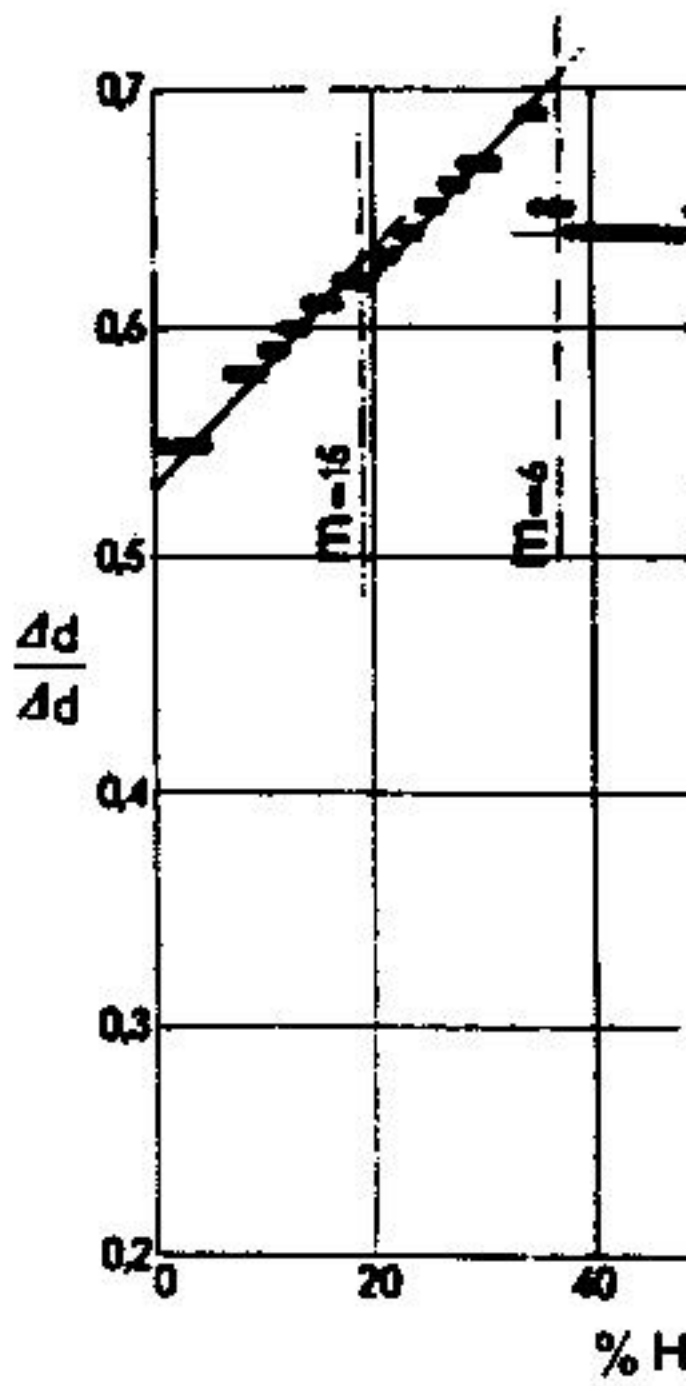
$$HNO_3: \ln \frac{\Delta}{\Delta_x} = -0.42$$

in agreement with the empirical formula (1).

It follows from this analysis that the rate at which a solute passes through an aqueous solution is determined by the concentration of water molecules.

An H_2O molecule adjacent to a solute molecule has its neighbors broken and is reoriented by the electric field.

Owe Berg: Born



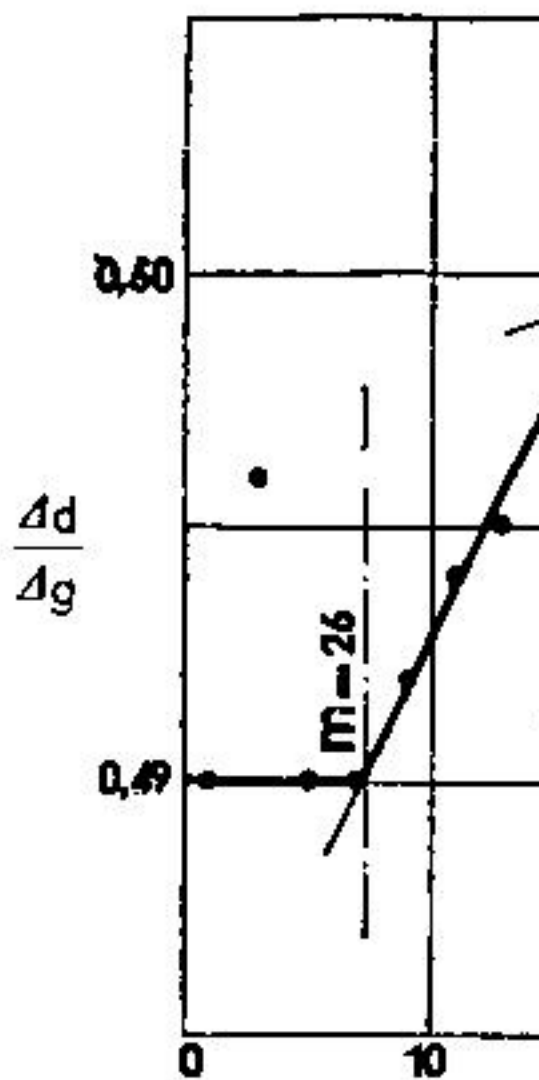


FIGURE 7. The derivative $\frac{\Delta d}{\Delta g}$ of the data of Åkeröf and Teare.¹⁵

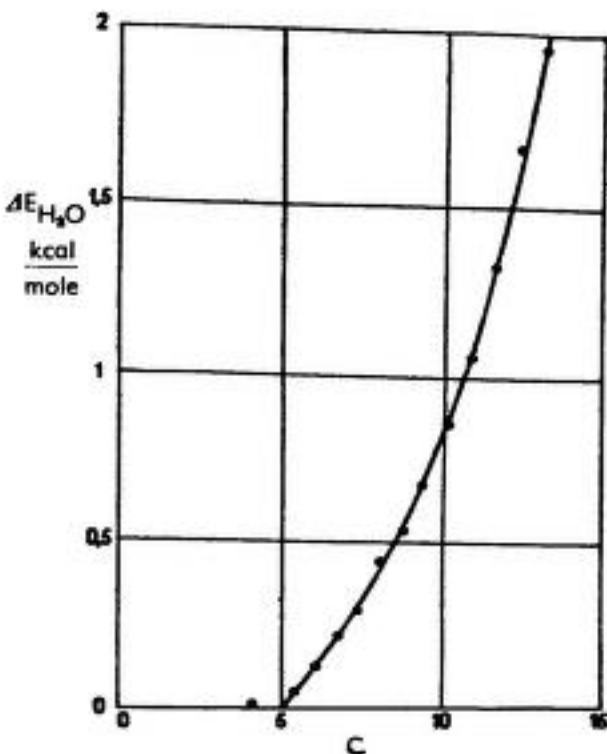


FIGURE 8. The relative heat of water vaporization ΔE in HCl solutions as a function of the concentration c from the vapor pressure data of Yannakis.¹¹

For the ideal solution, the former definition gives

$$W = \frac{m}{m+1} \quad (21)$$

i.e., the mole fraction of the solvent. The formula

$$p = \frac{m}{m+1} = 1 - \frac{1}{m+1} \quad (22)$$

is known as Raoult's law.

A plot of p against $1/(m+1)$ very rarely has unit slope. Thus, for HCl solutions the data give

$$p = 1 - \frac{3}{m+1} = \frac{m-2}{m+1}, m > 26 \quad (23)$$

This formula holds for $m > 26$ only. For $m < 26$, there is a deviation Δp from this formula

$$\Delta p = p - \frac{m-2}{m+1} \quad (24)$$

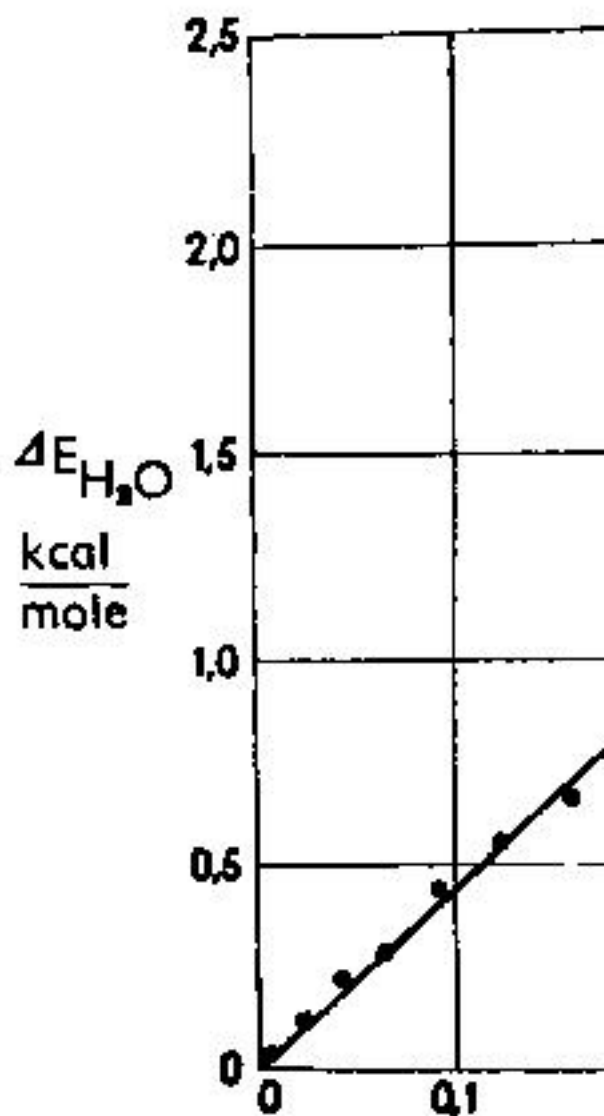


FIGURE 9. The data in FIGURE

6
Owe Berg: Bon

dicates that

$$\Delta p \approx -\frac{3}{100} \frac{26-m}{m+1},$$

and that

$$p = \frac{3}{100} \frac{26-m}{m+1} + \left(\frac{1}{m+1} \right)$$

The function

$$= \Delta p + \frac{3}{100} \frac{26-m}{m+1} +$$

is plotted against $\frac{1-\alpha}{m+1}$ in FIGURE 11

$$\begin{cases} \alpha = \frac{m}{5}, \\ \alpha = 1, \end{cases}$$

The data suggest a straight line through
2. Hence,

$$\Delta p = \frac{3}{100} \frac{26-m}{m+1} + \left(\frac{1}{m+1} \right)$$

Salt Solu

A brief reference will be made in th

SOLUBILITY OF

HCl mol./100 g.	NaCl solution	HCl mol./100 g.
0.0000	4.513	0.000
0.0438	4.474	0.096
0.0870	4.433	0.191
0.1756	4.346	0.385
0.3610	4.151	0.787
0.9263	3.605	1.993
1.6677	2.889	3.524
2.6740	2.055	5.552
3.5670	1.408	7.320

At saturation, a solution is at equilibrium with its solid phase; the energy difference is then zero,

$$\Delta F = \Delta H - T\Delta S$$

The NaCl solution is peculiar by having ΔS close to zero. Hence, there is little change in entropy when the solution and the precipitate. The

Owe Berg: Bon

$$\Delta S = 10 R \ln 2$$

The heat of neutralization at 18°C. is 13.5 cal./g. in heat content and the corresponding

$$\frac{\Delta E}{T} = \frac{13800}{291} = 47$$

Thus, the Second Law of Thermodynamics applies as for dissolution-precipitation at saturation.

Applications t

Chemical reactions in aqueous solution of inter- and intramolecular bonds, effected, by bonds between H_2O molecules, the fact that a redistribution of bonds does occur. Whether it occurs or not, actions results, are decided by the peculiarities of the reaction. An instance of such a process is the reaction of NaOH discussed previously.

Dilute and concentrated acid solution may form nitrates, concentrated nitric acid dissolves

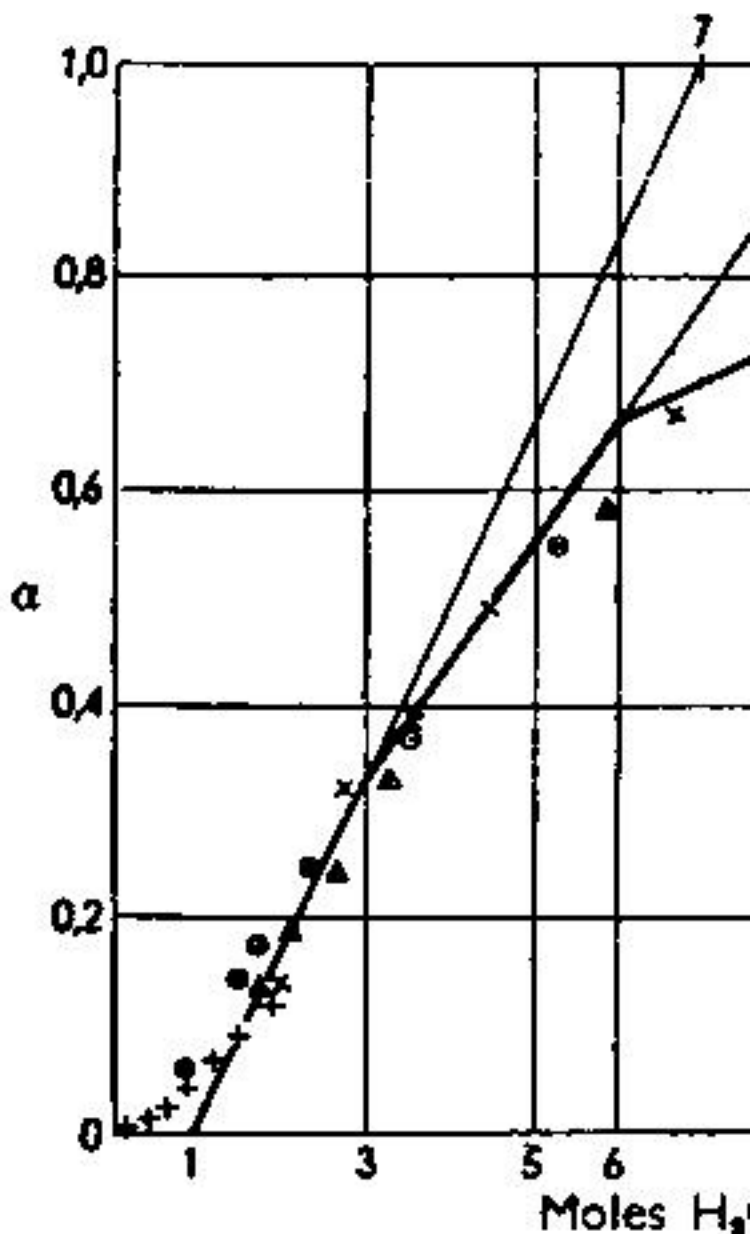


FIGURE 12. The degree of dissociation calculated from the structure. The data at 25°C are taken from Sen,²¹ Dalmon²² and Rao.²³

Owe Berg: Bon

done for various acids, e.g., HNO_3 ,¹⁷ H_2SO_4 ,¹⁸ and HCl .¹⁹ The result of such a calculation is shown in Table I, together with the results of Raman measurements. The distribution coefficients are given among these data. They agree very well with the values calculated by us.¹³ Figure 13 shows a plot of the rate of dissolution of the concentration of undissociated acid. The points plotted on the abscissa were calculated from the structural calculations.

Conclusion

It follows from this brief summary that the properties of concentrated aqueous solutions that they are comparable with the properties of the pure components of the mixture, i.e., the distribution of the components among the different phases with respect to each other. The structure of the molecules and their properties, particularly vapor pressure and solubility, may be derived from the properties of the pure components. Chemical properties may then be derived from the properties of the pure components. It should be added that the methods used in this paper have been selected for convenience of treatment. It is evident that other systems may be considered, and the method used does not affect the basic principles. It is evident that the properties of concentrated aqueous solutions are similar to those of dilute aqueous solutions.

20. CHÉDIN, J. 1937. Ann. Chimie 8: 2.
21. REDLICH, O. & J. BIEGELEISEN. 1.
22. DALMON, R. 1943. Mém. Serv. Chim. Min. 10: 1.
23. RAO, N. R. 1941. Indian J. Phys. 23: 1.
24. OWE BERG, T. G. 1951. Z. Anorg. A.

THE FORMATION OF IC INTERF

P. R. C

*U. S. Army Cold Regions Research
Hanover,*

INTRODU

Despite its rather obvious importance in metallurgical processes, the growth of surfaces has been studied very little, even to have been adequately described. The difficulties of face growth have been pointed out by S and confusing state of affairs in 1955. I gave little quantitative information and believe to be incorrect as will be developed. A qualitative description of some faces and some further review of the circumstances and here again inadequate formulation of hypotheses which seem ther experiment as will be shown. The

With this state of affairs, it has been possible to make an experimental study of the way in which ice grows on various surfaces of various kinds. As a part of this work, the principal structures which appear in the ice have been observed for three very different surfaces, and the growth velocities of the ice film have been measured at different face temperatures.

Two types of experiment will be described. In the first, a stream of water is passed horizontally from a vertical wall, so that it falls onto a horizontal surface to permit observation of the growth of the ice film. It is found that, although there is no initial ice film, there is a small amount of ice at the interface before appreciable growth begins. This is due to the fact that the temperature of the water is below the freezing point of the ice. The growth velocity of the ice film is determined by the temperature of the water, and the form of the ice film is determined by the temperature of the water and the temperature of the interface. The temperature of the interface is determined by the temperature of the water and the temperature of the ice film.

The second kind of experiment will be described. In this, the growth velocity of the initial layer of ice as it spreads over a horizontal surface is determined by observation from above of a horizontal surface. The growth velocity of the ice film is determined by the temperature of the water and the temperature of the interface. The temperature of the interface is determined by the temperature of the water and the temperature of the ice film. The form of the ice film is determined by the temperature of the water and the temperature of the interface. The interface can be determined by observing the growth velocity of the ice film.

VERTICAL WALL EXPERIMENTS

The vertical wall experiments were made in a large tank.

Camp: Ice Formation at

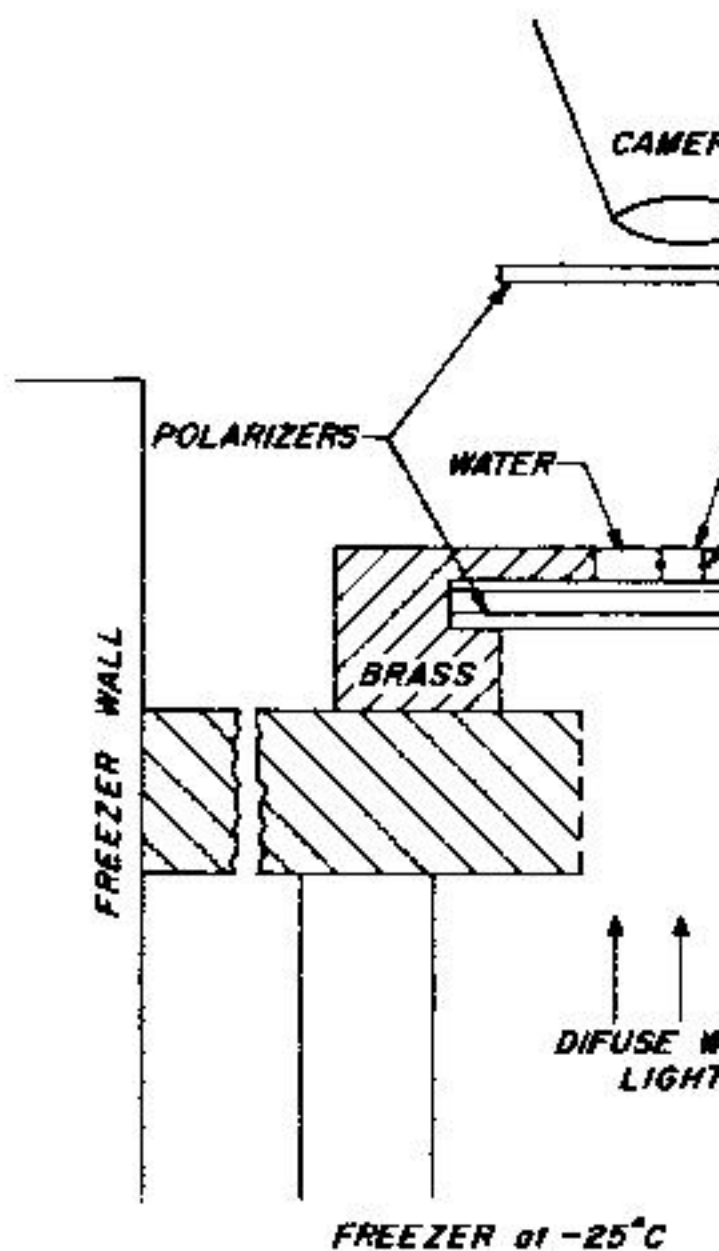


FIGURE 1. Apparatus used in the

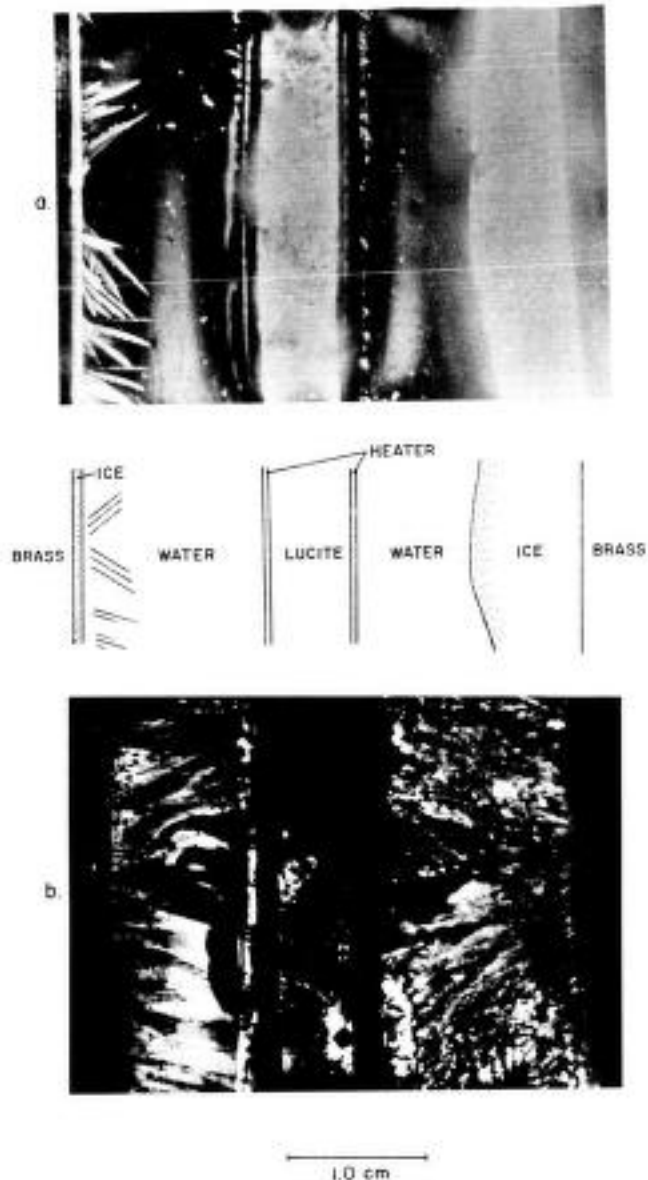


FIGURE 2. Different stages of development of ice in the vertical wall experiment. *Top left:* Dendrites have grown out into the water and an ice wall is just moving out from the brass. *Top right:* The dendrites have melted back and been overtaken by the advancing ice wall. *Bottom left and right:* The experiments of the top left and right after growth is complete.

Camp: Ice Formation at
gulfed the dendrites. FIGURE 2*b* shows
growth is nearly completed.

HORIZONTAL E

It was apparent from the vertical observations that the initial growth along the interface, is dependent upon a solid surface. Accordingly a horizontal experiment was devised to study its characteristics. The nature of the mechanism giving rise to this growth is unknown. However, the experiments seem to fall into three categories: electrical, chemical, and mechanical. Therefore, the materials chosen for the experiment were aluminum, glass, and two insulators one which is not wettable by water and one which is wettable by water. The apparatus used for all three experiments is shown in FIGURE 3. The apparatus used for aluminum is shown in FIGURE 3.

A heavy aluminum plate is mounted in a commercial chest-type freezer in which there is a fan. This acts as a cold plate of fairly uniform temperature. On this cold plate is mounted a rectangular block one-half inch milled out of a one-inch thick aluminum plate. A hole is bored vertically into the end of the plate accomodating a thermocouple probe to measure the surface temperature and horizontal growth.

Because air pockets, which inadvertently fall directly on the cold plate, lead to thermal coupling between the cold plate and the inner wall of the dish, the inner wall is burnished by light strokes to create a surface which is smooth without depolarization. The dish is viewed with plane polarized light directed through the ice at different angles and is photographed from above through the ice at different angles. Depolarization occurs even when the optic axis is parallel to the direction of polarization. In this way ice films only a few tenths of a millimeter thick are photographed. Multiple nucleation experiments show that the growth of ice did not extend appreciably beyond the boundaries of the nuclei.

The experiments were conducted in a dish 2 mm. in diameter and 2 mm. deep. The water was fairly constant temperature. (The water bath was used to vary the temperature of the water.) When the temperature of the water was reached, growth was initiated by the addition of a few drops of water. At temperatures close to 0°C., growth commences at the solid interface with an ice crystal.

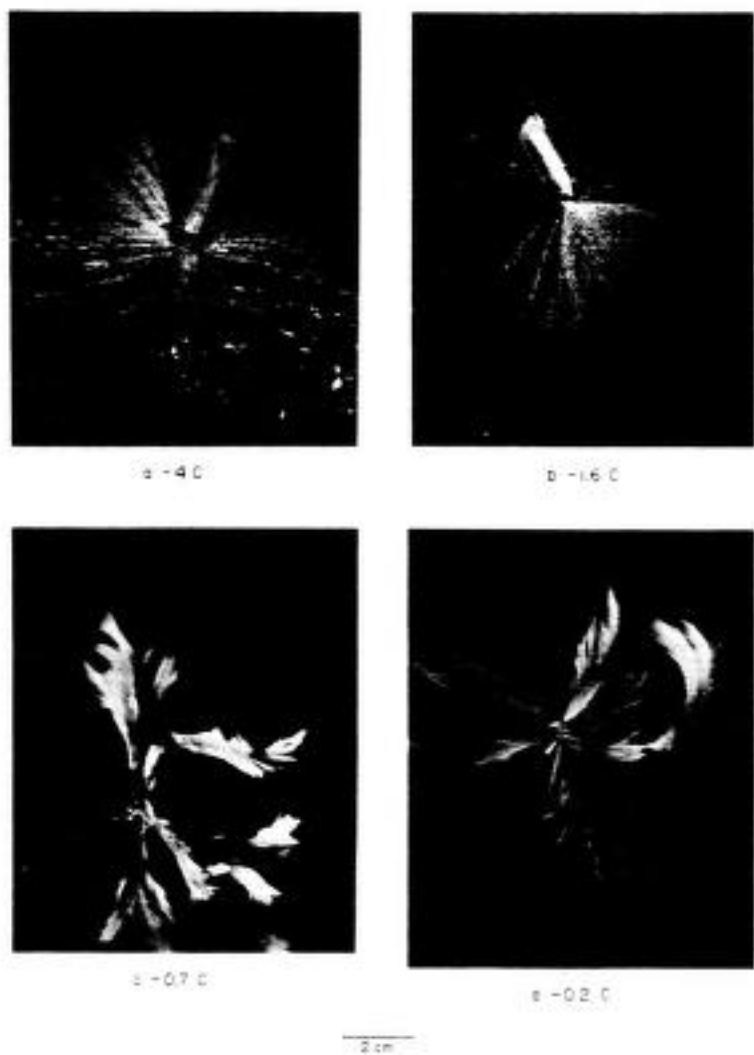


FIGURE 4. Growth structures appearing on aluminum at various temperatures, a. -4°C, b. -1.6°C, c. -0.7°C, d. -0.2°C. Arrows indicate the direction of c-axis in the seed crystal.

This is characterized by better defined tightly bound feathers for which the c-axis makes a low angle to the interface. In the intermediate range it is possible to favor one kind of growth or the other by using a seed with c parallel or perpendicular to the plate.

The velocities for both modes of growth were measured and the results are plotted in FIGURE 5. For the mode with the c-axis nearly perpendicular to the surface, the data are plotted as circles. For the other, the data are

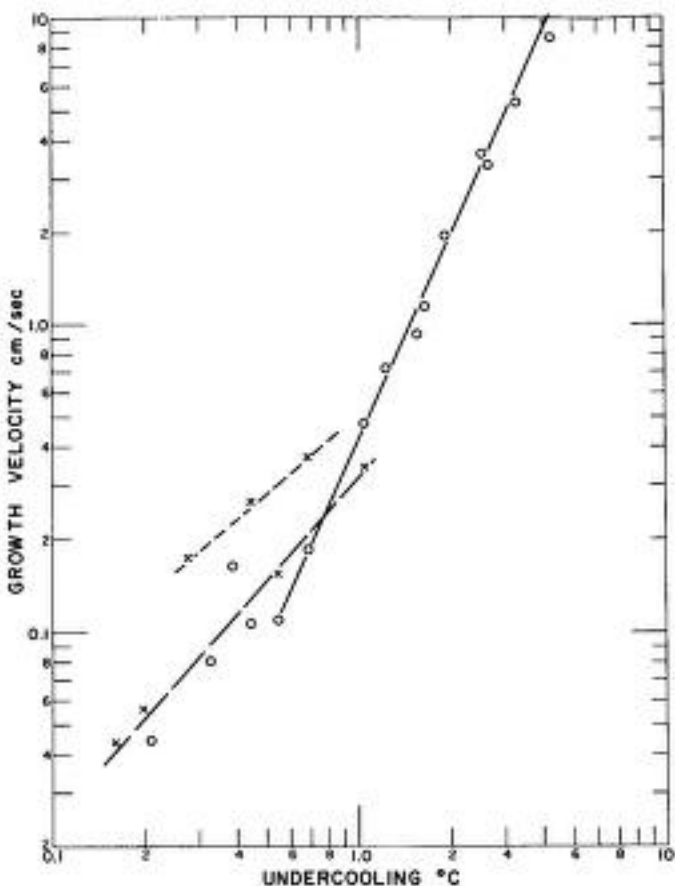


FIGURE 5. Growth velocity (cm./sec.) of ice on aluminum vs. undercooling (°C.). Circles indicate growth with c-axis nearly perpendicular to the interface. Crosses, x, indicate other modes for which the c-axis makes a small angle to the interface. (The points at 3.3°C. and 4.3°C. may be in error by ± 0.3 °C., the others by ± 0.1 °C.).

plotted as crosses. Within the limits of experimental error, the c perpendicular data can be summarized by

$$v = (0.42 \pm 0.1) \Delta t^{2.2 \pm 0.1} \text{ for } 5 > \Delta t > 0.8 \text{ °C.} \quad (1)$$

Where v is the growth velocity in cm./sec., Δt is the undercooling in °C. and t is the centigrade temperature. Above about -1 °C. there seems to be systematic departure from Equation 1. Although this is in a region in which experimental errors are large, we believe that the departure is real. It should be noted that in this temperature region the c perpendicular growth structure becomes more open and rounded than at lower temperatures.

Camp: Ice Formation at

The data for the low angle growth must be some parameter not considered important in determining the growth rate. It indicates the existence of at least two low angle growth mechanisms, indicated by the dashed lines in FIGURE 5. The crystal whose c-axis was in the plane of the interface, the structures grow along the interface at various angles to the seed of 0, 30, 45, 60 and 90 degrees. It is not clear whether a given curve might correspond to several such relations. Nevertheless, points belonging to a particular line on a plot of $\ln(\dot{V}/V_0)$ versus time for a given structure; the upper line resulting from a higher temperature than the lower.

However this may be, it is quite clear that the low angle growth mechanism has a rate which exceeds that for the high angle growth mechanism at low temperatures but which rises more slowly with temperature so that there is an opportunity to occur, either by delamination or by nucleation at a surface imperfection, at a temperature which is higher than the high angle growth mechanism at high temperatures. The cross over occurs at a temperature which is higher than the temperature at which the high angle growth mechanism becomes dominant. The final structure depends quite critically on the temperature at which the cross over occurs.

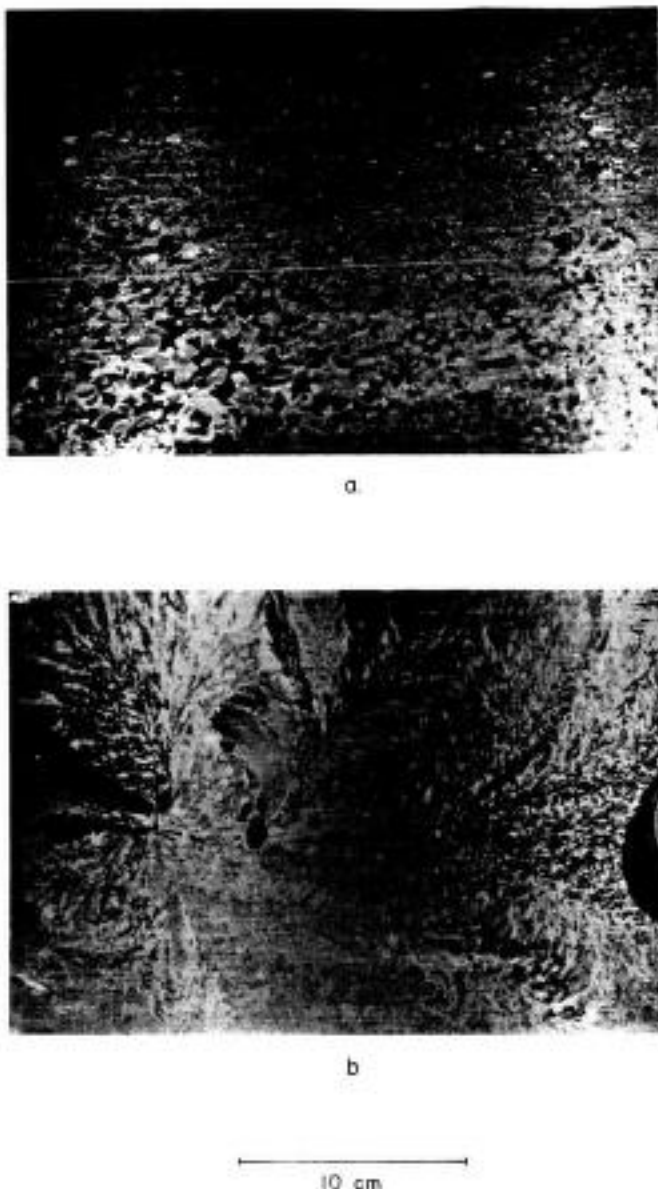


FIGURE 6. Grain development in the early stages of growth. (a) Same as FIGURE 4a but 22 minutes later. (b) Same as FIGURE 4c but 16 minutes later. In both the ice is about 3 mm. thick. Arrow indicates the direction of c-axis in the seed crystal.

Camp: Ice Formation at

thermal conductivity of lucite, it was decided to use aluminum chips instead of aluminum chips for thermal imbedding of the thermocouples in the lucite. With the chips we found it difficult to prevent temperature gradients from occurring. Also because of the low thermal conductivity we had to modify our method of imbedding thermocouples in the lucite, by using 0.5 x 0.5 cm. pieces of 5 mil brass sheet metal which were soldered inside of our lucite dish. The thickness of the brass sheet was 0.3 mm. The dish itself was made of 1/8" lucite and was painted black around it. The bottom (outside) of the dish was also painted black to provide a reflecting surface which would reflect most of the incident light.

The results for lucite are quite different from those obtained on aluminum. The characteristic structures are shown in Figures 1, 2, 3 and 4. At temperatures of -5.8, -2.6, -1.2 and -0.6°C. regular modes of ice formation are apparent. At -5.8°C. a mode parallel to the surface is dominant but the dendrites are somewhat different from those found on aluminum. There are at least two modes having c at a low angle. One is a very straight needle-shaped dendrite extending almost in a vertical plane. The second is a curved dendrite from which seems to spawn new curved

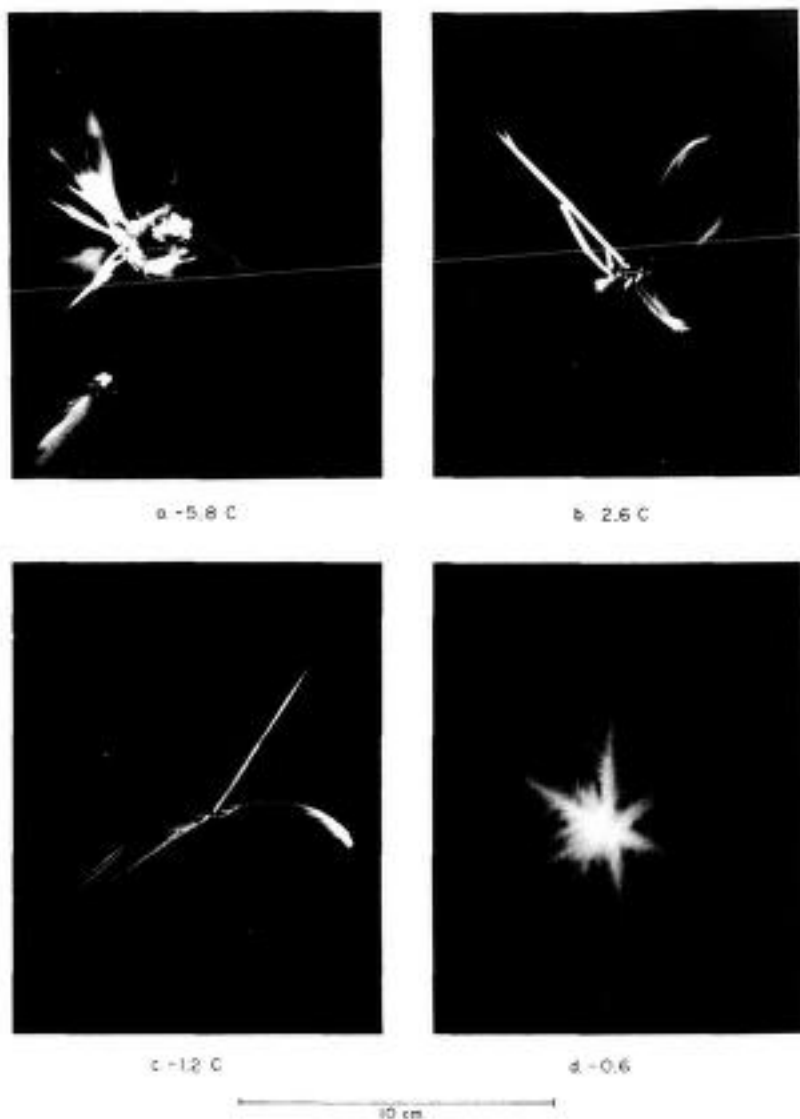


FIGURE 7. Growth structures appearing on lucite at various temperatures, (a) -5.8°C , (b) -2.6°C , (c) -1.2°C , (d) -0.6°C . In (b), the smaller straight member has been deliberately moved with a probe and broken in the middle as mentioned in the discussion. Arrows indicate the direction of *c*-axis in the seed crystal.



FIGURE 8. Later stages in the development of (a) FIGURE 7b (after 140 seconds) and (b) FIGURE 7c (after 15 minutes). Arrows indicate the direction of c-axis in the seed crystal.

of the northeast-southwest diagonal reproduction.

At somewhat smaller undercoolings, the growth rate appears to be the same (see FIGURE 7c). However, the top growth does not appear and the bottom growth shows thicker trunks and shorter secondary branches. Some of this should be evident in the photograph of FIGURE 7c, 15 minutes later.

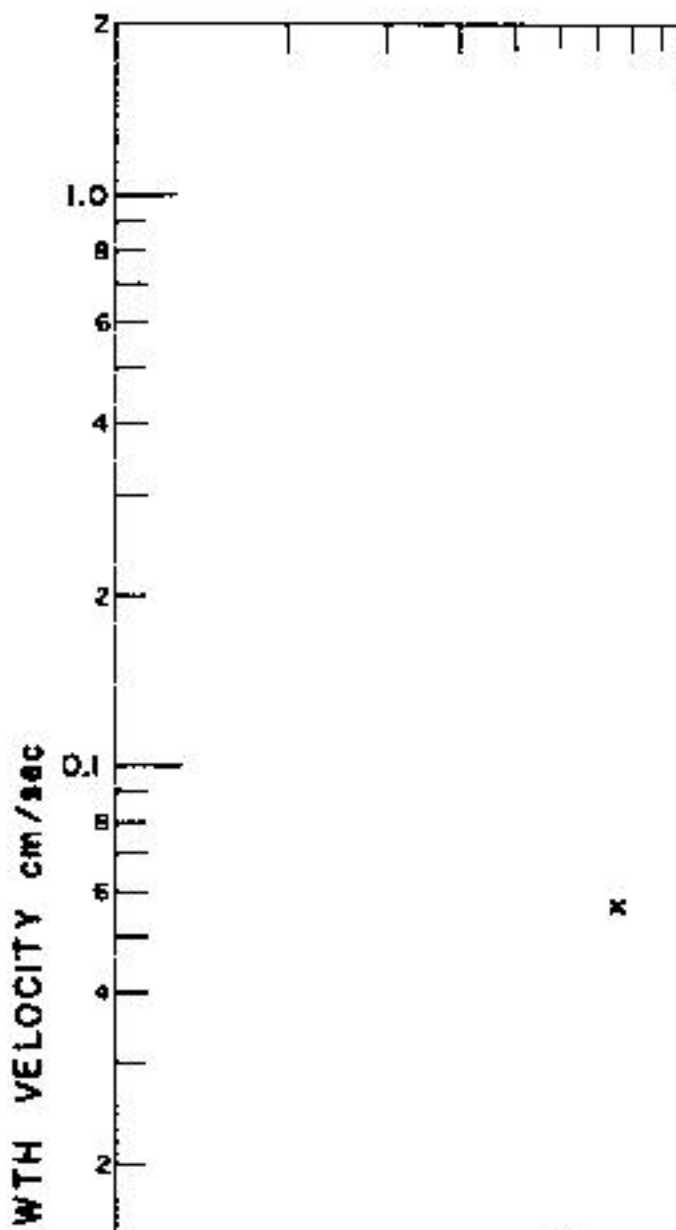
Finally at small undercoolings, the growth rate decreases rather quickly in a perpendicular to the interface direction (-0.6°C). In this same experiment, the growth rate does not show on the reproduction.

A set of rate experiments similar to those for the periclase-lucite with the results shown in FIGURE 8 were made at a distance of 1 mm from the interface, plotted as circle diameter versus velocity-temperature relation.

$$v = 9.2 (\pm 0.4) \times 10^{-3} T^{0.75}$$

over the temperature range -0.5 to -0.1°C . The data for the low angle growth modes are shown in FIGURE 9 represent the data for those for the curved blades. It is seen that the perpendicular structure grows much more slowly than the

Camp: Ice Formation at



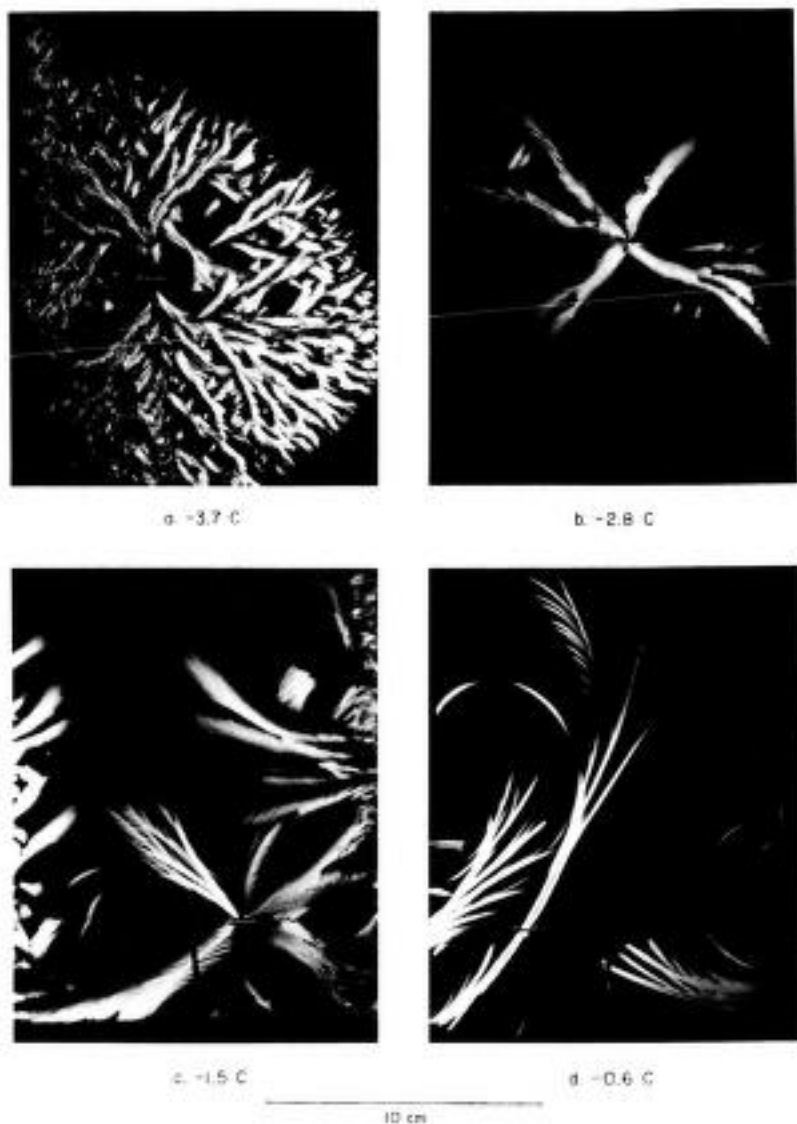


FIGURE 10. Growth appearing on glass at various temperatures: (a) -3.7 °C., (b) -2.8 °C., (c) -1.5 °C., (d) -0.6 °C. Arrows indicate the direction of c-axis in the seed crystal.

growth occurs producing the slightly more ordered structure of FIG. 11a which shows the sample of FIGURE 10a eleven minutes later.

A slight increase in temperature to -2.8 °C. brings about a fairly dramatic change. It is a little as if the picture at -3.7 °C. had been magnified. The predominant structure is still vinelike but much larger and more

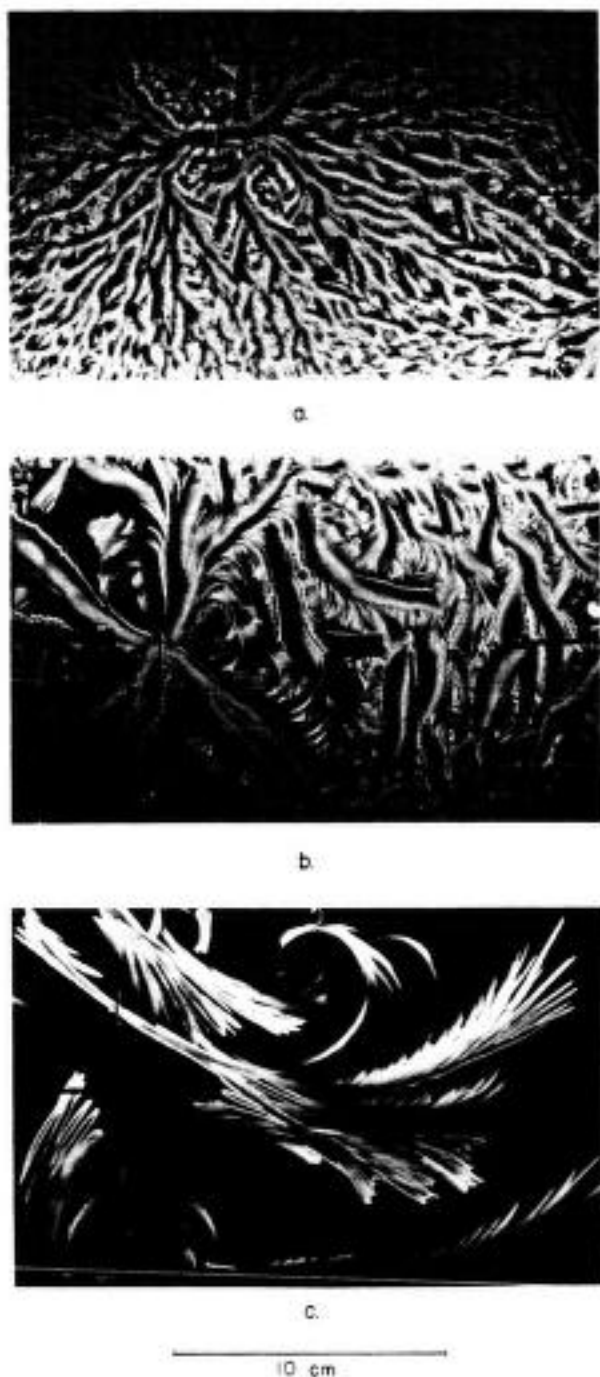


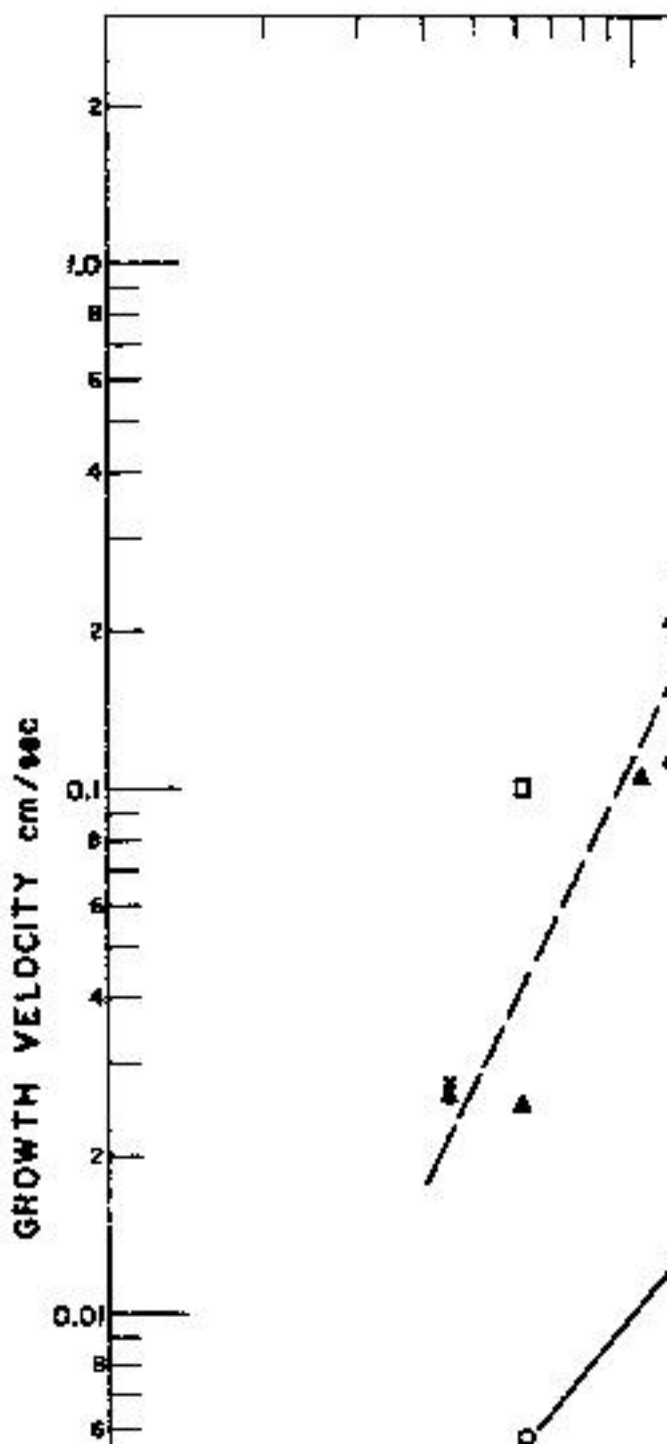
FIGURE 11. Later stages in the development of (a) FIGURE 10a (after 11 minutes), (b) FIGURE 10b (after seven minutes) and (c) FIGURE 10d (after three minutes). Arrows indicate the direction of c-axis in the seed crystal.

orderly. It is still hard to define the structure shown in FIGURE 11*b* taken seven minutes after the "bark" of the vine has peeled back. The area partly enclosed by these curves has been exposed to the interface.

At somewhat higher temperature the vine structure begins to take new form. The new growth, is made up of fine long-evaluated fibers which we have designated the "feathers" on both sides with short fine feathers growing in the direction of growth. These two types of structures are shown in FIGURE 11. As growth continues the vine structure and the feathers change as did the vine structure and the feathers which the c axis makes a high angle with the fiber axis.

At still higher temperatures, -0.1° C., the feathers become sharper and more magnified and take on a more definite structure. It becomes apparent that a long slim fiber is a needle or a needle-like structure. The needles present a similar problem. They appear to consist of circular arcs which must have their centers at the same point. Much less of the total surface becomes exposed to the interface and consequently more high angle

Camp: Ice Formation at



in the 0 to -5°C. range, winter is much more prosaic.

In considering the data of FIGURE 1, its somewhat tentative nature but to assign to a given structure a name so forth, because these forms themselves while we show points as straight may really be of the same species. To be able to resolve these matters the low angle growth by the dashed lines have given the most weight to the confidence. With the reservations concerning angle growth

$$v = 0.01 (\pm 0.003)$$

and for the low angle growth

$$v = 0.12 (\pm 0.03)$$

DISCUSSION

When water freezes on aluminum, heat is extracted through the solid, the sensible nucleation at the interface (either a layer of ice grows rapidly across it,

Camp: Ice Formation at

TABLE
RATE PARAMETERS ASSUMED

Surface material	a
High angle modes	
Aluminum	0.4
Lucite	0.0
Glass	0.0
Low angle modes*	
Aluminum, upper dashed line	
Aluminum, lower dashed line	
Lucite Δ	
Lucite x	
Glass (average)	
From Lindenmeyer ³	
Brass 3°C. t 1°C.	
Bulk Growth Hillig 1958 ^{8†}	
Growth ⊥ c	

that the kind of surface does indeed affect its rate. Even the low angle growth on flat sides by water seem to be effected when the edge is touching. In this connection it is interesting to note that on lucite at small undercoolings (about 10°) the film is rigidly bonded to the substrate and can be easily pushed off by pushing it with a glass probe. This is shown in the photograph where the tip of the shorter of the two needles moved and then broke in the process shown in the photograph.

Moreover, it is clear that the growth is affected (perhaps even largely) by the thermal gradient. For example, this is evident from the fact that the growth on lucite can be either greater or less than that on the temperature. (The two curves in Fig. 11 were obtained in preliminary experiments on a lucite substrate.) The very thin film of vacuum-deposited aluminum film is too small to have a large effect on the interface and yet the velocity of growth is greater than that on the clear side, the velocity being intermediate between that for plain lucite and that for the water-grown film.

It was mentioned in the introduc-

Camp: Ice Formation at V

curvature of a dendrite which makes interface is because the heat of fusion angle to the interface is somewhat tra growth is faster on the other side. We bei ing curved growth as being of special : two hypotheses with the following obs be sure of a somewhat different struc which the surface is a much better he growth as well as long straight growt poorer heat sink than glass. (3) In our half of which is covered by an evaporat which cross from one section to the oture on the aluminized section than on t growth on both lucite and glass, partic quently terminates in a perpendicular gr is less than that of the curved growth. (6) is higher than that of water and the cont (6) The curved blades are in contact thermal properties of the substrate can the blade joins it. Knight (FIGURE 4) make an obtuse angle with the base o In another experiment we have delibe

(several millimeters) and c-perpendicular to all three surfaces. A particularly Another contention is that the temperature important influence on the result indicates that for zero temperature is chaotic and for a large positive tends to become parallel to the interface. Temperature gradients were small (c produce a surface c-perpendicular to the substrate. We believe our experiments demonstrate that neither the thickness nor the temperature gradient at the moment to the structure of the interface. The temperature of the interface is important in the manner of nucleation is impos-

ACKNOWLEDGMENT

It is a pleasure to thank Mr. C. L. Smith and Mr. J. E. Goss for their help in conducting these experiments. We also thank Walter Kiszenick for preparing the

REFERENCES

1. SHUMSKI, P. A. 1955. The growth

by insertion of an ice single crystal of selected orientation into the free surface of a water sample uniformly supercooled. As temperatures above about -5°C. it has been found that growth follows the orientation of the nucleating crystal, in the form of thin dendrites (with 60° branches) growing parallel to the basal plane of the ice structure. Below this temperature, dendrites grow from the site of nucleation, in several directions, not necessarily related to the orientation of the seed crystal. With decrease of temperature, dendrite arms become narrower and more closely spaced, being $\sim 10\mu$ at -10°C. The crystallization velocity increases approximately as the square of supercooling being $\sim 30 \text{ cm.sec.}^{-1}$ at -20°C. The presence of a solute has two effects: to change the habit of growth (relative velocity along different crystallographic directions) and to change (lower) the velocity of growth—molecules have a diffusion barrier to growth. When dendrites meet a solid surface (FIGURE 1) the form of growth changes strikingly to that already shown by Camp, and if the supercooling is sufficiently great, curved growth, and nucleation of new crystal growth directions may occur in addition. The surface may act in two ways—as a sink for release of latent heat and as a site to nucleate new crystals at the

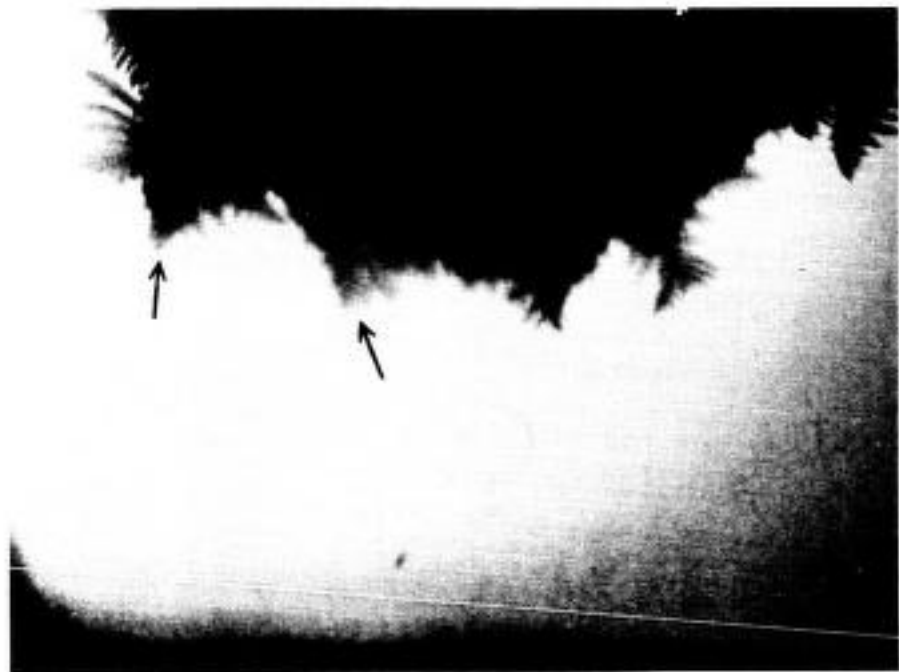


FIGURE 1a. Crystal growth in rabbit serum at -5°C., nucleated by a single crystal in the upper free surface. Growth (arrowed) in the bulk of the liquid occurs as dendrites with straight arms.



FIGURE 1b. As the dendrites meet the outer glass walls the velocity of propagation increases and the growth becomes curved.

interface with the crystal which grows from the bulk liquid. The crystallization velocity is therefore greater on the surface than in the bulk of the liquid.

In any closed system — a water or solution drop in air, a plant or animal cell — the final form of the ice (its spacial distribution) and its petrographic structure, will depend critically on the amount, and spacial distribution of supercooling before nucleation took place, and also on the distribution of nucleation sites. The form of crystals which grow first, into the supercooled liquid, will depend on the supercooling, and on the thermal and crystallographic characteristics of the membrane surface where nucleation occurs. Whether the growth is characteristic of the surface or the bulk liquid will also depend on the supercooling and, particularly, the cell dimensions. The second stage of freezing will depend entirely on the efficiency with which heat can be removed and how the shell of ice growing inwards from the periphery interacts with the initial growth of fine dendrites— separating the solute into small regions with dimensions related to dendrite size, which would be equivalent to the final spacial distribution of any eutectic which might form. Previous work has not been concerned with investigating cell damage in relation to this initial distribution of

Camp: Ice Formation at V

ice — (which may change subsequently) like to suggest that a full understanding of cell damage will not be achieved until the freezing processes have been made.

As has been discussed in the text, one idea that the surface acts merely as a nucleation. Interfacial growth occurs on better as a heat sink than is water and surface layers of foreign substances (which alter the velocity of interfacial growth) accept interfacial free energy as importantistics of interfacial growth and probably of the interfacial forces involved.

ELECTRICAL PROPER

H. D.

*Electromedical Division, Moore
University of Pennsylvania*

Water bound to the surface of macromolecules may be considered as a physical properties of a macromolecule which cannot be accounted for by the properties of the individual macromolecules. I shall report here some of the results of our studies on macromolecular suspensions observed in the last few years. However this may imply for the electrical properties of macromolecules some macroscopic and valid concepts will be presented. The experimental dielectric data to those observations will be presented and an interpretation will be attempted.

The dielectric properties of proteins in aqueous solution have been investigated during the 1940's through the work of Oncley and his associates. The dielectric properties of the data could be understood in terms of the ion-pair mechanism.

$$\epsilon^* \quad \epsilon_\infty +$$

The changes which result from the addition of 1 g. protein to 100 cc. suspending medium are called dielectric increments if they are positive, and decrements if they are negative. Increments are observed at frequencies which are low in comparison to about 1 mc. and decrements at frequencies much above. Low frequency dielectric increment values permitted Oncley to determine protein dipole moments. High frequency dielectric decrements result from the fact that the dielectric constant of the hydrated protein is lower than that of the replaced electrolyte. However, the decrement values obtained by Oncley near 10 Mc. are not as low as one might predict if the dielectric constant of the hydrated protein is rather low in comparison with that of the replaced electrolyte.

Decrement values were also obtained during the 1950's at microwave frequencies above 1000 Mc. (Buchanan 1952). They are of a higher magnitude than those observed by Oncley and of reasonable magnitude if the dielectric constant of the hydrated protein is assumed to be very small compared to that of electrolytes. Clearly, another relaxation process is indicated at frequencies between those employed by Oncley and by Buchanan. Li and Schwan have determined the dielectric properties of hemoglobin in 1955 in the frequency range from 10 to 1000 Mc. (Li 1955; Schwan 1957). They observed a dispersion due to this anticipated relaxation effect. It is the purpose of this presentation to first summarize some of these results and then to interpret them.

Material and Method

Hemoglobin was prepared with toluene (Haurowitz, 1930). Investigations were also conducted on packed erythrocytes which were diluted with distilled water. It is known that the resultant erythrocyte ghost suspensions behave at frequencies above 100 Mc. exactly like hemoglobin of equal concentration since the ghost membranes are of negligible impedance and hence do not affect the dielectric properties (Fricke & Curtis 1935; Schwan 1957). Indeed, results obtained with hemoglobin and erythrocyte ghost suspensions were noted to provide the same information with regard to dielectric decrements. Data were taken at various concentrations. Measurements extended usually over the frequency range from 150 to 1000 Mc. and in some cases from 0.5 to 1000 Mc. They were repeated to check reproducibility.

The determination of the dielectric properties throughout the range from 150 to 1000 Mc. was conducted with a transmission line, operating in a resonance mode. Details have been given previously (Schwan & Li, 1955). Measurements from 0.5 to 150 Mc. were conducted using General Radio Bridges 1601A and 916A and a sample cell described elsewhere (Schwan, 1963, Figure 37). Dielectric constants were obtained accurate within about one half dielectric unit and electrical conductivities accurate within two

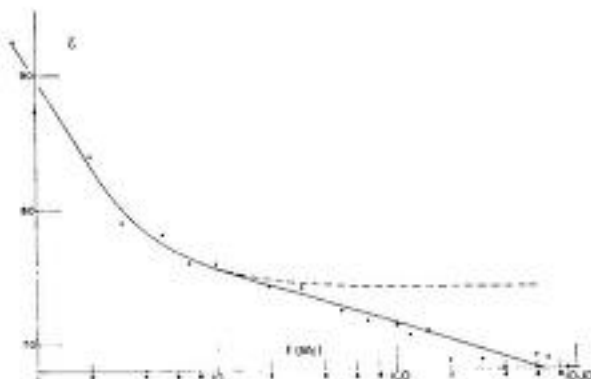


FIGURE 1. Frequency dependence of the dielectric constant ϵ of a 10 per cent Hb — suspension.

to three per cent, depending on frequency and dielectric loss. All data were taken at about 25°C.

Results

FIGURE 1 illustrates the frequency dependence of the dielectric constant ϵ of a 10 per cent hemoglobin suspension. The steep slope of the curve which is drawn for a best smooth fit of the data represents the greater part of the radio frequency relaxation behavior mentioned above. The dashed curve extending above 20 Mc. illustrates the high-frequency behavior obtained from an extrapolation of the radio-frequency relaxation effect. Its deviation from the continually decreasing curve constitutes the evidence for an additional relaxation mechanism.

TABLE I
DIELECTRIC DECREMENT VALUES FOR HEMOGLOBIN FOR FOUR
DIFFERENT CONCENTRATIONS

	100 Mc	300 Mc	600 Mc	900 Mc
5%	0.79	0.97	1.23	1.29
10%	0.75	0.87	0.98	1.08
15%	0.71	0.85	0.97	1.03
20%	0.71	0.8	0.86	0.88

Decrement values are given in terms of dielectric unit change per 1 g. Hb in 100 cc. Concentrations are given in terms of weight percentage. Accuracy ± 0.05 .

Schwan: Electrical Properties

Dielectric decrement values have been plotted in FIGURE 1 and are given together with TABLE I. The decrement values are fairly constant up to a weight percentage figure of about 10%. Further, the frequency dependence becomes more pronounced as the concentration increases, the mechanism which is responsible for the decrease in dielectric decrement becoming less effective at higher concentrations. There is also a change in approach at low frequencies for all concentrations. This value is close to the one observed by Schwan (1943). The decrement value approaches zero within experimental error with the value of 0.001.

Conductivity data are presented in FIGURE 2.

Interpretation

A. Dielectric constant of hydrated hemoglobin. It is assumed that the macromolecules are lumping together whatever amount of water they contain. The polarization resulting from the hydration shell can be represented by a dielectric constant ϵ_e . It can be shown (Schwan, 1943) that the dielectric constant ϵ_s of the macromolecules and the dielectric constant ϵ of the suspension ϵ are interrelated by the equation

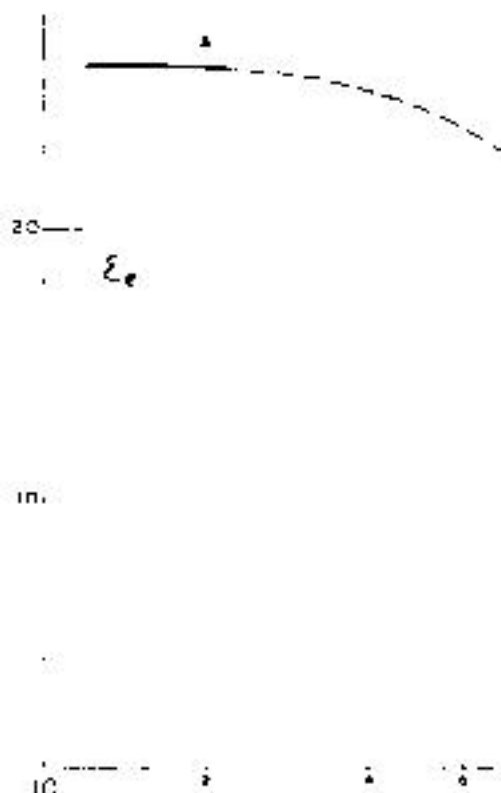


FIGURE 2. Frequency dependence of Hb-molecule ϵ , for two assumed hy-

magnitude of the dispersion of ϵ independant on the assumed hy-

FIGURE 3. Hydration and ϵ_r -values at different frequencies. Most probable value is 0.4. At frequencies above 1000 MHz ϵ_r is approached. However, below 1000 MHz ϵ_r decreases with increasing frequency.

Schwan: Electrical Properties

range of change from 100 to 1000 Mc²/sec., those characteristic of the rotation of constants are proportional to molecular weight, the rotating subunits is probably about hemoglobin.

2. The water bound to the protein seems to change in dielectric properties.

The concentration dependance of the dielectric constant appears to favor the second hypothesis. A concentration dependance might be anticipated at concentrations above 20 per cent, individual hemoglobin molecules could interact. However, if hydration values are considered, the volume of the hydrated protein is greater than that of the unhydrated one. Thus, interaction between proteins is not expected to occur at the 20 per cent level. If bound water structure extends further than the thickness which one would derive from

B. *The dielectric constant of bound water* has been used to calculate the dielectric constant of the effective dielectric constant of the protein per se ϵ_p :

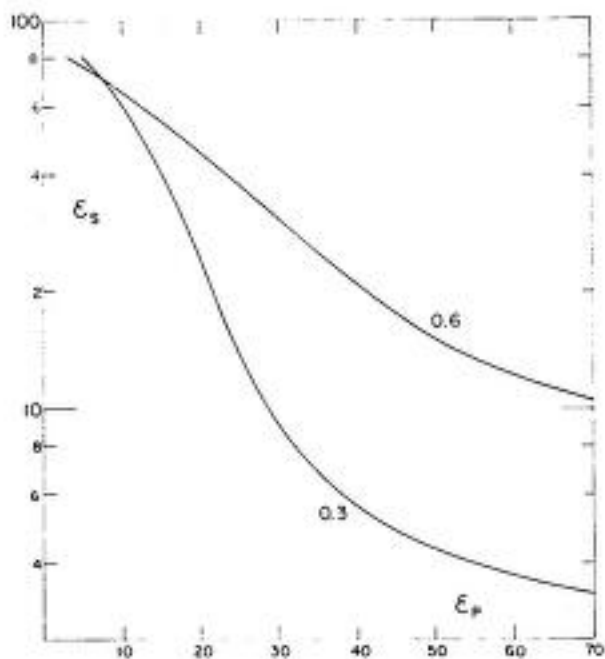


FIGURE 4. Dielectric constant of bound water ϵ_b versus assumed dielectric constant ϵ_0 of Hb for two assumed hydration values.

In FIGURE 5 we have plotted the dielectric constant of bound water, giving preference to the first possibility, i.e., assuming that the dielectric constant ϵ_b is reasonably small. The values for bound water are compared with those for normal "free" water and ice. Bound water relaxes at frequencies between those characteristic of the corresponding behavior of ice and normal water. Thus bound water appears to stand from a structural point of view

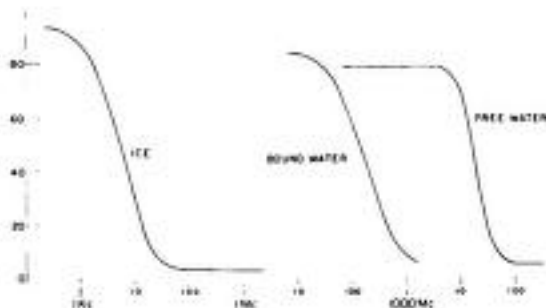


FIGURE 5. Frequency dependence of the dielectric constant of ice, bound and normal (free) water. All three curves have comparable limit values. The curve for bound water is less steep than the others.

Schwan: Electrical Properties

between normal water and ice. The slope of the water is flatter than that of ice and probably reflects a broader spectrum of time constants associated with bound water. This indicates variations in the activation energy of water associated with different activation processes.

C. Conductivity. Additional information can be obtained from the electrical conductivity κ of suspensions of normal water and electrolytes at microwave frequencies characterized by one single time constant (Debye equation)

$$\epsilon^* = \epsilon_\infty + (\epsilon_0 - \epsilon_\infty) e^{-t/\tau}$$

The subscripts 0 and ∞ refer to limiting cases. The following conductivity equation

$$\kappa_w = \kappa_{\infty} + (\kappa_0 - \kappa_{\infty}) e^{-t/\tau}$$

where a conductivity term κ_{∞} has been added to account for frequency independent contributions to the conductivity.

$$\kappa_\infty = \kappa_{\infty} - \frac{\epsilon_0 - \epsilon_\infty}{18}$$

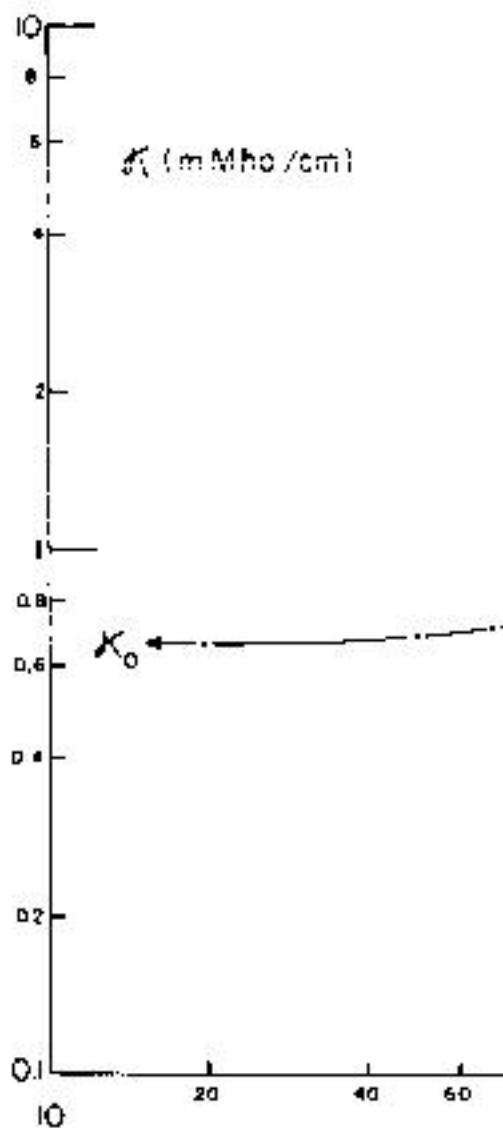


FIGURE 6. Frequency dependence of water (κ_w). A contribution κ_0 is char-

Schwan: Electrical Properties

Another independent estimate of κ_{∞} at 1000 Mc. is obtained as follows. If the relaxation process can be described by a single relaxation time, the conductance and dielectric constant will be related by the equation

$$\frac{G}{G_0} = \frac{\kappa}{\kappa_{\infty}} = e^{-t/\tau}$$

This equation is often found to be quite accurate for the case of protein hydration, where the conduction process involves a spectrum of times, each with its own average time constant. For the case under consideration, the frequency dependence observed appears to be exponential. Below 100 Mc. decrement values approach unity, while above 1000 Mc. they decrease rapidly. The changes at lower frequencies are due to the protein hydration, while those at higher frequencies are due to the water. Above 1000 Mc. on the other hand, the decrement values are greater than those anticipated if the hydrated protein were the only factor influencing the dielectric constant and a significant further decrease is observed. It is concluded that an average relaxation time of about 300 Mc. pertains. For the case of protein hydration, the dielectric decrement values quoted in Table I give four dielectric units over frequency ranges from 100 to 1000 Mc. The value of $\kappa_{\infty} - \kappa_{\infty}$, as calculated from Equation (1), is 0.0001, which is satisfactorily close to the estimate of 0.0002.

D. Protein hydration determination from dielectric measurements. The outlined estimates of the conductance and dielectric properties of

1. The effective dielectric constant goes a relaxation process which is value above 1000 Mc. is lower than The magnitude of this dispersion sumed amount of bound water.
2. The electrical conductivity of ample for the ease of a 20 per cent ion caused by the hydrated Hb m nearly 1 mMho/cm. as the frequ Changes in conductivity and dielect be related as demanded by relaxati
3. The mechanism responsible for constant and conductivity is likely characteristics of bound water. B frequencies somewhere near 300 Mc energies. Its structure appears t normal water.
4. A new technique to determine utilizes microwave conductance de 0.1 g. H₂O/g. Hb at best. Furth possible and are indicated.
5. A value of $0.3 \pm 0.1\pi$ between

THE EFFECT OF VARIOUS ON PROTON CONDUCTIV ENERGY

F. Hein

Pioneering Rese
U.S. Army Natick
Natick, I

Protons participate in numerous biologically important processes. There are two distinct proton transport mechanisms in biological systems:

(a) Diffusion, like other ions.

(b) Transfer between adjacent molecules. The second mechanism is the more rapid and it contributes mainly to the high proton conductivities found in living systems. The transfer process is not entirely clear. It has been suggested that the transfer may be due to the movement of water molecules. This suggestion has been made by performing experiments on the transfer of protons between adjacent water molecules. The transfer process has been studied by measuring the electrical conductivity of various biological structures. The results show that the transfer of protons between adjacent water molecules may be the dominant mechanism of proton transfer in biological systems.

Most conductivity studies involving ionic species in biological systems have been performed on pure water or on mixtures of water and other solvents. The results of these studies have shown that the transfer of protons between adjacent water molecules is the dominant mechanism of proton transfer in biological systems.

A.C. conductivity measurements were carried out in concentration equilibrium (in about 20 minutes) and no drift in conductance values, but it did not reach constant conductivity value. In terminating experiments, it was concluded that equilibrium conditions are sufficient for the factors which influence proton

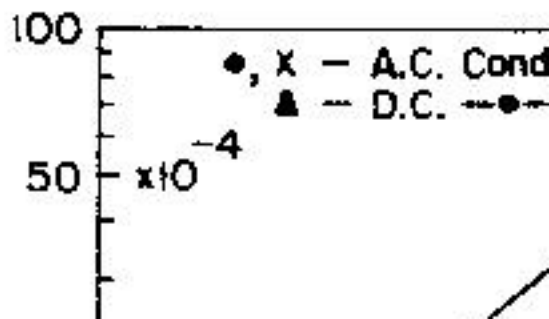
Experimental Results

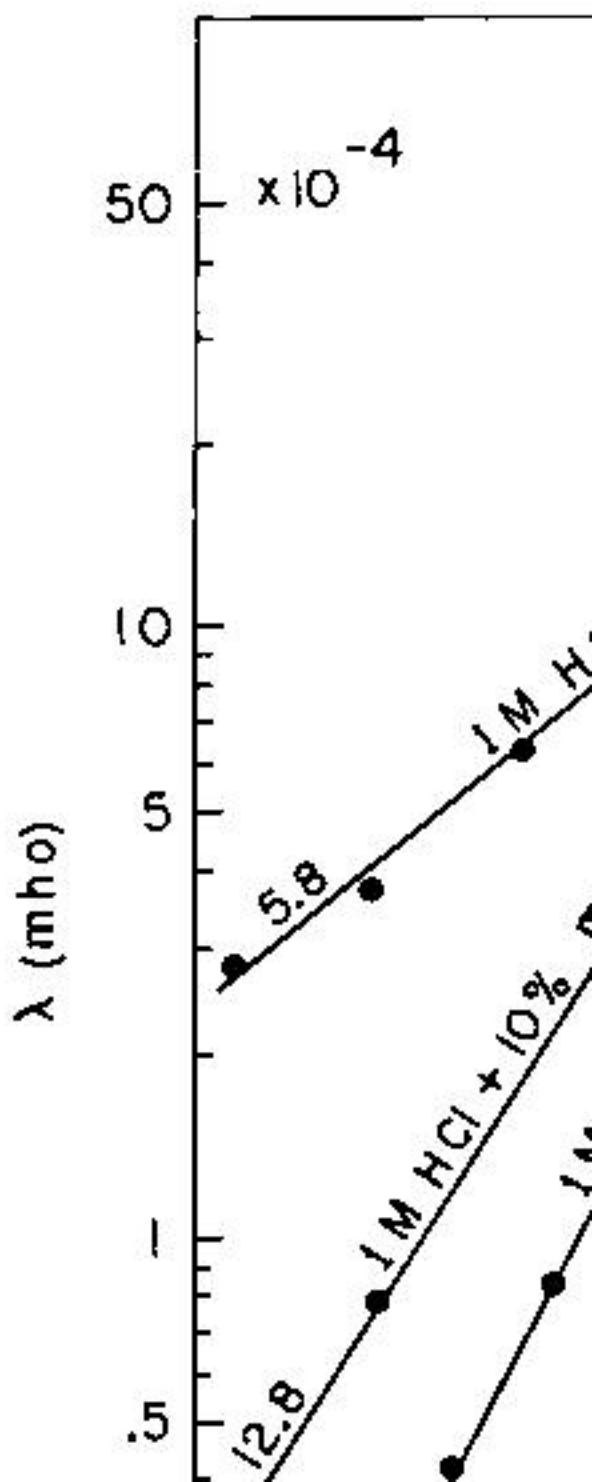
Conductivity during supercooled experiments was to determine the conductivity of a solution of HF and ice at the same temperature as a function of time during the minimum time required for ice formation. The solution was cooled to -6.0° and a glass rod was inserted into the solution; this initiated rapid ice formation.

Heinmets: Effect of

ductivity-U cell had an additional center-measuring device. FIGURE 1 shows conductance as a function of time. It is evident that heat is liberated to raise the temperature of the ice. During this time conductance is reduced from -6° to -6° and the rapid rise is again down to -6° and the rapid rise. After that a slow drift of conductance occurs until it becomes constant.

Effect of proton concentration. In HCl-protonated ice at various concentrations at a given absolute temperature. Absolute conductances are not comparable since different cells had to be used for each type of ice. The primary interest here is the effect of proton concentration on the rate of proton transport as a function of time. The slopes of conductivity curves are more

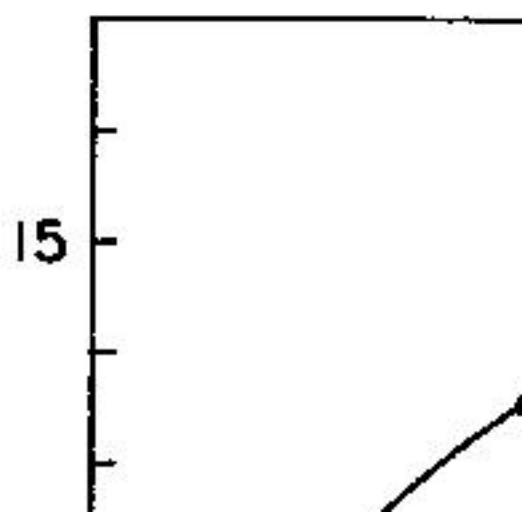




Heinmets: Effect of Biolog

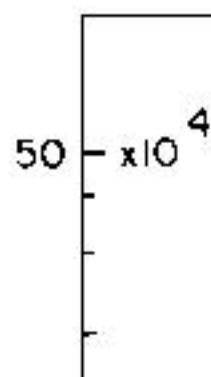
value of 6. Conductivity measurements particular interest since OH-ion transport but the mechanism is considered to be different. This is supported by the conductivity log conductivity of 1 M NaOH-ice is more than that of 1 M HCl-ice.

Effect of addition of various biolog no significant effect on activation energy present in solutions in the liquid state. high concentrations (20 per cent gelatin) a significant reduction of slope value changes were nonlinear and activation single numerical value. Gelatin solut



drastic expansion of ice and cells were discontinued. In contrast, in the presence of various biological values drastically. In the presence (1 gr. per 100 ml. of .1M HCl) activation energy values 18.7, 17.8 and 14.2 kcal. It appears reduction in activation energy values .1 M NaCl solution activation energy (2 g. agar per 100 ml. .1 M HCl) yields.

Further studies were carried out activation energies. FIGURE 3 shows the activation energy value when 1.0 M NaCl effect is produced in 1 M HCl-ice shows the effect of glycerol concentration a rapid rise of activation ene-



Heinmets: Effect of B

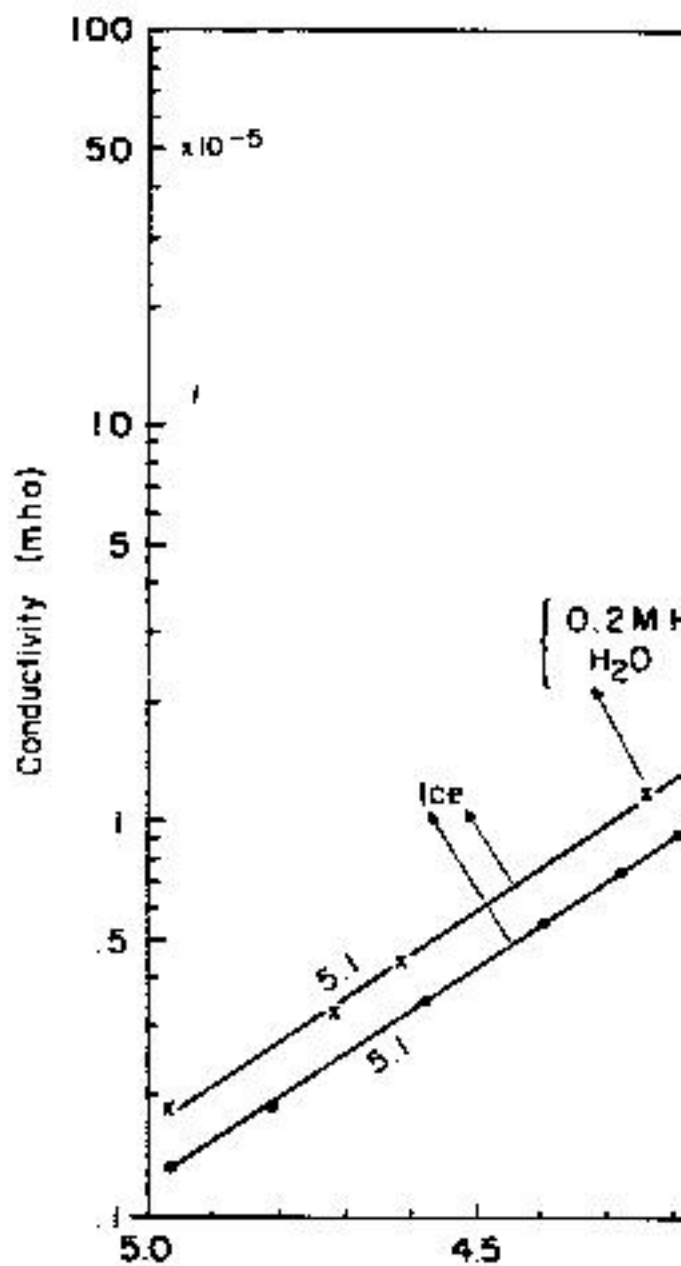
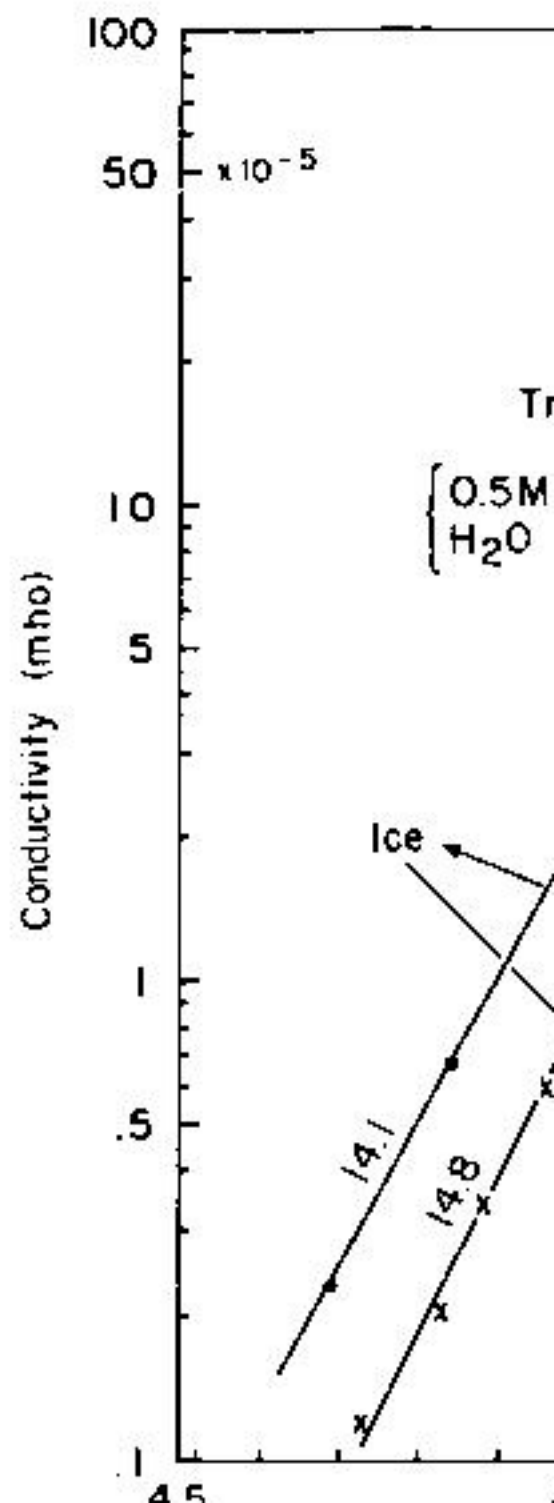
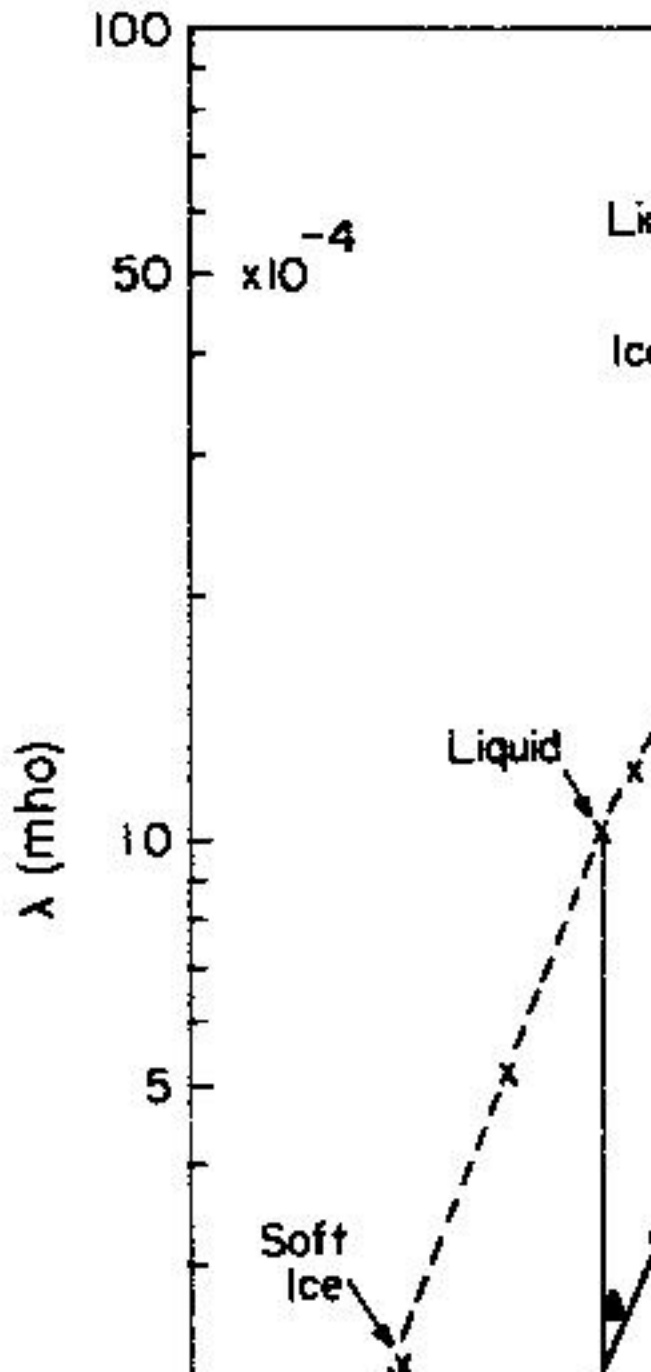


FIGURE 6. Log-conductivity of 0.2 M H_2O



Heinmets: Effect of B



perature. At lower impurity concentrations.

Some exploratory experiments were made to determine if the energy is not affected by change of concentration. This observation may have some bearing on the transfer mechanism.

Received

1. GROSS, G. W. 1965. Ion incorporation in ice. *This Annal.*
2. HEINMETS, F. & R. BLUM. 1963. *Trans. Faraday Soc.* 59: 1141.

HYDRATION STRUCTURE MACROMOLECULES

H. J. C. Berendsen et al.

*Department of Physical Chemistry,
University of Groningen, The Netherlands*

It is generally assumed that macromolecules affect the structure of water in their immediate surroundings. In particular, one might, in analogy with known properties of water,¹ venture to predict the following:

- (a) Polar side chains are expected to exert a structure-breaking influence beyond the hydration shell.
- (b) Nonpolar side chains will induce changes similar to the effects of nonpolar solutes.
- (c) Backbone structures with no available hydrogen-bonding acceptors (as the α -helix) will act as nonhydrating agents.
- (d) Backbone structures able to change the relative geometry of hydrogen-bonding sites, such as the β -sheet, will be able to induce changes in the hydration shell.

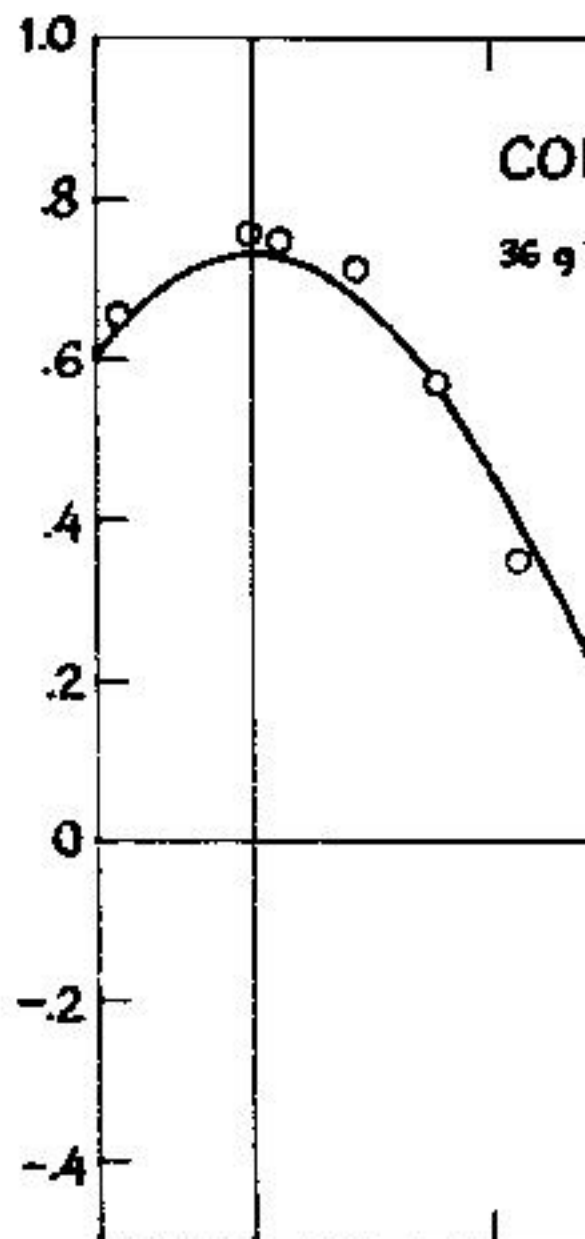
molecules (collagen, silk fibroin, oriented samples. These experiments. In Part II we describe the influence of water in hydrated collagen.

Part I: Fibrous Materials

Collagen. The protein collagen and it has been observed that over (20–90 per cent) the resonance signal consists of three peaks. The two outer peaks are symmetric about the central peak and are a result of the angular dependence of the distance between the protons, of the order of one gauss. In FIGURE 1 the spectrum of water protons is shown for a sample of collagen fiber containing 36 g. water per 100 g. fiber direction and magnetic field. It follows precisely the dipolar interaction between fiber direction and magnetic field, so that the water molecules rotate anisotropically being in the fiber direction. This is compatible with any simple rotation of the fiber around its axis.

Berendsen & Migchelsen:

peak separation
(gauss)



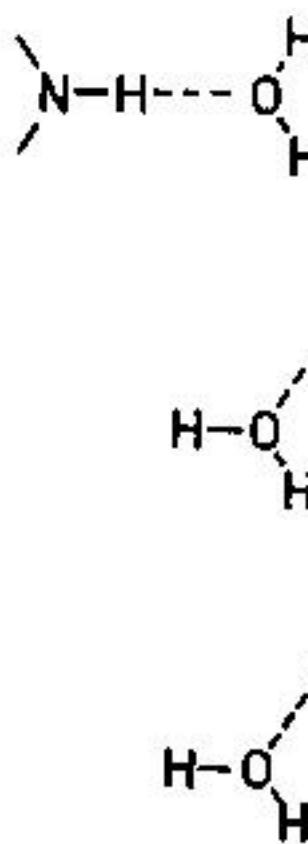
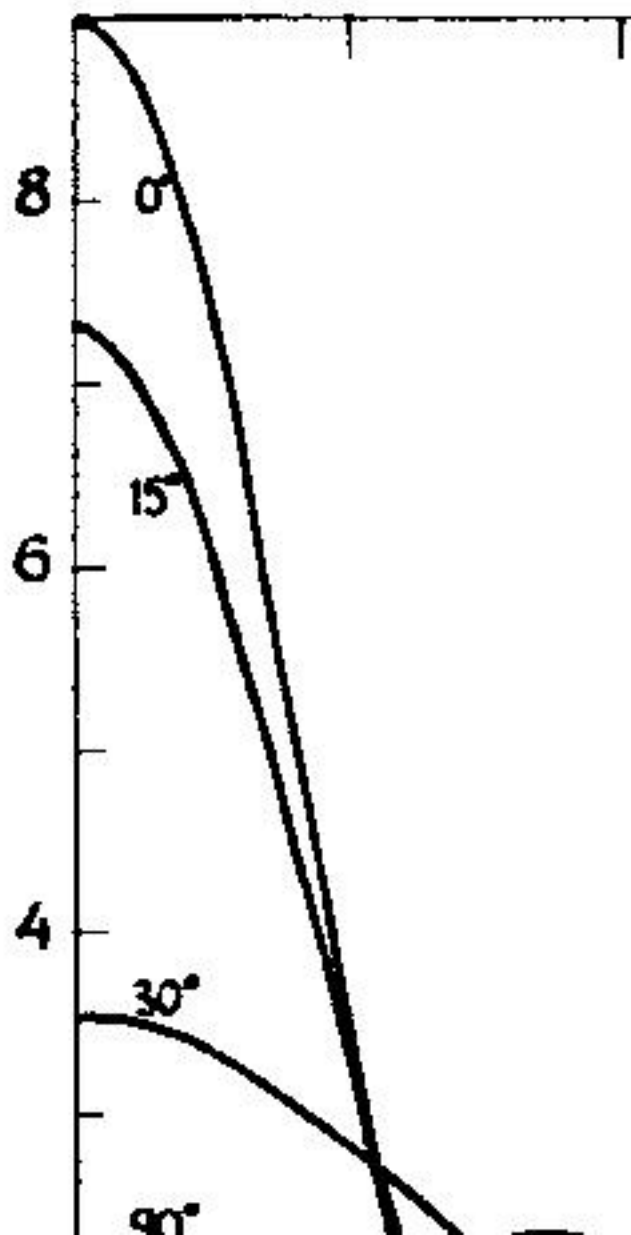


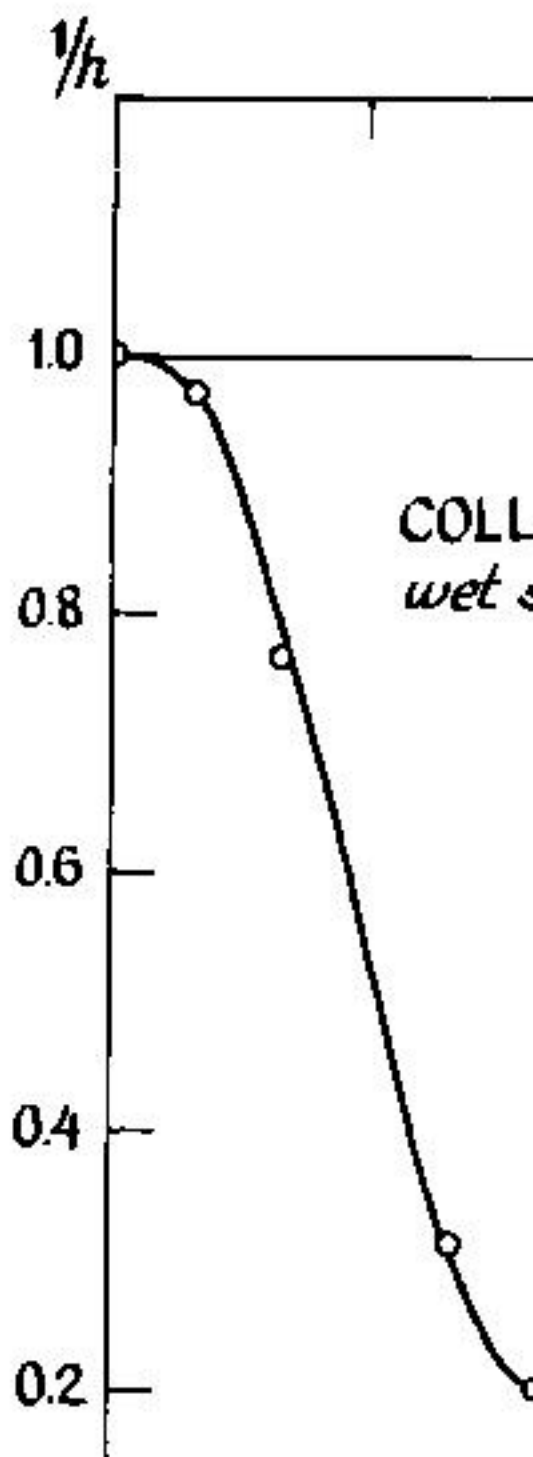
FIGURE 3. Proposed chain-like structure of collagen at relative humidities below 90 per cent. The partial structures of the collagen backbone are shown. The dashed lines indicate hydrogen bonding in this figure.

horse hair), it was found that non-crystalline cellulose from all sources had a

Berendsen & Migchelsen:

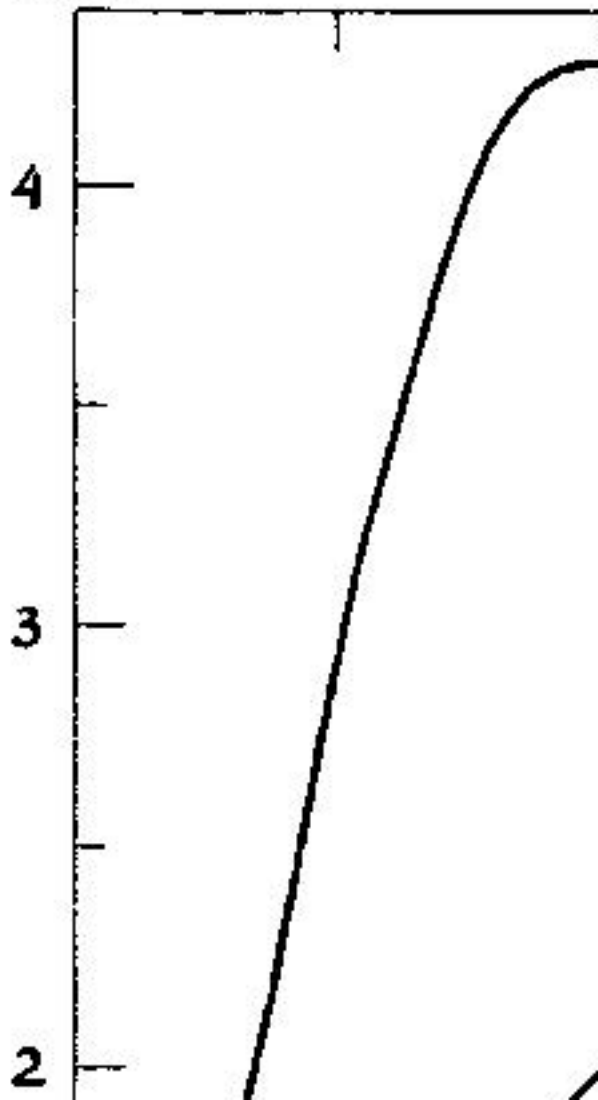
$S(\alpha, \varepsilon)$
in units of μ^2/r^6





Berendsen & Migchelsen:

$$\frac{S(t)}{S(0)}$$



$\frac{1}{h}$

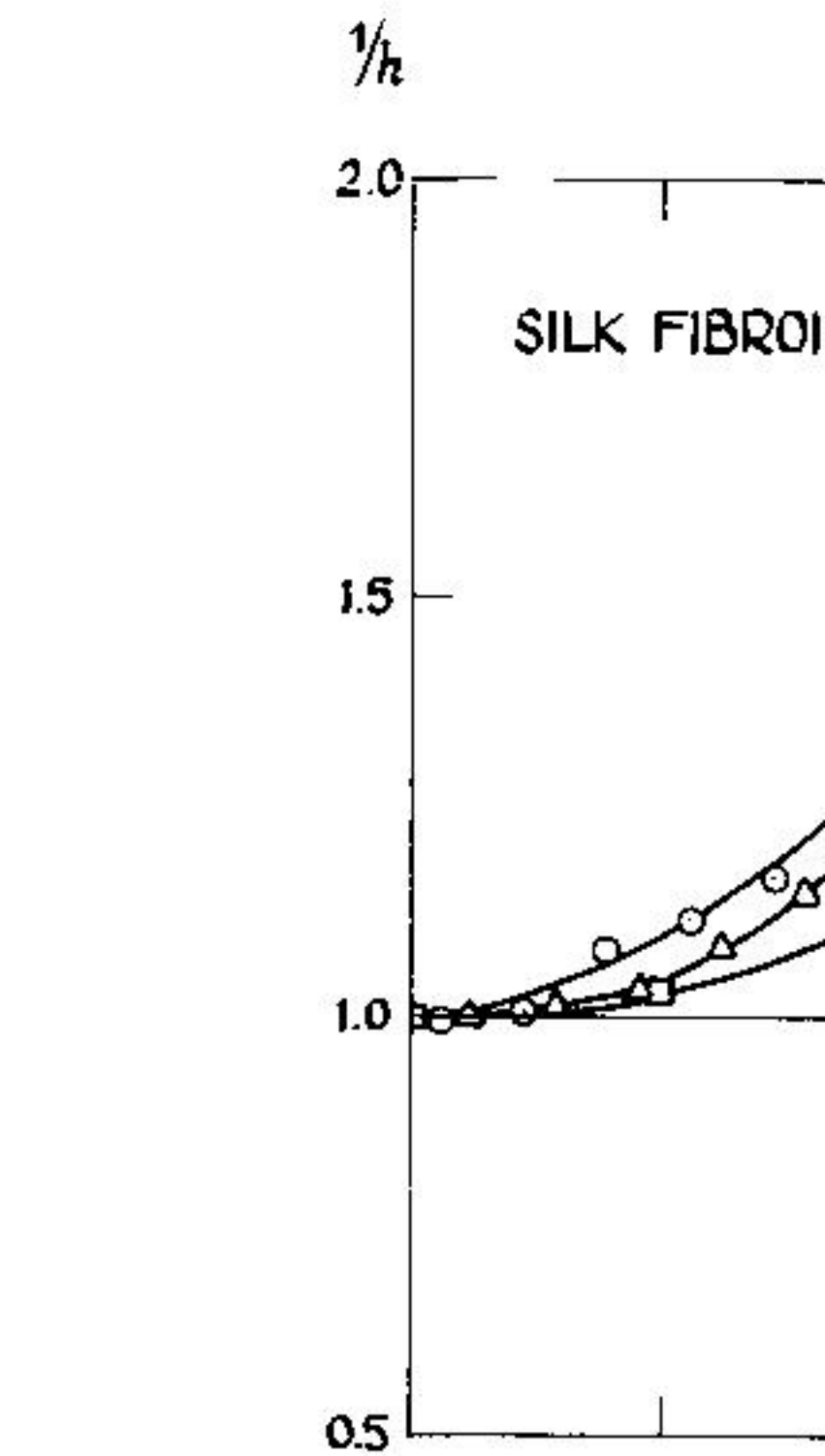
2.0

1.5

1.0

0.5

SILK FIBROI



Berendsen & Migchelsen:

η/h

2.0

DNA

1.5

1.0

0.5

1

2

3

4

5

6

7

8

9

10

11

12

13

14

15

16

17

18

19

20

21

22

23

24

25

26

27

28

29

30

31

32

33

34

35

36

37

38

39

40

41

42

43

44

45

46

47

48

49

50

51

52

53

54

55

56

57

58

59

60

61

62

63

64

65

66

67

68

69

70

71

72

73

74

75

76

77

78

79

80

81

82

83

84

85

86

87

88

89

90

91

92

93

94

95

96

97

98

99

100

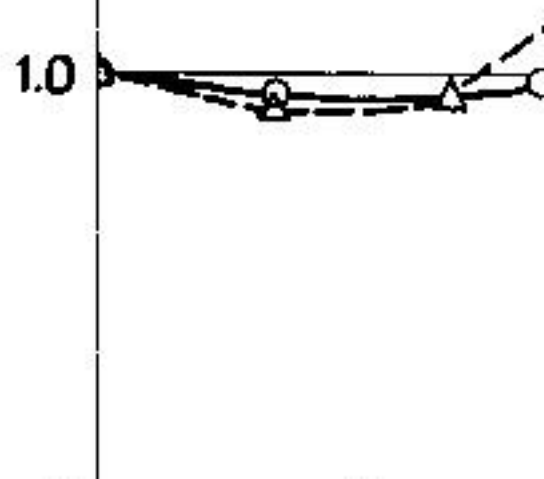
$\frac{1}{h}$

2.0

1.5

1.0

HAIR KER.

 α : unstretched β : partly stretched

Berendsen & Migchelsen:

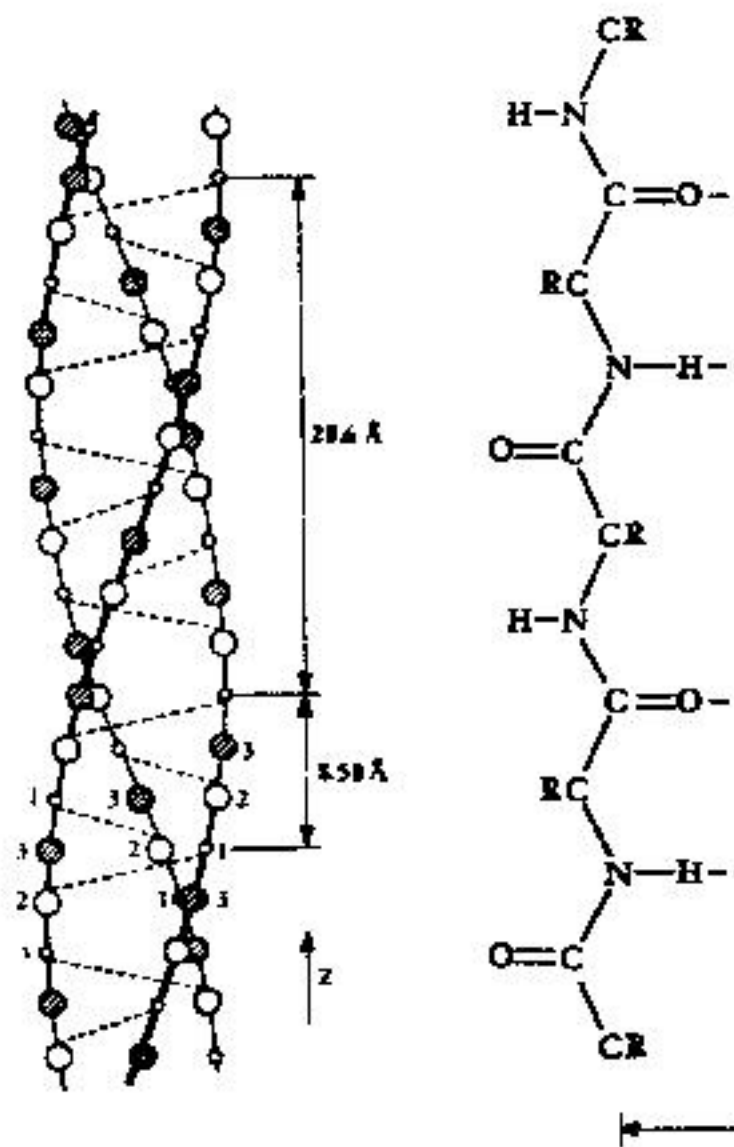
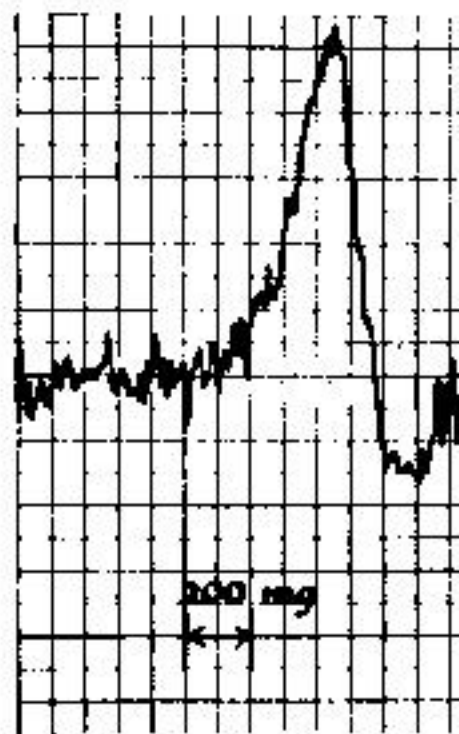
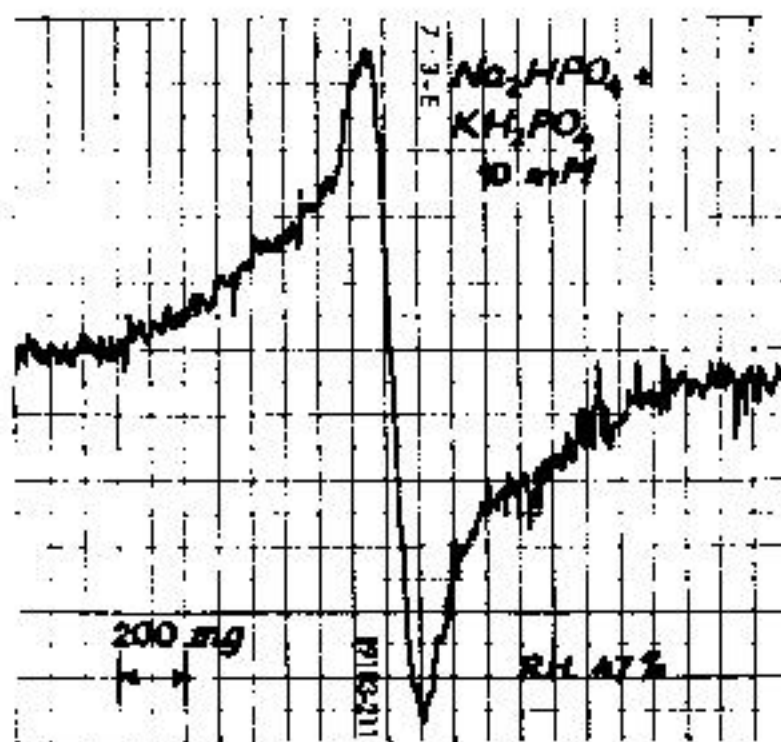
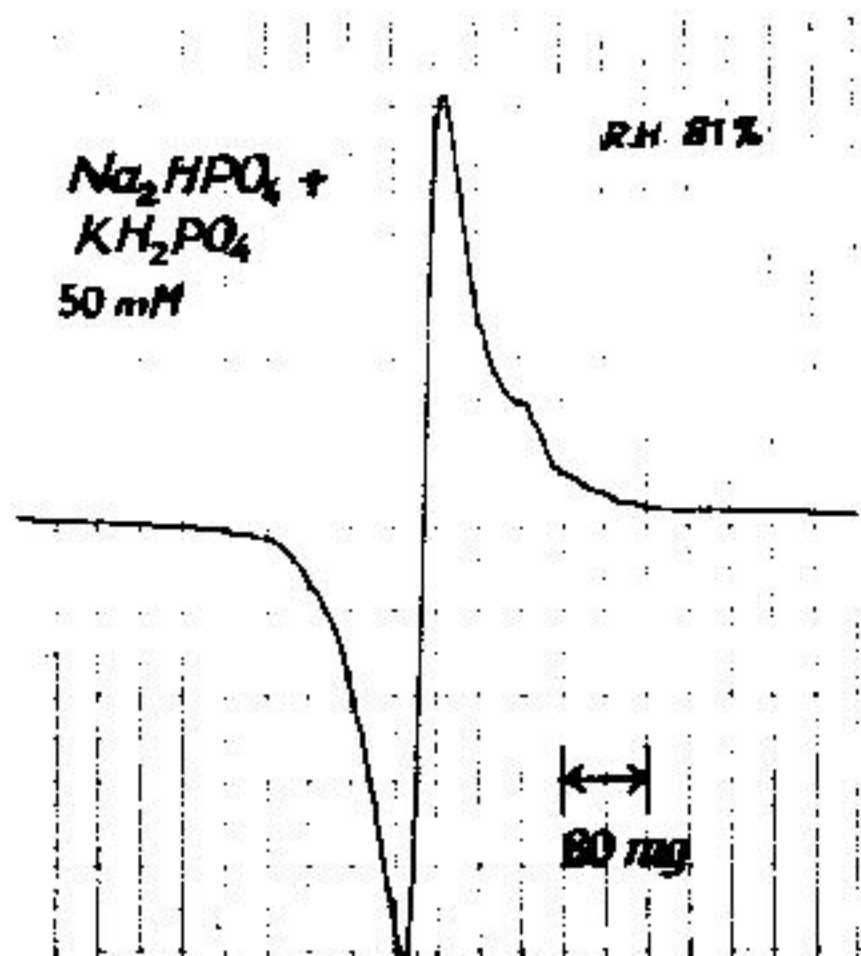


FIGURE 10. Basic structure of (a) collagen repeat distances in the macromolecules.



Berendsen & Migchelsen

myosin, and they suggest that the effects are a consequence of very general effects of the solvent, which in turn may actions involved in the stabilization or of a few selected salts according to the conformation is:



K phosphate > (NH₄)₂SO₄
LiCl > NaBr > LiClO₄

Salts to the left of NaCl stabilize, to the right destabilize, the alpha conformation.

Since phosphate occurs at one extreme of the scale, it is of interest to break the organized water structure. The effect of other salts of this series. By titration of the NMR spectra of solutions of K-Na-phosphate (pH 7.0) at 150 mM. concentration. After bath cooling to 20°C., the curves were equilibrated to 81 per cent relative humidity (in a saturated urea solution); the curves of the water protons, remaining after subtraction of the NMR line indicates a marked splitting of the water molecules, interpreted as the existence of two forms. The absence of such splitting indicates the absence of organized water. Both phosphate and ammonium sulphate have no appreciable influence on the water structure. It is, however, that NaCl also breaks the organized water structure when 150 mM. is used. The breaking effect of ammonium sulphate, while in K-Na-phosphate is more pronounced than in NaCl. By lowering the temperature by fivefold the results of FIGURE 13 have been obtained.

Berendsen & Migchelsen:

conformation of macromolecules, which Hippel and Wong that the influence on effect.

It now appears that a structure-breaking agent has at least on the hydration of collagen, measured by NMR, a marked influence on macromolecular conformation. One possible explanation is that the native conformation induces more ordered water molecules than does the denatured conformation, so that a structure-breaking agent will increase not only due to the macromolecular conformation, but also due to the presence of an agent that reduces the order of the water molecules around the macromolecule will increase the entropy of the system without changing the entropy of the denatured state. Thus the entropy increase on denaturization is greater than the entropy decrease of a structure-breaking agent as with the native state.

The measurement of NMR absorption provides a discriminative and sensitive tool for the study of the effects of various agents on the 'organized' state of a biological system. It seems to be very promising, especially as new methods are available.

ION INCORPORATION AND CONDUCTIVITY OF CONDENSER ICE

Gerardo W.

New Mexico Institute of Mining and Technology, Socorro, New Mexico

The direct-current conductivity of ice samples doped with ionic impurities has been measured as a function of concentration, and temperature. Electrolytes used were sulfuric acid, hydrochloric acid, potassium chloride, and sodium chloride.

Technique. The preparation of samples for conductivity measurements has been described previously,¹ however, an important modification has been made in the technique for preparing nonpolarizing electrodes. Disk electrodes prepared under high vacuum had been used previously.¹ These are now replaced by circular electrodes made of sintered platinum or palladium spheres having diameters and porosities of up to 25-35 per cent. The manufacturer's specifications. Platinum electrodes have a size, 34.5 mm. and 27.5 mm. diameter, and a weight of about 1.3 gm./cm.². A

The disks are manipulated with teflon-tipped forceps. Their performance equals or excels that of palladium-coated filter paper. They can be reused indefinitely.

The samples used for these experiments were polycrystalline with a strongly preferred orientation of the c-axis in the direction of growth. The average freezing rate was of the order of one millimeter per minute. Experiments with single crystals have recently been started and thus far seem generally to confirm the results obtained with the polycrystalline samples.

All freezing solutions were prepared with high-grade conductivity water (1×10^{-7} mhos/cm. or less at 25°C.) and the purest reagents commercially available.

Concentrations indicated in this paper as in the ice or in the melt refer to the melted ice phase at room temperature.

Discussion of Results

Experimental results are tabulated in TABLE 1. Sample curves are shown in FIGURE 1.

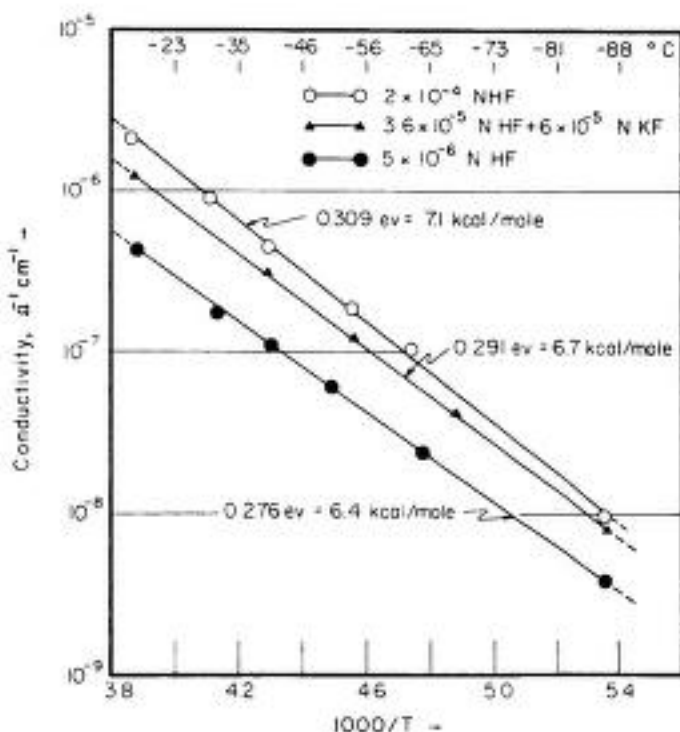


FIGURE 1. Arrhenius plots of ice samples grown from dilute solutions of hydrofluoric acid and of potassium fluoride.

TABLE I
SUMMARY OF ACTIVATION ENERGIES; TEMPERATURE RANGE: -10°C TO -86°C.

Solute	Molarity in the melt (moles per liter)	Number of samples	E/2 (mean values)	
			ev	Kcal/mole
HF	10^{-4} to 10^{-8}	33	0.30 ± 0.04	6.9 ± 0.92
HF*	2.8×10^{-3}	1	0.325 ± 0.005	7.5 ± 0.12
HF†	Not stated	Not stated	0.338	7.8
HCl	10^{-5} & 1.7×10^{-4}	5	0.29 ± 0.01	6.7 ± 0.23
KF‡	HF: 4 to 10×10^{-6} KF: 3 to 15×10^{-5}	5	0.31 ± 0.02	7.2 ± 0.46
KF§	HF: 4 to 6×10^{-5} KF: 4 to 7×10^{-5}	7	0.31 ± 0.02	7.2 ± 0.46
CsF†	Not stated	Not stated	0.294	6.8
NH ₄ F	10^{-2} to 10^{-5}	8	0.39 to 0.28	9.0 to 6.5

*C. Jaccard (1959).

†Computed by A. Steinemann (1957) from low-frequency measurements.

‡Open circuit.

§External shunt, 10 Kilohms.

The electrical conductivity of ice is largely determined by hydrogen ions associated with ionic impurities built into the lattice. In the case of the halogenic acids, hydrofluoric and hydrochloric, the conductivity at constant temperature is proportional to the square root of the acid concentration in the ice (FIGURE 2). This leads to the following expression for the conductivity as a function of acid concentration and temperature:

$$\sigma \propto [H_3O^+] = K(T) [HA]^{\frac{1}{2}} \quad (1)$$

where σ is the conductivity, $[HA]$ is the molarity of the ice of hydrofluoric or hydrochloric acid, and T is the absolute temperature.

$$K(T) = C \exp(-E/2kT) \quad (2)$$

where E is the energy of ionization, according to the theory of Jaccard (1959).

The activation energies of TABLE I have been computed from the slope of Arrhenius plots such as those of FIGURE 1. They represent the numerical value of $E/2$ in Equation 2.

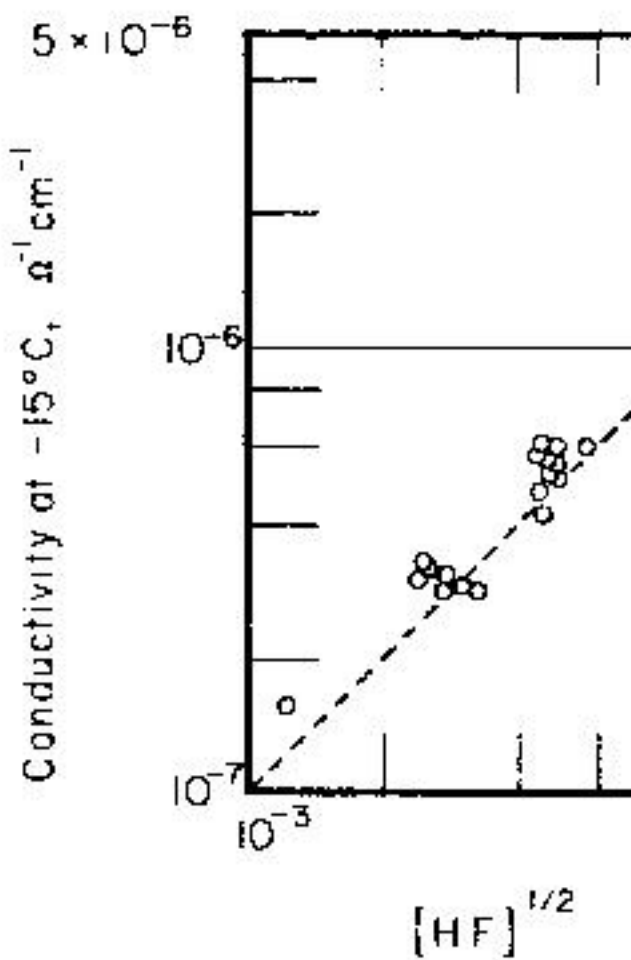


FIGURE 2. Conductivity at -15°C . vs. the square root of HF concentration for samples grown from dilute solutions of HF. The dashed line is a straight line extrapolated to zero conductivity. It passes through the origin and the point corresponding to the granular precipitation of HF. The samples were taken at various stages of the precipitation process at high concentrations.

Hydrofluoric and hydrochloric acid. The results of the experiments made by Stoyanov et al.¹ are summarized in Table I.

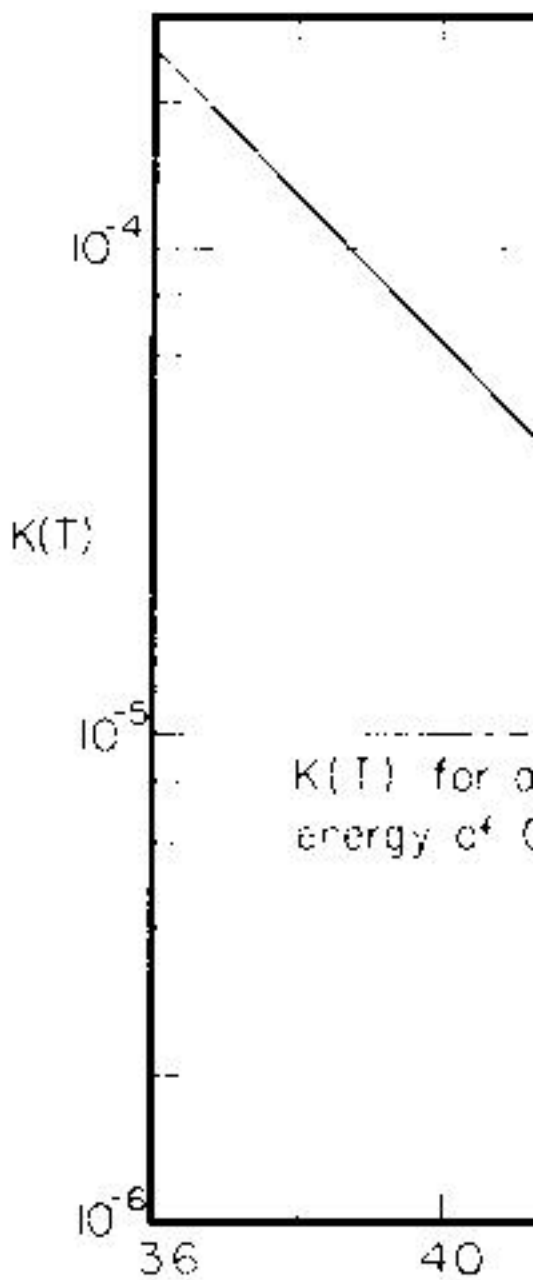


FIGURE 3. The proportionality factor

The potassium ion, therefore, does not appear appreciably to influence the conduction process. It is possibly not incorporated into the ice structure at all but rather accommodated interstitially. Furthermore, in spite of its considerably smaller radius (1.33 Å), its behavior is similar to that of cesium (1.65 to 1.69 Å). The latter ion was investigated by Steinemann (1957). His results are nearly identical to those for KF here presented (TABLE 1).

If, prior to freezing a 2.5×10^{-4} M solution of potassium fluoride is brought up to a pH of about 7 by means of potassium hydroxide, the activation energy of conduction remains the same or perhaps increases slightly, but the conductivity is reduced by a factor of between 10 and 20, as compared to samples of similar hydrogen-ion content prepared from hydrofluoric acid alone. The additional base shifts the hydrogen-ion concentration equilibrium in the freezing solution. As a result, fewer hydrogen ions are available for neutralization of fluoride ions incorporated into the ice (Cobb, 1964). The rate of fluoride-ion incorporation is, therefore, diminished. But in addition, this preliminary result suggests that the base introduces into the ice a defect structure which affects the conductivity. A further investigation of this question in a controlled, carbon-dioxide-free atmosphere is currently being initiated in our laboratory.

Ammonium fluoride. Several investigators have reported that the resistivity of ice doped with ammonium fluoride rises by orders of magnitude as the concentration is increased from 10^{-5} to 10^{-2} M (Workman, 1951; Brill, 1957; Iribarne et al., 1961). The present investigations not only have confirmed this remarkable phenomenon but have shown in addition that the activation energy also increases with concentration in this range, provided the samples have been grown at average rates of one millimeter per minute or more. At concentrations below 10^{-5} M, the activation energy

TABLE 2
ACTIVATION ENERGIES OF ICE SAMPLES DOPED WITH AMMONIUM FLUORIDE.
AVERAGE OF TWO SAMPLES AT EACH CONCENTRATION

Concentration in the melt (Moles per liter)	E/2	
	ev	Kcal./mole
7×10^{-3}	0.39 ± 0.01	9.1 ± 0.2
9×10^{-4}	0.35 ± 0.01	8.0 ± 0.2
9×10^{-5}	0.32 ± 0.01	7.4 ± 0.2
8×10^{-6}	0.28 ± 0.01	6.4 ± 0.2

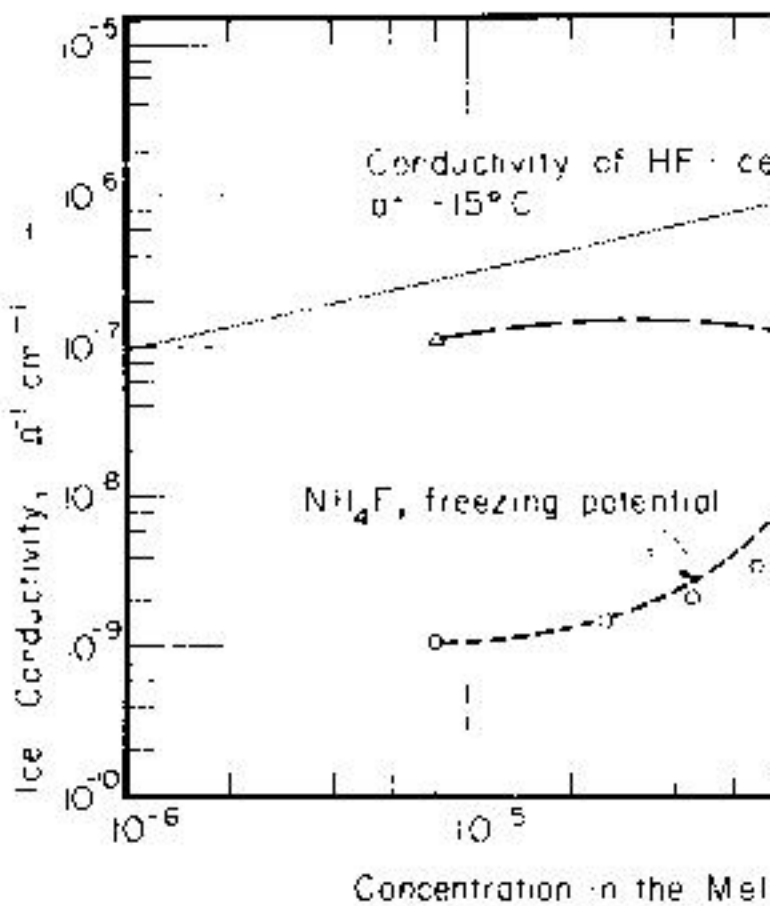


FIGURE 4. Conductivity at -15°C . as a function of concentration, for ice solutions. For comparison, the curve concentration of hydrofluoric-acid ice is shown.

approaches the value observed for solid ice (TABLE 2).

FIGURE 4 shows measurements, m-

Gross: Ion In

tude of about 5×10^{-6} M) appears independent of ice conductivity. However, because of the low concentrations, this result must still be considered tentative until more accurate measurements are made.

As the ammonium fluoride concentration increases in the melt, the highest value of the freezing point depression is reached shortly after the beginning of a freezing cycle. The cause of this rise for the rise is the increased number of ions in the melt. The layers adjacent to the interface or the interface itself become more ordered. As the concentration is increased further, the concentration in the ice becomes smaller and the concentration in the melt increases.

At NH_4F -concentrations in the melt which are higher than the highest value reached by the freezing point depression curve, it passes through a maximum. This is possibly due to the formation of a partially ordered ice structure (Lodge *et al.*, 1955). The ratio HF : NH_4F is constant at 1.0 throughout the range of the measurements, as does the ratio HF : NH_4F . The ratio HF : NH_4F is constant at 1.0 throughout the range of the measurements.

At the low concentration end (less than 10^{-6} M) the freezing point depression curve for ammonium fluoride in ice is identical with that for ice doped with hydrofluoric acid alone.

The curves suggest that the NH_4^+ -ion has a greater influence on the structure of ice than the fluoride ion. The effect of the fluoride ion is reduced by the presence of the ammonium ion. The effect of the ammonium ion is reduced by the presence of the fluoride ion.

Samples doped with cesium fluoride at the same temperature and concentration as those doped with hydrofluoric acid show incorporation taking place at the interface by water molecules diffusing into the water and replaced by hydroxyl ions available for incorporation, and hence the difference in incorporation rate of the two samples. In ice frozen from dilute aqueous ammonia, the hydrogen-ion concentration, the incorporation rate, and the ice-water interface reaction rates may be greatly reduced by a factor of 10. The freezing potential also depends on all components present in the solution.

In ice frozen from dilute ammonium fluoride solutions, the conductivity and activation energy depend on the ratio HF : NH₄F. The effect of this ratio has not been investigated because, except at the highest ratios, the degree of ionic separation and the fraction of HF modify the results. The influence of the freezing solution influences the conductivity of the ice, which will be considered in future investigations.

Acknowledgments

Professor Roland Lise made valuable contributions to this work.

Gross: Ion In

- LODGE, J. P., M. L. BAKER & J. M. PIERRARD
in dilute solutions by freezing. *J. Ch.*
STEINEMANN, A. 1957. Dielektrische Eigen-
Dielektrische Untersuchungen an Eis-
tomen. *Helv. Phys. Acta* 30: 581-610.
WORKMAN, E. J. & S. E. REYNOLDS. 1950
ing the freezing of dilute aqueous so-
to thunderstorm electricity. *Phys. Rev.*
WORKMAN, E. J. 1951. Some electrical p-
solutions. Final Report on Thunders-
Corps, U.S. Dept. of the Army.

MECHANISM OF THE ELECTRICAL CONDUCTIVITY IN ICE

C.

*Swiss Federal Institute for
Weissfluhjoch-*

The Electrical Conduc-

As ice belongs to the most common substances known to man, it has been studied by many scientists for a long time, but its electrical properties could be elucidated only recently by means of new techniques (e.g. neutron diffraction) which have been developed for the investigation of the properties of crystalline solids. Investigations performed since the beginning of this century have now yielded the following picture.

Pure ice is altogether a bad conductor of electricity. Its electrical conductivity¹⁻³ has a value of 10^{-17} ohm⁻¹ cm⁻¹ at 0°C. It is to be mentioned that all values given in this article are at 0°C unless otherwise specified. The response to temperature changes follows the Arrhenius law with an activation energy of about 0.54–0.61 eV, but recently a smaller value of 0.35 eV has been reported.⁴ It has been shown by electrolysis experiments that the electrical con-

Jaccard: Electrical C

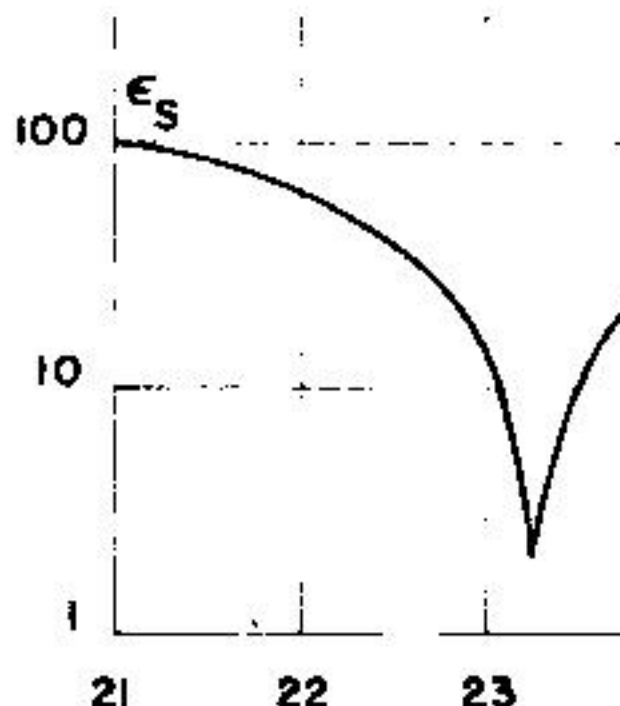


FIGURE 1. Dependence at -3°C . of the dielectric constant ϵ_s on the concentration n (HF) of hydrofluoric acid (according to Steinemann¹⁰).

creased, but the most interesting effect was observed at the lowest concentrations (FIGURE 1). As the HF concentration increased beyond the critical value, which are very near to ϵ_{∞} in homogeneous mixtures, the mechanism responsible for the dielectric breakdown breaks down.

Although it was obvious that the physical properties of this peculiar behavior



FIGURE 2. Ice lattice, seen perpendicular to the plane of the paper. The oxygen atoms and the dark hexagons are horizontal.

DC conductivity. Therefore, one has to consider as a result of fluctuations in the transverse

Jaccard: Electrical C

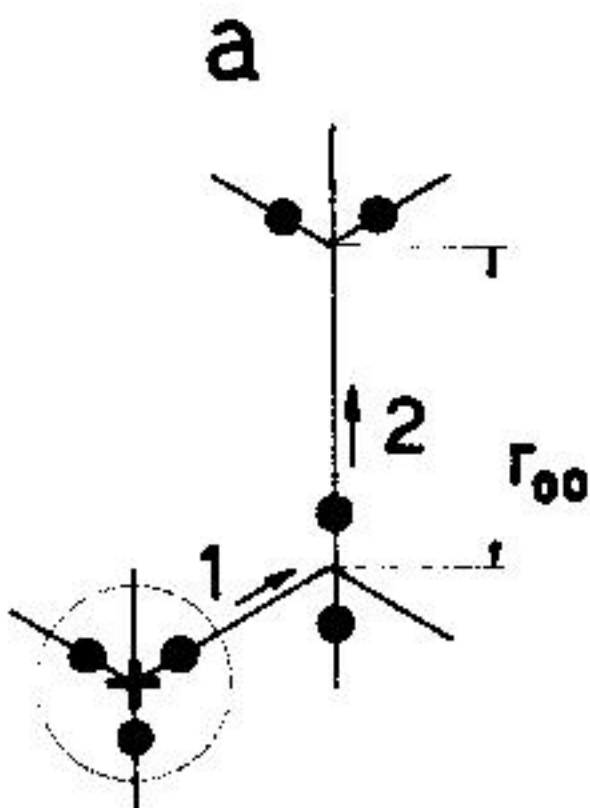


FIGURE 3a. Motion of a positive ion
protons according to the arrows 1 and 2
state on a distance $4/3r_{00}$ along the c-axis
(gen atoms not being shown.)

If a defect state jumps from one lattice site, r_s , it is accomplished first by the jump of the original site, and simultaneously by the nuclei and electronic clouds which go

defined by the following relation:

$$\mathbf{e}_{\text{defect}} \cdot \mathbf{r}_s =$$

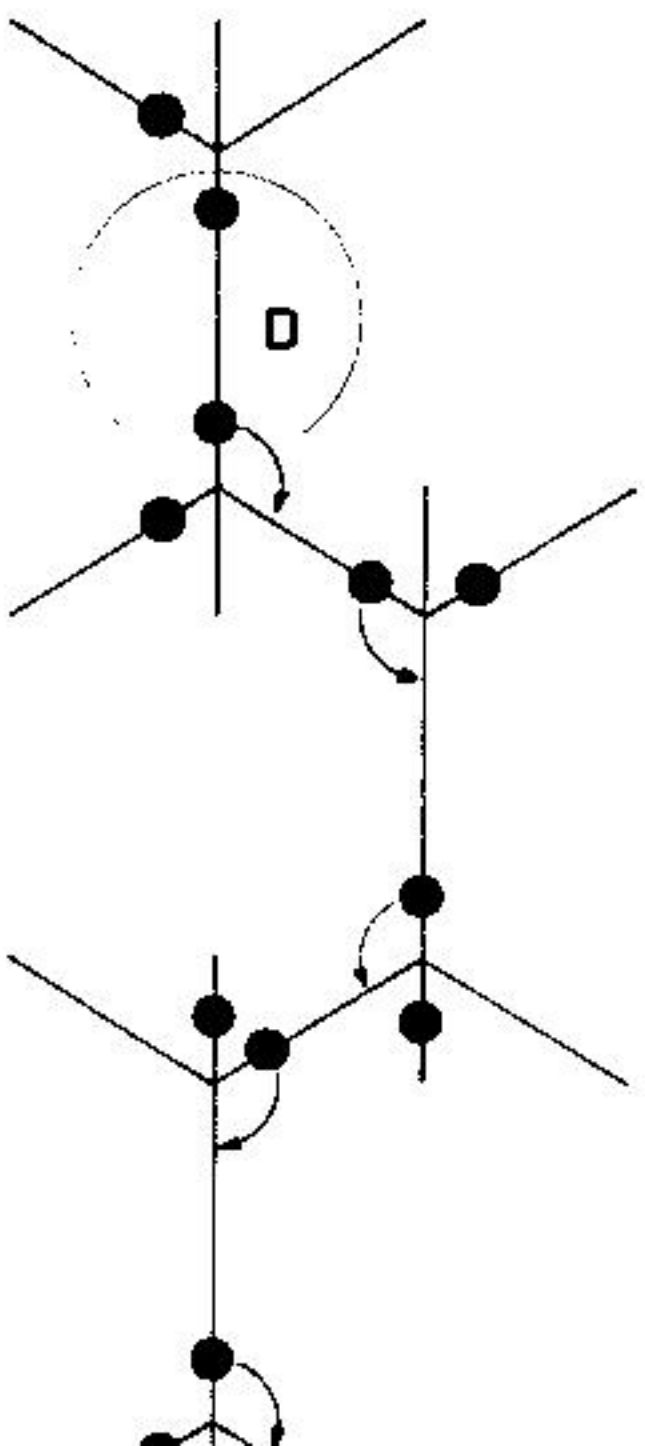
where the integration occurs on the path transferred along the distance \mathbf{r}_s . As above, it is in the most general case of conductors which do not need to be parallel to the direction of motion. Effectively the defect in its travel trajectory, it can be measured from outside the charges of the ionic defects having opposite signs ($e_+ - e_- = e_{\pm}$). There are also \pm defects ($e_D = -e_L = e_{DL}$), but they are transported through the lattice in both sorts of defects in order to share the charge. Consequently, the proton has no net charge:

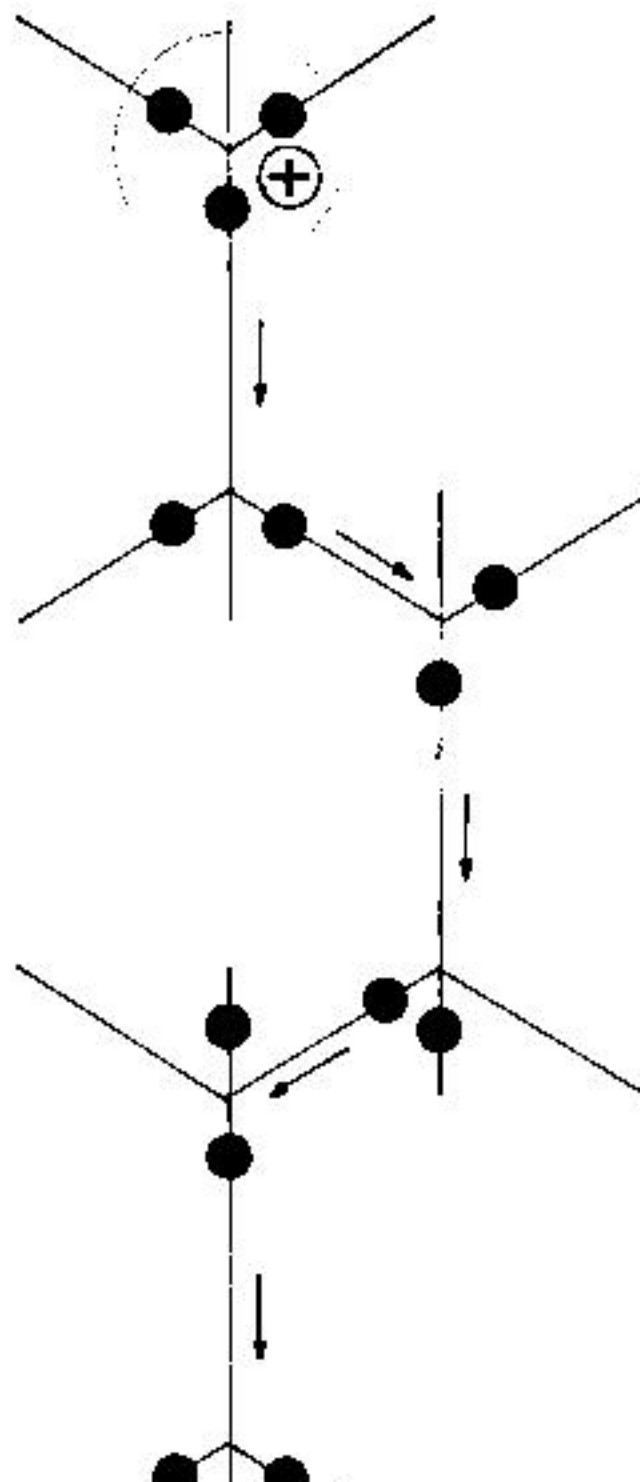
$$e_+ + e_- = 0$$

Mechanism of

The quantitative description of the different points of view¹⁻¹⁶ practical to nonvanishing DC conductivity, we leave to another paper. One of them may be the major carrier

Jaccard: Electrical C





Jaccard: Electrical Conductivity

determined by other methods,³ and amounts to 1.2 ohm⁻¹ cm⁻¹. The mobility of the positive ions has a value of 1.2 cm²/volt sec.

Thermodynamics

The quantitative phenomenological treatment of the conductivity in *Mechanism of the Conductivity* has been modified in view of the thermodynamics of irreversible processes. It is the same as those from the previous treatment (with differences in numerical factors) but allows the consideration of complicated effects where the electric field is not uniform and there are temperature gradients. The determining factor is the entropy production from the change in configuration. In the first approximation it has the form

$$\dot{S}_k = - \frac{8}{\sqrt{3}} k r_{00}$$

where Ω is a "configuration vector" related to the lattice configuration and defined by

$$\Omega = \int_{\text{cell}} (\mathbf{j}_+ - \mathbf{j}_-) \cdot d\mathbf{l}$$

The \mathbf{j} are the defect currents, k is the Boltzmann constant, r_{00} is the distance between two neighboring oxygens, and $d\mathbf{l}$ is the differential vector element along the boundary of the unit cell.

tween the defects. It is called a "p

$$e_p = \frac{\sigma \pm}{\sigma \pm}$$

It relates the lattice polarization

P

In pure ice, where the Bjerrum de
the "polarization charge" is the s

e_p (pure)

This charge can be virtually attached
action with the lattice polarization
and the polarization exerts a force on

$$\eta_k = e_k F$$

F being the electric field, ϵ_0 the di
 η_k being ± 1 . As it was pointed out
of polarization," corresponding to
produced as a change in the proton
related to the static dielectric cons

$$\epsilon_0 \epsilon_s = e_p^2$$

Thus, the matching of the partial
according to Equation 8 and also o

Jaccard: Electrical C

step. This is suggested at first by the value of the activation energy, which is of the order of magnitude occurring generally in ice. It has been shown experimentally⁴ that the activation energy is about 0.23 eV, giving the height of the potential barrier.

The situation is different for the ionization of the proton. The activation energy is very high, about 400 times higher than the thermal energy kT. This cannot be accounted for by a classical mechanical tunnel effect. In fact, as is prevailing now, the protons go through the potential barrier by means of the quantum mechanical tunnel effect. The step height is about 0.76 eV, which is about 40 times the thermal energy kT, i.e. about 0.02 eV, at 273°K. The tunneling length is about 0.76 Å, but certainly larger. The low frequency stretching of the lattice, which is about 0.76 Å, allows a penetration of the protonic wave function through the potential step and, therefore, a transfer of energy. This is the cause of the low frequency stretching of the lattice. The transfer of energy is about $2 \times 10^{12} \text{ s}^{-1}$ (whereas it is only $2 \times 10^8 \text{ s}^{-1}$ for the thermal tunnel effect) and this together with the defect of the DC conductivity in pure ice.

Although it has not been proven experimentally, it is reasonable to assume that the proton must be present in the mobility of the ions. When the proton is moving, it must pass through the jump of the former, the proton is being transferred from one lattice site to another. This is the case in the case of the tunnel effect, where the proton is transferred through the potential barrier. The transfer of energy is about $2 \times 10^{12} \text{ s}^{-1}$ (whereas it is only $2 \times 10^8 \text{ s}^{-1}$ for the thermal tunnel effect) and this together with the defect of the DC conductivity in pure ice.

This description does not preclude the possibility that the ice may also have a bearing on certain physical properties of the ice. For example, when the ice is doped with a solute, the complicated situation is not yet clearly understood.

Acknowledgments

The author is indebted to Mr. W. H. Barnes for his critical reading of the manuscript, to Dr. M. de Quervain for his interest and constant interest in the problems of the ice, and to the Swiss National Academy of Sciences for a travel grant.

References

1. JOHNSTONE, J. H. L. 1912. Proc. Roy. Soc. A, 84: 101.
2. GRÄNICHER, H., C. JACCARD, P. SCHERER & H. EIGEN. 1957. Helv. Phys. Acta, 30: 100.
3. BRADLEY, R. S. 1957. Trans. Faraday Soc., 53: 100.
4. JACCARD, C. 1958. Helv. Phys. Acta, 31: 100.
5. EIGEN, M., L. DE MAEYER & H. DECROLY. 1958. Helv. Phys. Acta, 31: 100.
6. DECROLY, J. C., H. GRÄNICHER & C. JACCARD. 1958. Helv. Phys. Acta, 31: 100.
7. HUMBEL, F., F. JONA & P. SCHERER. 1958. Helv. Phys. Acta, 31: 100.
8. AUTY, R. P. & R. H. COLE. 1952. Proc. Roy. Soc. A, 207: 100.
9. STEINEMANN, A. 1957. Helv. Phys. Acta, 30: 100.
10. BARNES, W. H. 1929. Proc. Roy. Soc. A, 100: 100.
11. PAULING, L. 1935. J. Am. Chem. Soc., 57: 100.
12. WOLLAN, E. O., W. L. DAVIDSON & R. H. COLE. 1952. Proc. Roy. Soc. A, 207: 100.
13. PETERSON, S. W. & H. A. LEVY. 1952. Proc. Roy. Soc. A, 207: 100.
14. RABINOWITZ, J. N. & R. H. COLE. 1952. Proc. Roy. Soc. A, 207: 100.

THE PHYSICAL STATE OF WATER AS A MODEL

Gilbert Nirenberg

*Department of Molecular Biology in
Division of Medicine, Pennsylvania State University*

Living cells, as a rule, contain 15 to 70 per cent water. We now know that it is the proteins that underlie biological phenomena, and that the nature of one amino acid residue may produce profound differences in the properties of the system in which this protein is a part.¹ Yet, important as these biological phenomena are, there can be no life unless there is water. Water is found in the form of contractile proteins or in the extracellular fluid and in the plasma always contains water; the unique character of living systems is not the behavior of the proteins per se, but the behavior of the water in these systems. The question arises: In what way does water function in living systems? Does it function merely as a solvent of the proteins?

In recent years, considerable evidence has been presented that water is not merely a

The views on the physical state of water in living cells, however, are widely divergent.

According to the classical membrane theory, the intracellular water is permanently and entirely (or almost entirely) in the form of normal water such as is found in a 0.1 M KCl solution. The well-known asymmetry in the distribution of ions and nonelectrolytes between the intracellular and extracellular water is attributed to the critical pore size on the cell membrane or to a continual pumping by "Na pumps" and "permeases" located in this thin structure.

Gortner¹¹ advocated the view that cell water is bound; his concept, however, was not accepted largely because of a lack of truly convincing evidence.^{11,12}

According to Troschin's sorption theory¹³ the cell water has different solubility properties for nonelectrolytes, amino acids and ions than normal water; it does not offer molecular interpretations as to the mechanism of this difference in solubility.

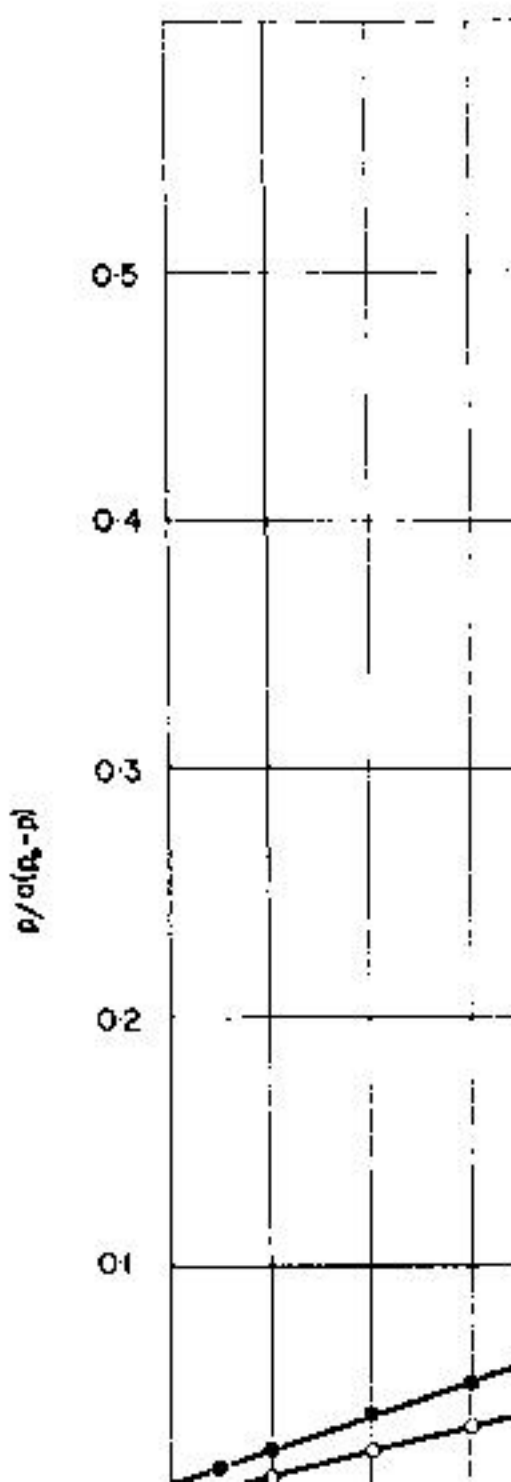
The association-induction hypothesis^{14,15} which deals with a broader topic agrees in essence with Troschin's sorption theory concerning ionic and nonelectrolyte distribution problems, although the two theories were developed independently. The association-induction hypothesis offers, however, specific molecular interpretation of the differences in solubility properties of the cell water in terms of restricted rotation of polyatomic non-electrolytes and de facto polyatomic hydrated ions¹ and of differences in the H-bond formed in the protoplasmic system.¹ The theory also stresses that the living protoplasm and hence protoplasmic water does not exist in one single physical state but as a rule, exists reversibly in more than one metastable cooperative states in the course of its normal physiological activity. Anticipating the evidence to be presented, we may state that it is our purpose in this paper to demonstrate that all or nearly all water molecules in a living cell can be considered to exist as polarized multilayers oriented on the surfaces of cell proteins. To demonstrate this, however, one cannot apply the direct approach which one uses on water sorption studies of stable inanimate systems because in living cells, the protein water systems are metastable; removal of water may bring about changes that are irreversible. Instead, we shall employ an indirect method which involves the three following steps: (1) establish multilayer adsorption of polarized water in one or more nonliving stable model systems; (2) choose properties exhibited by the water in living cells during its quiescent resting state; these properties must be significantly different from those of ordinary water and yet can be studied in the living cell without producing serious injury; (3) establish that this same property is also exhibited by the water in the nonliving model systems mentioned.¹

Ling: Physical St

In the following analyses, we have considered the properties of nonelectrolytes and of ions as the properties of water. In this paper we shall use strong electrolyte solutions, such as collagen from carp's swim bladder and serum albumin. The question of ionic distribution is complete and one of the properties of nonelectrolytes are still in progress. Nevertheless, these properties are included in this presentation as they represent different facets of the problem.

Polarized Water

Association of proteins with water can be studied by the sorption of water vapor on purified protein. The amount of water sorbed is plotted against the relative vapor pressure. This gives an S-shaped curve typical of sorption of gases on solid surfaces. Theories of such gas sorption have been proposed by Langmuir¹⁶ and Zwikker¹⁶ and by Bradley¹⁷; both suggest the action of van der Waals' attraction (or induction) as the cause of the build-up of water molecules. Brunauer, Emmett and Teller¹⁸ severely criticized the Langmuir theory (and of Bradley's theory on inductive action) and showed that the inductive action on gas molecules is quantitatively trivial; they offered instead the BET theory. The BET theory is, in



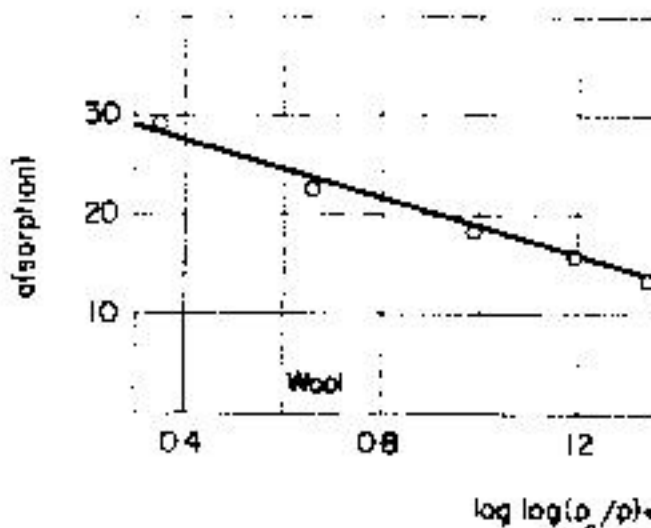


FIGURE 2. Water vapor sorption on sheep Bradley isotherm. Same data as in FIGURE 1.

agreement suggests that the polypeptide capable of orienting and polarizing suc-

In FIGURE 2 and FIGURE 3, the same and wool that appeared in FIGURE 1 are equation (Equation 1).† There is good agreement that in collagen and in wool, water polarized multilayers.

SELECTIVE EXCLUS
Namelectrolyte Ex

Copper ferrocyanide gel. Sheets to possess what later van't Hoff example, water but not sucrose to century, Moritz Traube²³ searched lar attributes; among those he (Cu₂ Fe(CN)₆) precipitation merely one of the best, if not the best a significant property of the Cu₂ Fe accommodates little if any sucrose. bran²⁴ studied the equilibrium dis- persion of Cu₂ Fe (CN)₆ gel; a m found in the clear supernatent so distributed in all the water with water is 100 per cent inaccessible each molecule of Cu₂ Fe (CN)₆ c an amount of water so large that lattice or on the surface of the sa water is "imbibed by the gel"; in fact, refers to water adsorbed in

"Coacervate." The same may a

Ling: Physical St

TABLE
DISTRIBUTION COEFFICIENTS OF NONELECTROLYTES
SULFONATE EXCHANGE RESINS AND ITS

	Dowex 50(H ⁺) (Wheaton and Bauman)	Rexyn RG 50(H ⁺) (25°C)	Amberlite IR-120 (25°C)
Urea	—	—	22.5
Methyl alcohol	0.61	0.94	2.2
Ethylene glycol	0.67	—	0.8
Glycerol	0.49	0.56	0.7
Xylose	—	0.23	0.6
Glucose	0.22	0.23	0.6
Sucrose	0.24	0.29	0.6

concentration of the fixed ions is usually low, i.e., 5. Wheaton and Bauman²⁷ report distribution of various alcohols and sugars and the external solution. Their data are similar to our studies on similar sulfonate-polystyrene

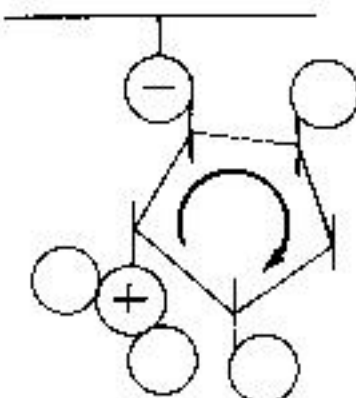
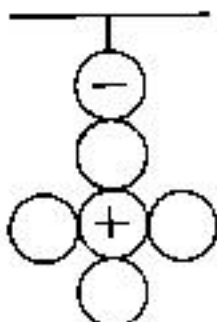
CATION EXCHANGE
RESIN

FIGURE 4. Diagram of a possible cation exchange resin, illustrating the form of H-bonds in the resin and hence size of arrows illustrates the relative

TABLE 2
DISTRIBUTION COEFFICIENT OF NONASSIMILATED SUGARS BETWEEN CELL WATER
AND EXTRACELLULAR WATER

Sugar	Frog muscle	Rat diaphragm muscle	Rat uterus (castrated adrenalectomized)	Rat adrenal gland
D-Xylose	—	0.52 ⁽⁴¹⁾ 0.341* ⁽²⁸⁾	0.82 ⁽²⁸⁾	0.79 ⁽²⁸⁾
Galactose	0.32 ⁽¹³⁾	—	—	—
Sucrose	0.29 ⁽¹³⁾	—	0.36 ⁽²⁸⁾	0.06 ⁽²⁸⁾

Data from references (13) and (41) were derived from *in vitro* studies; those from reference(27) from *in vivo* studies.

*Concentration of cellular sugar on the basis of fresh tissue weight instead of cell water.

"pumps"; yet, the water molecules differ from normal water only in that they are polarized and oriented in one way or another. Considered together, the data suggest that intracellular water may also be polarized and oriented and in this state, it excludes sugars.

SELECTIVE IONIC EXCLUSION

Ionic Exclusion in Living Cells

As in the case of nonelectrolytes, the earlier interpretation of asymmetrical distribution of ions was in terms of permeability or impermeability of the cell membrane. Thus, K⁺ ion was recognized as permeant and found in high concentration within the cell; Na⁺ ion, which is found at high concentration in the plasma, but low concentration in the tissue, was considered impermeant. As in the case of nonelectrolytes, however, advancing techniques (in particular, radioisotope techniques) soon proved unequivocally that Na⁺ ion is in fact also permeant.^{25,26} To remedy this failure of the original theory, the Na-pump was proposed. This was a very reasonable assumption at the time it was introduced, since similar "pumps" for Na⁺ and for nonelectrolytes undoubtedly operate across such biological "membranes" as intestinal mucosa, frog skin and kidney tubules, etc., at the expense of metabolic energy. Thus, it was thought that Na⁺ ion was an exception to the rule; by introducing the Na pump, or original

TABLE 3
MINIMAL ENERGY REQUIREMENT OF THE Na⁺, Ca⁺⁺ AND Mg⁺⁺ PUMPS IN
FROG MUSCLE CELLS IN COMPARISON WITH MAXIMAL
AVAILABLE METABOLIC ENERGY

Extracellular concentration (mM./l.)	Theoretical (Donnan equilibrium)		Intracellular concentration (experimental) (mM./l.)	"Permeability constant" (hr ⁻¹)
	Donnan Ratio	Intracellular concentration (mM./l.)		
K ⁺	2.4	53.4	128.0	0.077 ((1), p.292)
Na ⁺	105	53.4	16.9	1.223 (31)
Ca ⁺⁺	4.0	53.4	5.7	2.45 (32)
Mg ⁺⁺	2.5	53.4	15.8	4.16 (33)

concept of a sieve-like membrane may still be considered adequate to explain the distribution of all other ions and nonelectrolytes. In reality, this turned out not to be the case.

Extensive tracer studies have long since proven that many ions, hitherto thought to be impermeant, are in fact, also permeant. These include Ca,⁺⁺ Mg,⁺⁺ orthophosphate, lactate, sulfate ion, free amino acids, and many sugars.¹ The question is: Do they all follow equilibrium distributions predicted on the basis that the intracellular water is entirely the same as in an 0.1 N KCl solution? The answer is no. Thus the anticipated intracellular concentrations (on the basis of an assumption of equilibrium distribution in normal intracellular water) are for Mg⁺⁺ 3565 and for Ca⁺⁺ 5704 mM. per liter of intracellular water. In reality the intracellular Mg⁺⁺ and Ca⁺⁺ ion concentrations are 15.8 and 5.7 mM./l. respectively.

The same criteria (permeability and distribution not following that of Donnan equilibrium) that led to the postulation of the Na⁺ pump also fully apply to these ions. If the pump theory is not an *ad hoc* but general theory which supplements the pore-size concept whenever needed, there is no choice that there must be Mg⁺⁺ pump and Ca⁺⁺ pump as well. TABLE 3 summarizes calculations we have presented elsewhere in greater detail.²⁴ Even if each of the pumps operates at 100 per cent efficiency, the overall

Ling: Physical St

TABLE
MINIMAL ENERGY REQUIREMENT OF
FROG MUSCLE CELLS IN COM-
AVAILABLE METAB

	Fraction of nonenergy consuming efflux according to pump model	Electrochemical work per mole of ion pumped (volt-Faraday)	Efficiency assumed
K ⁺	100%	0	—
Na ⁺	0.1%	0.148	100%
Ca ⁺⁺	0.4%	0.142	100%
Mg ⁺⁺	0.15%	0.116	100%

striction of rotational (and to some extent translational) motion, hence a lowered entropy of ions and a corresponding increase in viscosity is summarized by the following equation. A similar version of this equation is used in studying the effect of ion size.

$$[p_i^+]_{in} = K_i [p_i^+]_{ex}$$

where $[p_i^+]_{ex}$ and $[p_i^+]_{in}$ are the concentrations of the ions outside and inside of the *i*th cation; $[p_s^+]_{ex}$ is the excess concentration of any one of the *m* other ions present in the system, which refers to any one of the *m* sites available for the *i*th. Where $[f_j]$ refers to the fraction of the *j*th site occupied by the *i*th ion among the *N* types of similar sites. K_{ij} and K_{is} are the equilibrium constants for the *i*th ion with the *j*th and *s*th monovalent cations on the same site. If we assume that $f_j = f_i$ (see below) for the *i*th ion with a high valence cation, $[f_i]$, one may on first approximation assume that $K_{ij} = K_{is}$. Then, if we drop the *J*th, rewrite and simplify Eq. (1), we get

$$[p_i^+]_{in} = \frac{K_i [p_i^+]_{ex}}{1 + \tilde{K}_{ij} [p_i^+]_{ex}}$$

where p_i refers to another multivalent cation. From a number of experimental studies, concentrations of the ions except the *i*th and *j*th, then, are assumed to be constant.

Ling: Physical S

TABLE
THE DISTRIBUTION COEFFICIENT OF Na⁺
AND OF SHEE

Frog sartorius mu

q_{Na}	ΔF° kcal./mole
0.19 (0°C.)	1.04
0.13 (25°C.)	

Sheep's wool

q_{Na}	ΔF° kcal./mole
0.16 (25°C.)	

is found to be 0.8. However, this e total water of the swim bladder t collagen tissue in the form of adh of K_{Na} between water in collagen a

The pattern of ion uptake in shee similar to that found in muscle c Equation 7. Wool contains 33 per of 0.16 at 25°C. and 0.1 at 37°C.

Molecular Mechanism of I

From data just given, one can librium:

$$|Na|_{in} \approx$$

to have a value of 1.247 kcal./mole. ΔH° is -3.15 kcal./mole and the a Thus, the Na^+ ion would have ac tration higher than that in the ex large entropy loss which more tha shown, by Guggenheim and Fowler atomic structure; as such by fa hence entropy) is the rotational pa entropy of Na^+ ion in the water in

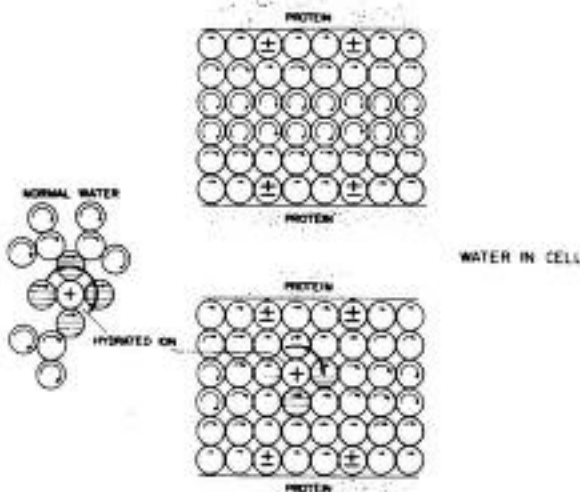


FIGURE 5. Diagram illustrating the physical state of water in the living cell in a region with hydrated ion (*lower right*) and in a region without a hydrated ion (*upper right*). Left figure is a diagram of a hydrated ion in normal water. The length of the curved arrows indicated the degree of rotational freedom of each water molecule; a progressively greater rotational freedom is shown for water molecules further away from the proteins. The merging and mutual reinforcement of the polarization (arising from the ion and from the proteins) and the anchoring effect of the fixed proteins produces a microscopic "droplet" of water molecules. In this "droplet", water molecules have greatly reduced rotational motion.

Chambers and his coworker²⁸ and later confirmed in more than one laboratory. A single frog muscle cell was supercooled to -6°C. Formation of one to many ice "spikes" progressed from the cut end of the muscle fiber when it was touched with an ice-tipped micropipette. The orientation of the "spikes" followed the orientation of the muscle fiber, straight when the muscle fiber was straight, twisted when the muscle fiber was twisted. The shape of ice crystal was different in other cells, being feather-like, for example, in sea urchin eggs. When the freezing was very rapid hundreds of such ice "spikes" could form in a single muscle fiber. A comparison of the cross-section of such a frozen cell²⁹ with a similar cross-section of a frog muscle fiber seen through an electron microscope³⁰ suggests that the ice formation occurs between the protein filaments which run longitudinally along the length of the muscle fiber. Thus, the frozen portion of the cell water must correspond to the water occupying intracellular space farthest away from the polarizing surfaces of the protein molecules. The fact that (1) water not in the form of ice remains in cell proteins after the completion of the intracellular freezing and that (2) no branching or horizontal propagation of ice "spikes" occurs²⁹ also suggests that the layer of

water immediately adjacent to the proteins is strongly oriented and that transformation of their structure to ice is energetically unfavorable. All these are in complete accord with the physical state of cellular water which is deduced from the study of ions and nonelectrolyte distribution reported in this paper.

SUMMARY

Sorption of water vapor on collagen and on sheep's wool fits the BET theory up to 50 per cent vapor saturation; the same data fits the Bradley multilayer adsorption isotherm of polarized molecules to near saturation, suggesting that water in these systems is polarized and oriented in multilayers. It was shown that Na^+ ion is excluded from this water in wool so that it reaches an equilibrium concentration of about 0.1 that in the external medium; a quantitatively similar situation exists in living frog muscle cells. In both, the equilibrium distributions have negative enthalpy values and large negative entropy values suggesting that the water in the hydrated shell of Na^+ ion merge with and reinforce polarized water in the system and form stronger H-bonds, but this advantage favoring distribution in the wool (or cell) is more than offset by the large entropy loss in the restricted rotational freedom.

REFERENCES

1. LING, G. 1962. A Physical Theory of the Living State: The Association-Induction Hypothesis. Blaisdell, New York, N. Y.
2. FORSLUND, E. 1952. Proc. Swed. Cement Concrete Res. Inst. No. 16.
3. JACOBSEN, B. 1955. Svensk. Kem. Tidskr. 67: 1.
4. SZENT-GYÖRGYI, A. 1957. Bioenergetics. Academic Press, New York, N. Y.
5. KLOTZ, I. M. 1958. Science 128: 815.
6. BEEMAN, W. W., P. GEIL, M. SHURMAN & A. G. MALMON. 1957. Acta Cryst. 10: 818.
7. HEARST, J. E. & J. VINOGRAD. 1961. Proc. Nat. Acad. Sci. 47: 1005.
8. RITLAND, H. N., P. KAESBERG & W. W. BEEMAN. 1950. J. Chem. Phys. 18: 1237.
9. BERENDSEN, H. J. C. 1962. J. Chem. Phys. 36: 3297.
10. GORTNER, R. A. 1938. Outlines of Biochemistry. 2nd. Ed. New York. Gortner, R. A. 1937. Selected Topics in Colloid Chemistry. Chap. 8. Ithaca, New York.
11. BLANCHARD, K. C. 1940. Cold Spring Harbor Sym. Quant. Biol. 8: 1-8.
12. WEISMANN, O. 1938. Protoplasma. 31: 27.
13. TROSCHIN, A. S. 1958. Das Problem der Zellpermeabilität. Fischer, Jena, Germany.
14. LING, G. N. 1962. In Phosphorus Metabolism. W. D. McElroy & B. Glass, Ed. (2): 748. John Hopkins Press, Baltimore. (2): 748.
15. LING, G. N. 1964. Texas Rep. Biol. Med. 22: 244.
16. DE BOER, J. H. & C. ZWICKER. 1929. Z. Physik. Chem. B3: 407.
17. BRADLEY, S. 1936. J. Chem. Soc. : 1467.
18. BRUNAUER, S., P. H. EMMETT & E. TELLER. 1938. J. Am. Chem. Soc. 60: 309.
19. BRADLEY, S. 1936. J. Chem. Soc. : 1799.
20. BULL, H. 1944. J. Am. Chem. Soc. 66: 1499.
21. HNOJEWYJ, W. S. & L. H. REVERSON. 1959. J. Am. Chem. Soc. 63: 1653.

Ling: Physical St

22. MELLON, S. R. & E. F. HOOVER. 1950. J.
23. TRAUBE, M. 1876. Arch. Anat. Physiol.
24. McMAHON, B. C., E. J. HARTUNG &
Soc. 33: 398.
25. EDSELL, J. T. & J. WYMAN. 1958. Biophys.
New York, N. Y.
26. LONG, F. A. & W. F. McDEVIT. 1952. Ch
27. WHEATON, R. M. & W. C. BAUMAN. 19
28. HECHTER, O. & G. LESTER. 1960. Rec.
29. STEINBACH, H. B. 1952. Am. J. Physiol.
30. HEPPEL, L. A. & C. L. A. SCHMIDT. 19
31. LEVI, H. & H. H. USSING. 1948. Acta. Ph
32. TASAKI, I., T. TEORELL & C. S. SPYRO
33. CONWAY, E. J. & G. CRUESS-CALLAGH
34. LING, G. N. 1965. J. Gen. Physiol. 24: S
35. LING, G. N. & M. OCHSENFELD. 1965.
36. FOWLER, R. H. & E. A. GUGGENHEIM
Cambridge Univ. Press. New York, N.
37. LING, G. N. 1955. Am. J. Phys. Med. 34:
38. CHAMBERS, R. & H. P. HALE. 1932. Proc.
39. LUYET, B. J. 1965. This Annal.
40. HUXLEY, H. E. 1957. J. Biophys. Bioc
41. KIPNIS, D. M. & C. F. CORI. 1957. J. Bio

THE STRUCTURE OF WATER PEPTIDES AND AMINO ACIDS DIELECTRIC

Edward

Physics Department, Guy's Hospital,

With the exception of Schwan's dielectric studies on protein solution regions of the protein molecule investigations are found in the literature. *Infrared* and *radiofrequency* measurements at microwave frequencies previous measurements for egg albumin (cf. *Dielectric Properties of Proteins*, *et al.*, 1952) who made measurements at 1000 m. and 10 cm. wave length. In view of the fact that no previous measurements for egg albumin have been made at the same frequencies as those used in the present work it was decided to make such measurements for this purpose.

In this paper the results on both the infrared and radiofrequency measurements in terms of the protein molecule size

Grant: Structure

TABLE
DIELECTRIC DECREMENTS

Temperature	Egg Albumen		$C = 0.001$
	$f = 250 \text{ Mc/s}$	$f = 450 \text{ Mc/s}$	
0	$1.05 \pm .08$	$1.02 \pm .08$	
10	$0.87 \pm .08$	$0.94 \pm .08$	
20	$0.80 \pm .07$	$0.89 \pm .07$	
25*	$0.74 \pm .07$	$0.85 \pm .07$	
30	$0.69 \pm .07$	$0.80 \pm .07$	
40	$0.56 \pm .05$	—	

Bovine serum albumen			
Temperature	$f = 250 \text{ Mc/s}$	$f = 450 \text{ Mc/s}$	$C = 0.001$
0	$1.03 \pm .08$	$1.06 \pm .08$	
10	$0.89 \pm .08$	$0.92 \pm .08$	
20	$0.84 \pm .06$	$0.87 \pm .06$	
30	$0.76 \pm .06$	$0.80 \pm .06$	
40	$0.61 \pm .05$	—	

* $\delta_0 = 0.70$ (Onokey, 1943); $\delta_0 = 0.95$ (1943).

water in order to account for the volume occupied by the protein molecules, and the precise nature of this correction is unknown.

Consequently all deductions about the dispersion parameters have been made from the decrement variation. It is only possible to make a complete analysis for egg albumen at 25°C. since this is the sole case where the decrements at very low (δ_s) and very high (δ_∞) frequencies are known. For egg albumen at 25°C. the relaxation region is represented by the Cole-Cole equation

$$\frac{\delta}{\delta} = \delta_\infty + \frac{\delta_\infty - \delta_s}{1 + \left(\frac{j \lambda_s}{\lambda} \right)} 1 - \alpha \quad (3)$$

where the symbols have their usual significance. The value of α is 0.15 ± 0.15 which indicates the probable existence of a small distribution of relaxation times, but is incompatible with a wide distribution of relaxation times as was reported for hemoglobin by Schwan (1957). The limits of error are necessarily wide in this type of investigation due to the required parameter being deduced from a small difference between two large measured quantities.

The relaxation wavelength (λ_s) was calculated as 100 cm. (300 Mc/s) at 25°C. and the activation energy (ΔH) was deduced from the variation of λ_s with temperature to give the result 16 ± 5 kcal./mole (TABLE 2).

In the derivation of $d\lambda_s/dT$ it was assumed that the variation of decrement with temperature at the frequencies of measurement $d\delta/dT$ was very much greater than $d\delta_s/dT$ or $d\delta_\infty/dT$. This is true when the frequencies of measurement are near the relaxation frequency, and leads to a linear relationship between $d\lambda_s/dT$ and $d\delta/dT$. The assumption is further justified if $d\delta_s/dT$ and $d\delta_\infty/dT$ are in opposite directions, which is likely.

Owing to the lack of results at high and low frequencies it is impossible to make analyses of egg albumen at any temperature other than 25°C. Nevertheless, it is clear from TABLE 1 that δ varies strongly with frequency at all other temperatures, and strongly with temperature at all frequencies. Similar behavior is exhibited by serum albumen as seen from TABLE 1. These results, taken together with Schwan's observations for hemoglobin, show that this subsidiary dispersion occurs for at least three proteins, and

TABLE 2
SUBSIDIARY DISPERSION IN EGG ALBUMEN

Cole-Cole Parameter α	λ_s (cm) at 25°C	ΔH (kcal./mole)
0.15 ± 0.15	100	16 ± 5

Grant: Structure

it will be interesting to extend this to other proteins.

Interpretation of Dielectric Parameters

The preceding sections of this paper establish the existence of a relaxation around 300 Mc/s with an activation energy. The more difficult task, however, is the interpretation of the data with the same amount of confidence.

Both in this Conference and previously I have advanced the idea that bound water may have activation energies which has not provided activation energies. Gelatin adsorbed to silica gel is reported as having an activation energy of 1.2 e.v. (Hasted, 1961). It therefore seems a reasonable dispersion observed in the present work. A more mathematical analysis on these lines will be given later.

In a previous communication (Grant, 1961) it was shown that most known dielectric mixture formulae can be written as

$$\epsilon_M = \epsilon_w + kV,$$

where ϵ_M refers to the mixture and ϵ_w , ϵ_k and V refer to the pure components and the volume fraction of the dispersed phase respectively. The volume fraction V is a constant equal to or greater than

molecular picture of bound water. three hydrogen bonds, that is, in bound water molecule can rotate in

Although the rotation of the bound water molecule is not the only explanation for the observed dispersion of the protein molecule. There are many polar groups present in the albumen molecule bearing both positive and negative charges. The 52 glutamic acid residues and 20 lysine residues in their water environment would be expected to occur in the same frequency.

A quasimacroscopic explanation of the dispersion of the protein molecule by the albumen molecule of an N. S. Aoki (1957). The N and F forms of the protein molecule are interconvertible during electrophoresis, and the energy required for the conversion from one form to the other is 15 kcal./mole.

Peptides and Proteins

Some very recent measurements have been made on the dispersion of some amino acids and peptides, and the results are summarized in TABLE 3 (Aaron, 1964). This is the first time that the dispersion of

properties of amino acids and peptides over a temperature and frequency range, the previous measurements having been made over 30 years ago and at 25°C. only (Wyman & McMeekin, 1933). It is very interesting to notice, however, that there is substantial agreement between the dielectric increments obtained by Aaron and Wyman.

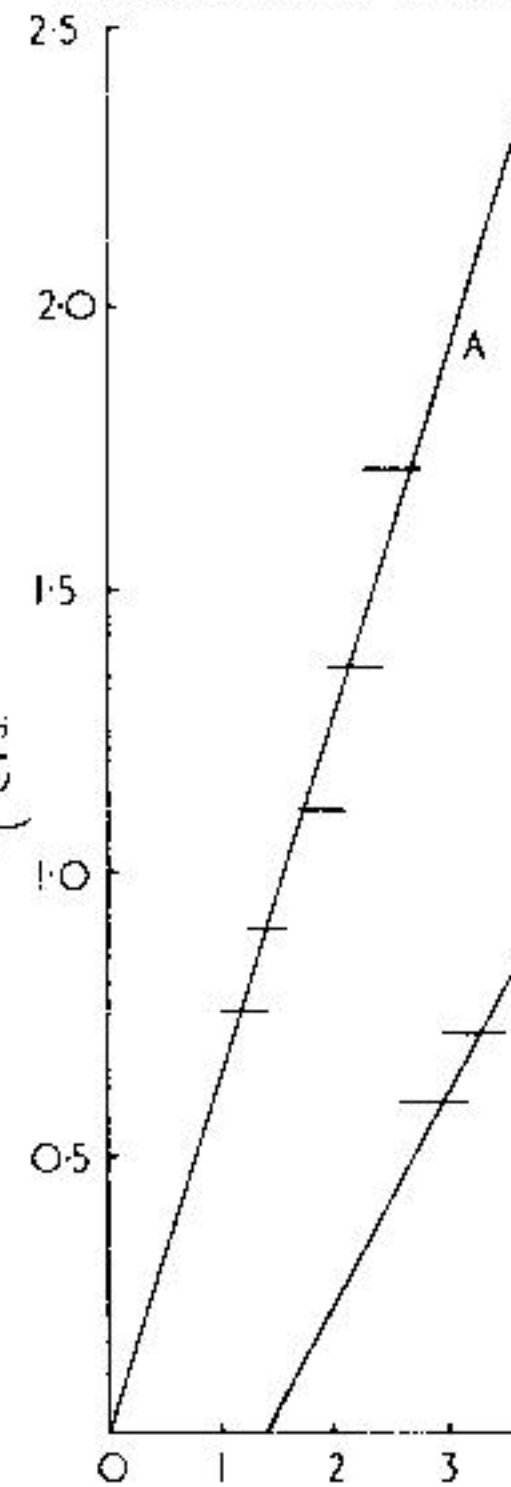
The dipole moments were calculated using Kirkwood's theory plus appropriate approximations (Kirkwood, 1943), and the charge separations obtained accordingly.

In the case of the three amino acids studied, the charge separation is in agreement with that expected from structural considerations, and it can be noticed that the larger charge separation in β -alanine gives rise to a much higher dielectric constant than for α -alanine.

On the other hand, the charge separation (τ) for the peptides is lower than would be expected for a linear ionic polymer. For example, the value of τ for diglycine as a linear molecule is calculated as 7.2 Å whereas the observed value is 6.0 Å and the relative difference for triglycine is greater. Even allowing for the approximations involved in using Kirkwood's theory these differences are significant and suggest that the peptide backbone is curved in solution, due no doubt to the electrostatic attraction between the polar groups on the ends of the molecule. That the curvature is not greater could be explained by the screening effects of the charges on the bound water molecules, i.e., the lone pair electrons on the oxygens in the case of the amino groups and the protons in the case of the carboxyl groups. Although the values reported in TABLE 3 are at 20°C. only, measurements were made over the range 0°C. - 50°C. for all six solutions and showed that the increment decreases as the temperature increases. It was also found for glycine, diglycine and triglycine that a straight line relationship exists between the dielectric increment and the number of carbon atoms between the NH_3^+ and COO^- groups.

The activation energies for dielectric relaxation (ΔH_7) shown in TABLE 3 are all compatible with the breaking or distorting of a hydrogen bond between the solute molecule and a neighboring water molecule. The bond energy is smaller for β -alanine than for α -alanine which is consistent with the observed behavior of the other molecules in TABLE 3 since ΔH_7 decreases as the charge separation increases. From the structure of the amino acids considered it may be expected that each molecule could form up to a maximum of five hydrogen bonds but the dielectric results show the molecules can rotate upon breaking one bond. This suggests that there must be many molecules which form an average of only two hydrogen bonds to their water environment at any one instant at 20°C.

Turning now to the three peptides, it is seen that the activation energy decreases with the size of the molecule, which is a somewhat unexpected revelation. In contrast, the actual magnitude of the relaxation wavelength increases with molecular size, as is usual. It would therefore appear as



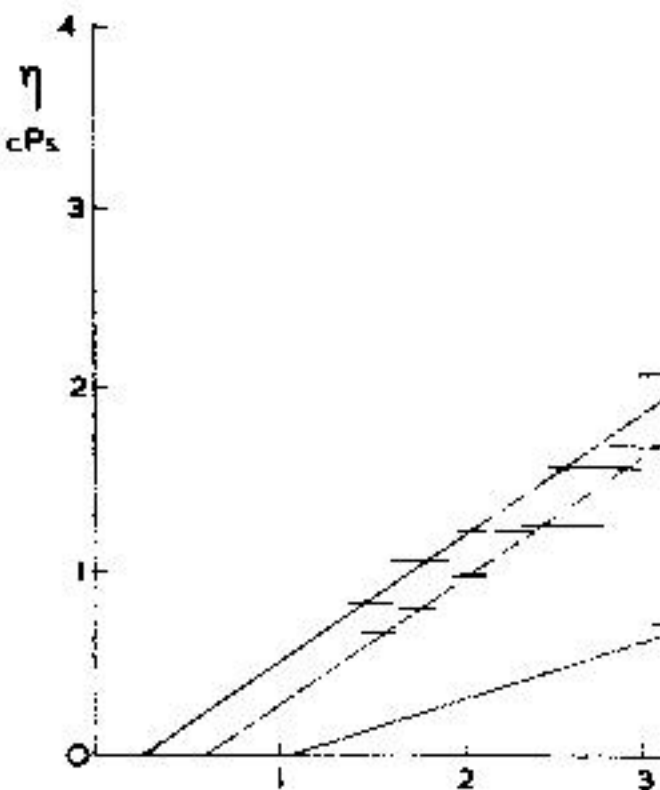


FIGURE 2. Relationship between relaxation viscosity for the alanines and glycylalanine. C — glycylalanine.

η_r T. The macroscopic dielectric relaxation is the molecular radius. Although a straight line is obtained for the first two, the deviation from the origin increases with molecular weight. It is also noticed for the peptide viscosity process (ΔH_{vis}) is greater than

from a few megacycles to hundreds for this process is such as to suggest that the molecules are "ice-like" rather than akin to liquids when dielectric properties are concerned.

In the case of the amino acids and peptides dielectric relaxation is governed by hydrogen bond linking the solute molecules. That the energy required to break the bond in peptides seems to suggest that the vibrational rotation involving the bending of the molecule is complete rupture of the bond. There is no evidence that the molecule relaxes. The activation energy for dielectric relaxation in the peptides is so small that one hydrogen bond is involved. It is suggested that for dielectric relaxation in the proteins there is a contribution due to the translational motion involved.

This work is being extended to other proteins and, when all the data is available, will be tentatively advanced in this present paper.

Acknowledgments

Thanks are due to Professor C. S. H. Williams, F.R.S., of Guy's Hospital Medical School, London, for his help and for providing the necessary facilities to enable this work to be carried out.

Grant: Structure

- SAXTON, J. A. 1952. Proc. Roy. Soc. A **213**: 4.
- SCHWAN, H. P. 1957. Advances in Biolog
demic Press, New York, N. Y.
- SCHWAN, H. P. 1964. This Annal.
- WYMAN, J., JR. & T. L. McMEEKIN. 1933.

SOLUTE BEHAVIOR IN DEXTRIN

N. V.

*Institute
University of*

The selectivity of neutral, or very weakly ionized, solutes has received considerable interest in recent years. The molecular sieving properties of starch, the selectivities of which the molecular sieve theory has been applied, have received particular attention particularly in the macroscopic range. The development of a general theory regarding the mechanism of molecular sieving in starch has been slow, and it is the purpose of this paper to review the available information on the molecular sieving properties of starch and other molecular nonelectrolytes in tightly cross-linked polymeric systems.

In general the molecular sieving properties of starch are similar to those of cellulose. The sieving range now includes all sizes of molecules, extending from the smallest proteins to the largest cellular particles.¹⁻⁴

The distribution of solutes in starch depends on both steric and interactional factors. The presence of a large number of hydroxyl groups makes it possible to study solutes in terms of their behaviour in terms of the

Marsden: Solu

Dextran, the parent of the dextran gels, is in an amorphous, non-crystalline state, and is high enough the mechanism of water-solubility a solution process. Starch¹⁶ and dextran are both relatively simple and possess crystalline areas which are easily ruptured. Clusky and Senti¹⁷ found that for absorption measurements in the infrared, starch showed little tendency to crystallize. Dextran, however, was treated the polymer as though it is a random coil, and was a good model up to about 65 per cent cross-linkage. Since dextran is a basic material for gels, dextran seems to have a relatively homogeneous structure, though the dextran used (B 512) used in the gels studied here showed some tendency to crystallize.¹⁸

The introduction of cross-linkages is intended to promote crystallization since this has been shown for dextran. Further, the use of glyceryl bridged cross-links in the gel structure of the gel is not essentially different from the cross-linkages of the gel DVS 920, which is a glyceryl linked G-10 of similar water content. The elution behaviour for some sugars and

where V_i is the effluent volume after the volume (void) of water outside the column and V_c is the volume of water in the column and V_g is the volume of particles of gel (water regain).

It will be assumed that the K_d values between the phases inside and outside the column (see below) were not affected if (1) the water regain was considerably increased¹⁰, (2) the equilibrium distribution coefficients measured on dextran gels containing glucose in a dextran gel (water regain) and on dextran gels containing no glucose in a dextran gel (water regain) values were similar, it has been reported good agreement for equilibrium distribution coefficients on a dextran gel type G-75, between the total volume of the system minus the volume of the gel and the volume of the system minus the volume of the gel as dextran is distributed. $H_2^{18}O$ was used to measure the total water space in a gel system. Tritium labeled water (THO) has been used instead of $H_2^{18}O$ because of the exchange of hydrogen under certain conditions with the three hydroxyl groups in the dextran chain (and the hydroxyl groups in the cellulose chain), since deuterium of D_2O was found to

Marsden: Solu

Samples of gel type G-25 dried for 4 hr were not sufficient to remove all traces of water containing THO. The tritium content was about 106 per cent of that expected if there were no water.

In gel DVS 9 (water regain 0.93) which has a cross bridge (with no exchangeable protons), $(V_1 + V_x)/V_1$ will have the value 1.1.

Solut

The main part of the data concerns gel DVS 9. Four series of solutes were used: (a) aldehydes, (b) aldoses,* (c) n-alcohols and (d) alkyl amide and acetone. In addition K_d values in gel type G-25 are given.

Concentration

In most cases solutes were loaded at concentrations below 0.1 M and determined in the effluent. Isotopically labelled derivatives, or cleavage products, appear to be largely independent of concentration. The results were unaltered in the following loading range:

cannot be characterized by an isotherm on the solvent and essentially independent of concentration. In addition to the great effect exerted by the solvent, the migration of an ion is influenced by the concentration of the solute and temperature. Studies on electrolyte migration in gel suspensions consisting of dextran gel suspensions have been made by several workers.¹⁷

Acyclic Sugars

The general formula for this series of hexitols is $C_6H_{12}O_n$, where $n = 3, 4$ in the present case. The values of α_D^2 are proportional to molecular weight as is shown in TABLE 2. The values of α_D^2 for the hexitols lie between the two hexitols and between the values for the corresponding disaccharides compared with the variations among the monosaccharides (see TABLE 3). Whether the other hexitols have similar values is not known, but Isherwood¹⁸ has reported values for sorbitol and dulcitol in paper.

As has been mentioned earlier, the values of α_D^2 reported in this paper represent quantities which are proportional to the size of the particles and thus are a measure of the size of the particles.

Marsden: Solu

TABLE
POLYHYDRIC ALCOHOLS

Polyol	Mol Wt	V_m^*
Ethane diol	62	100
Glycerol	92	100
Erythritol	122	100
Pentitol†	152	100
Hexitol‡	182	100

* V_m = molal volume calculated from

†Mean of ribitol and arabitol

‡Mean of mannitol and sorbitol

Various geometrical models of the gel structure have been proposed to account for the behavior of solute molecules. One suggested by Pedersen¹⁸ might be called the "gel chain model." According to these models is the assumption that the volume available for solute molecules within the gel matrix is limited by steric hindrance by the gel chains. The elution volumes of solutes from wet gel as a random suspension of fibers have given reasonable agreement with the relationship between some molecular parameters and the ratio of the Stokes radius and the elution volume. In this model the volume within the gel matrix depends on the distance of the center of the polyglucose chain of the gel at any point from the center of the solute. The greater the center-to-center distance, the greater the volume available for the solute. This model thus has the important implication to other models, that it does not require that the solute molecule may not penetrate the gel matrix. The gel matrices would therefore be able to penetrate the solutes. This difference would have to be discussed below.

The success of these models in predicting the relationship between the elution volume and a molecular parameter such as the ratio of the

Marsden: Solut

elasticity of the gel matrix, creating a mechanical potential of the solvent in the swollen outside the particles. To quote Flory¹¹ "the multiple role of solute, osmotic pressure device." The internal pressure will act within the wet gel. Thus

$$\pi V_i = -RT \ln$$

where π is the internal pressure of the gel, V_i partial molal volume of the solute, a_i activities in gel and external solution. It can be seen that for a given internal pressure, the concentration of a species within the gel will be proportional to its activity in the gel, and since the distribution coefficient is the ratio of activities in the two phases, this will also vary inversely with the concentration of the solute.

The difficulty in assessing the magnitude of the effect is that gels containing dextran gels with different internal pressures have different water regain values and hence different equilibrium swelling ratios. From a structural point of view, however, the glucose residues of the dextran chains are very similar to the glucose residues of the cellulose chains.

to have a small disordering effect. The "hydration" water are thermodynamically available to the polymer. It is conceivable that some of the water may be bound to the polymer. Glueckauf & Kitt¹⁶ give the hydration number K_d for the Li^+ form of the polymer as ~ 0.7 in a sulphonated polystyrene gel. The amount of the more swollen Li^+ form is however dependent on the "solvent" water available for the polymer.

More work is required to elucidate the mechanism of ion exchange. Laurent¹⁷ compared the behaviour of the polymer in carboxylic acid gels and solutions. There was no change in the equilibrium constant where the internal pressure should have been zero.

It is however of interest that the equilibrium constant for ion exchange was somewhat lower than that calculated from the acid concentration.¹⁷ It would be interesting to know if this factor contributed to the apparent increase in the equilibrium

A

The relationship between K_d and the properties of the polymer with the polyols, and the isomeric effect on the equilibrium constant in K_d values (FIGURE 1, TABLE 3), does not necessarily indicate the effect of other interactions on the equilibrium constant. Substitution of molecular weight by the reciprocal of the molecular weight indicates that the equilibrium constant increases with increasing molecular weight. This is in agreement with the results of Glueckauf & Kitt¹⁶ who found that the equilibrium constant increased with increasing molecular weight of the polymer.

TABLE
K_d VALUES OF FOUR ENANTIOMORPHIC A

Sugar	L-
Arabinose	0.647
Xylose	0.659
Glucose	0.576
Mannose	0.627

TABLE 2 shows that there was no significant difference in the K_d values of the D and L forms of arabinose and xylose. This suggests that specific adsorption to the polyols is not selective towards these sugars since the asymmetric glucose retains some selectivity towards enantiomorphs.

The point at which the K_d behaviour of the polyols changes from a linear relationship to the polyols coincides with the presence of marked conformational variations, particularly in the ring closure of the aldopentoses and aldohexoses.

Free forms of these sugars in aqueous solution exist in acyclic forms (polyhydroxyaldehydes) or their acetals. Ring closure of the open chain form may occur in different ways.

T

INSTABILITY FACTORS AND K_d VALUES
 [A anomer; AE composition of
 C1, 1C instability ratings in the
 weighted sum (Kelly) of instabilities;
 Ref. 18.]

	A	AE	C1
D-Arabinose	α		(1,2,3)
	β		(Δ 2,3)
D-Xylose	α		1
	β		-
D-Lyxose	α	76.0	1,2
	β	—	
D-Ribose	α	24.0	Δ 2
	β		
D-Galactose	α	1,3	
	β	3	
	α	29.6	1,4
	β	—	
	β	70.4	4

Applying this to the pyranose ring where, because of the asymmetry, each conformation produces a unique structure, Reeves¹¹ postulated that there will be two rigid "chair" forms (designated C1 and 1C) and an infinite number of flexible "boat" forms, which may be described in terms of six specific forms whose interconversion involves little ring strain. Interconversion of the rigid chair forms, on the other hand, involves considerable deformation and rotation of the ring valences.

The sugar in solution is thus an equilibrium of a number of conformations of the pyranose ring in addition to possible acyclic and furanose forms. The evidence seems to favour the predominance of chair forms of most of the aldopentoses and aldohexoses and an apparent correlation between the so called instability rating and the order of K_i values will be discussed below. The most stable form¹² will be that in which the substituents are staggered (chair form) with respect to each other; if viewed down the axis of a C-C bond the substituent group of the further atom would not be eclipsed, i.e. in line with the substituents of the nearer atom. This will occur in the boat forms and the substituents on adjacent carbon atoms will approach each other so closely that van der Waal's repulsion (destabilizing) forces will oppose this conformation. Thus energetically the "staggered" chair conformation will be preferred to the boat form unless other considerations make the chair form energetically unfavourable.

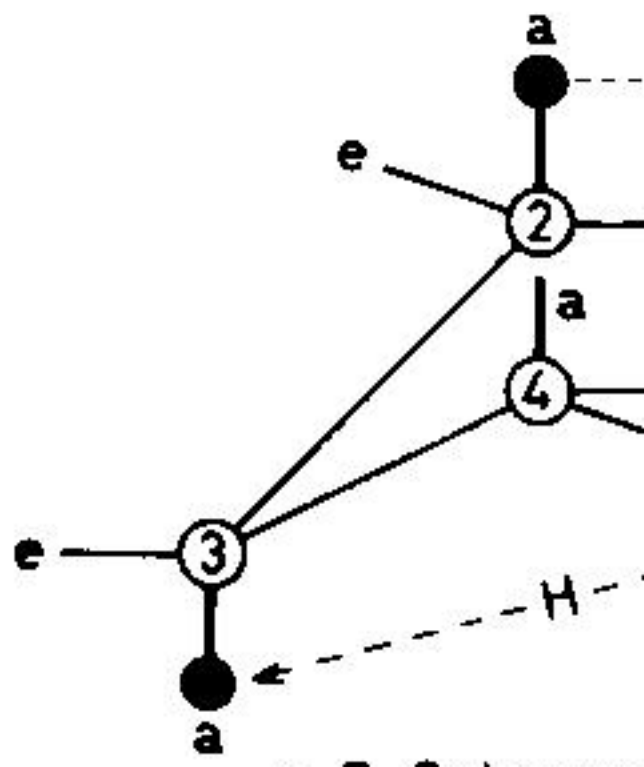
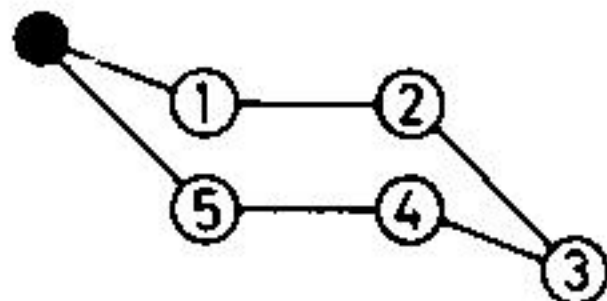
In the aldopyranoses the assumption of a chair form in solution means that in all cases except β -D-Xylose and β -D glucose some of the substituents (other than hydrogen) will lie axially.

FIGURE 2 illustrates the structure of the chair forms and shows (III) that equatorial groups (e_1, e_2) on adjacent carbon atoms are directed within 30° of the plane of the ring but do not eclipse each other, while axial groups (a_1, a_2) are nearly perpendicular to the plane of the ring. The staggering of the substituents means that if hydroxyls on adjacent carbon atoms are *cis* they will have different directions (i.e. ea or ae) while if they are *trans* they will be either both equatorial or both axial [FIGURE 2 (II)].

The positions of the hydroxyl groups at carbon atoms 1, 2, 3 and 4 (C_{1-4}) and the exocyclic carbinol group at C_5 affect the conformational stability and chemical reactions of the ring.¹³ An axial position creates instability, and in general the chair conformation most preferred will be that with most bulky or polar substituents equatorial. Most sugars could theoretically be arranged with all their hydroxyl groups equatorial in a boat form, and although a pure boat form is improbable on energetic grounds, it is possible that distorted boat forms exist because of this tendency of axial groups to become equatorial.¹⁴

The instability rating depends on the presence of axial groups and the weights attached to them. Two axial arrangements appear to be particu-

C 1



larly important.⁴¹ The Δ_2 factor occurs when the C-O bond at C₂ bisects the two C-O valences of C₁; this can only occur if the hydroxyls at C₁ and C₂ are *cis* and in the α anomer in the 1C form (FIGURE 2, III) and in the β anomer in the C1 form. The Hassel-Ottar (H) effect⁴² occurs when the carbinol at C₅ is axial on the same side of the ring as another axial hydroxyl (FIGURE 2, II).

Kelly⁴³ weighted the instability factors as follows: axial OH = 1 unit, Δ_2 = 2.5 units, C₂-CH₂OH axial, without H effect = 2.0 units, with H effect = 2.5 units.

If the instability rating (sum of the weighted instability factors) of the two chair conformations differ by one unit, or less, then the presence of both C1 and 1C forms is presumed. If the difference is more than one unit, it is assumed that the sugar is entirely in the conformation with the lower instability rating.^{41,44} Reeves⁴⁵ also proposed that whatever the difference a rating of 2.5 units or more would produce instability; this would mean that the Δ_2 factor alone could induce conformational instability.

When attempting to correlate these instability factors with other data, due weight should be given to the anomeric equilibrium, and it should also be borne in mind that, in addition to possible boat or distorted boat forms, furanose rings or acyclic forms may also be present in significant proportions in some cases.

TABLE 3 gives K_i values and instability data for the C1 and 1C forms of the aldopentoses and aldohexoses. Of the aldopentoses arabinose and xylose have low instability ratings and the lowest K_i values of the pentoses, while glucose and galactose have the lowest instability ratings and K_i values of the hexoses. Lyxose has a higher K_i value than xylose or arabinose and has a high instability rating, complex mutarotation and calculations of its molecular optical rotation suggest the presence of both C1 and 1C forms.⁴⁶

FIGURE 2. Chair conformations of the pyranose ring. I, the two conformations C1 and 1C; the terminal black circle is the ring oxygen atom. II, α -D-Galactose(1C) showing the relative positions of the hydroxyl groups (black circles). e and a refer to the equatorially and axially directed valences respectively. v is the ring oxygen atom and the carbinol group is axial at C₅. Note (a) that the carbon-oxygen (hydroxyl) bond at C₂ bisects the angle between the two C-O bonds at C₁ (Δ_2 effect) and (b) the Hassel-Ottar effect when there is another hydroxyl axial on the same side of the ring as the carbinol group at C₅. The instability rating is given below. III, A Courtauld model of the right hand end of the 1C form (viewed in the direction 'v' indicated in II). The ring oxygen atom is in dotted outline (O) with the bond to C₅ also dotted. The tetrahedra of C₁ and C₂ are shown (X is the C₁-C₂ bond) and the dotted arrow is the C₁-O bond. α (OH) and β (OH) refer to the anomeric hydroxyl group. The model shows (1) the bond angles and (2) the Δ_2 effect with a_2 bisecting the angle between e_1 and the C₅-O bond. This can only occur with a non-erected (equatorial) hydroxyl at C₁, i.e. in the α anomer in the 1C form and in the β anomer in the C1 form.

Ribose is apparently anomalous among pentoses and has a low instability to rotation and contains at least 8.5% of a form which may represent the acyclic aldehyde. The equilibrium constants for the interconversion of pentoses at pH 7.6 do not exceed unity, and the cyclic chain form would be expected, however (the two hydroxyl actions being equal) to reduce the equilibrium constant.

The three aldohexoses with the anomeric hydroxyl group in their probably preferred forms have the same value for the H factor in their 1C forms.

Erection of a hydroxyl group (either axial or equatorial) at C₂ or C₃ is associated with a change in the H factor being greater at C₂ (this involves the α and β anomers). Erection at C₁ appears to have little effect on the H factor except when the C₂ hydroxyl is also erected.

The effects of erection at C₁ are best illustrated by the fact that glucose exists as an anomeric mixture in solution. The values of the equilibrium constants for the interconversion of the anomers might be of help both in the estimation of the relative stabilities of the anomers and in the estimation of the contributions of the α and β anomers to the total equilibrium constant.

The right hand column of TABLE I gives the results of the column chromatography¹⁸ with an ethyl-acetate

TABLE 4
RATINGS OF HOMOMORPHOSIS SERIES
difference between hexose and methyl-pyranoside,
(same as in TABLE 3.)

		hexoses				-methyl hexapyranoside	
	A	$\Sigma(CI)$	$\Sigma(IC)$	ΔK_d^1	K_d	ΔK_d^2	
13	α	2	0	0.093			
	β	1	0				
76	α	3	3.5	0.034			
	β	3.5	4.5				
38	α	3	3.5	0.008			
	β	3.5	4.5				
	α	2	0				

bonding.³⁰ Thus the only interaction is between solute-gel and gel-solvent, but their

Equatorial hydroxyl groups in a glucose molecule are more strongly adsorbed than axial groups, and this is true in view of the lack of any difference in the temperature dependence of the equilibrium constants, which indicates the possibility of some interaction.

Kabayama and Patterson³⁰ suggested that glucose molecules with all their hydroxyl groups equatorially oriented would fit into a water lattice with all hydrogen bonds satisfied. If this were true, glucose groups will, on the other hand, involve some interaction with the solvent if the sugar is to be fitted into a water lattice.

Glucose and xylose have lower K_1 values than galactose. From an interactive view point this means that glucose has a relatively low affinity for the gel. It is interesting to note that their isomers with a hydroxyl group at C₁, i.e., galactose and mannose, have similar or slightly lower K_1 values. We do not have more information about the interaction of glucose with the gel from incorporation of an axial C₁ group, but we can compare it with the situation with other axial hydroxyl groups. The effect on the K_1 value much more.

Marsden: Solut

TABLE
ALKANE DIOLS: Gel I
[Concentration of diol loaded onto c

Diol	Mol. Wt
Ethylene glycol	62
1.2 Propane	76
1.3 Propane	76
1.3 Butane	90
1.4 Butane	90
2.3 Butane	90
1.5 Pentane	104
1.6 Hexane	118

K_d value a little less than that of 1.5 μ , there is some variation among the different diols.

Acetone, which is weakly polar, has a K_d value of 1.5 μ (FIGURE 1).

The effect of non-polar groups is illustrated by the changes in K_d produced by hydroxyl substituents.

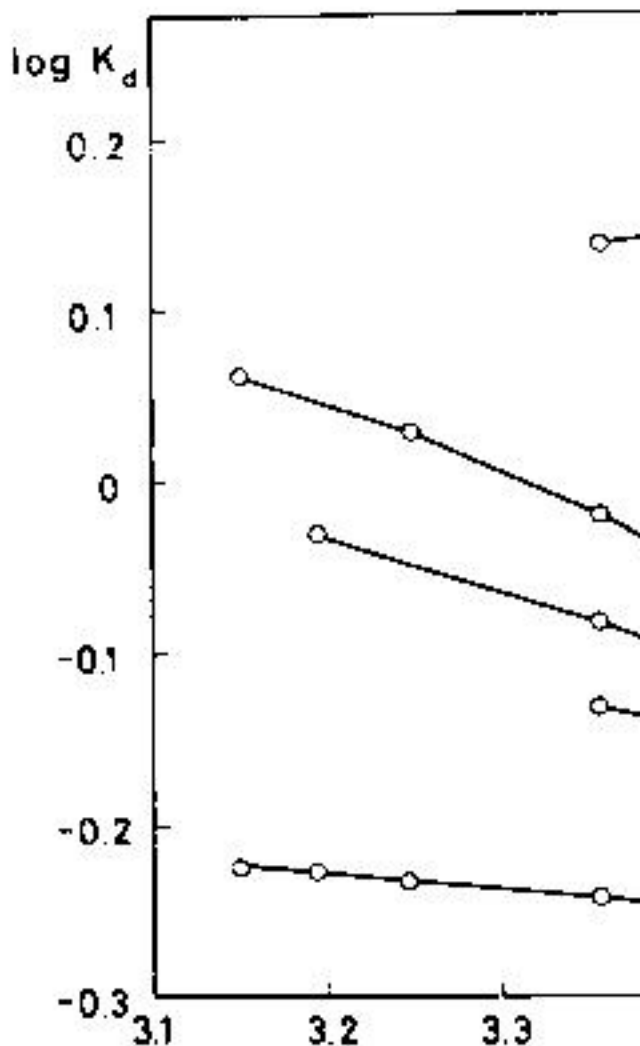


FIGURE 3. Gel DVS 9. The variation of $\log K_d$ with concentration of solutes eluted with deionized water. $u = n\text{-BuOH}$ = *n*-butanol and $n\text{-PeOH}$ = *n*-pentanol; temperatures correspond to 4.2°, 12.5°, 25°, 35°, 40° and 45°.

Marsden: Solut

TABLE
ENTHALPY, FREE ENERGY AND
(P-fluorobenzoate was only measured)
sumed to behave as the meta derivative.

	Gel	K_d	ΔH° cal. m
Methanol	DVS-9	0.74	+ 9
n- Butanol	DVS-9	0.83	+15
n- Pentanol	DVS-9	0.96	+25
Glucose	DVS-9	0.57	+ 4
Urea	DVS-9	1.30	-10
Thiourea	G-25	1.49	-16
o-hydroxybenzoate	G-25	1.69	-10
m-hydroxybenzoate	G-25	1.34	- 8
p-hydroxybenzoate	G-25	1.34	- 8
o-fluorobenzoate	G-25	1.02	
m-fluorobenzoate	G-25	1.21	
p-fluorobenzoate	G-25	1.21	

ΔH° is calculated between either 42°C or 25°C.
The values of ΔG° and ΔS° are for 25°C.

with temperature, there being a differ

Adsorption will only occur spontaneously if the free energy of the system decreases⁵³ ($\Delta G < 0$). This may be due to an exothermic reaction ($\Delta H < 0$) or an increase in entropy. For both urea and thiourea there is a decrease in entropy which is what would be expected for adsorption.

The n-alcohols, on the other hand, do not undergo any entropy changes. Adsorption may occur with a decrease in entropy if the increase in entropy is sufficient to overcome the decrease in entropy associated with the transfer of the solute from a solution on to a surface (i.e. the transfer from a three-dimensional space to a two-dimensional surface). If, however, solute-solvent interactions increase the entropy in the solution, the entropy of the solute can move to a position where it is more highly surrounded by the solvent, e.g. in the form of a cage.

Non-polar solutes such as the n-alcohols have been found to have high negative entropies of solution relative to their entropies in the pure liquid solution. Frank and Evans⁵⁴ suggested that this could be explained by increased organization of the molecules in the solution. Non-polar, non-hydrogen bonding molecules such as benzene would thus account for their excess entropy of solution due to their high positive entropy of vaporization and low heat capacity, since on raising the tem-

Marsden: Solut

methanol and ethanol, but between ethyl and propyl alcohols the latter would predominate.

Similar considerations would also account for the fact that $\alpha\omega$ -diols reverse their trend when the chain length is increased long enough (3 atoms).

If the peculiar structure of water is considered, it is clear that for values of weakly polar solutes, it should be possible to proceed in two ways. The ability of water to form hydrogen bonds increases with rising temperature. The excess ΔS_v values for the solvation of non-polar molecules should therefore fall with temperature, the higher the temperature the more rapid the fall.³⁴

More experimental points are required to test this prediction. In FIGURE 3 it can be seen that at the highest temperatures the slope of n-pentanol has apparently fallen below zero. This is because the maximum possible number of hydrogen bonds per molecule is approached by melting about 15 per cent of the hydroxyl groups. If sufficiently high temperatures could be obtained, still lower values might be achieved and the n- ΔS_v relationship similar to that of the acyclic diols.

Use of a hydrogen bonding solute such as water or formamide, e.g. formamide, should, other things being equal, reduce the effect of hydrogen bonding.

in water. The cross-linkages almost ties, the density of glucose residues calities. In view of the high amoun ent in the gel DVS 9 it might be be more in evidence. Up to now, h DVS 9 has not been shown to be contains about 70 per cent of wa similar diffusional specificity as in evidence does not suggest that sol to any particular influence of the problem awaits further study.

BENZOIC ACID DE *K_d Differences Induced by*

Although at pH 7.6 the hydroxy virtually completely ionized, their

FIGURE 4 shows that for each group have similar K_d values while and *o*-fluorobenzoate a much lower isomers. In addition all calculated

An intramolecular hydrogen bond between the carbonyl group and the hydroxyl group is observed in

Marsden: Solut

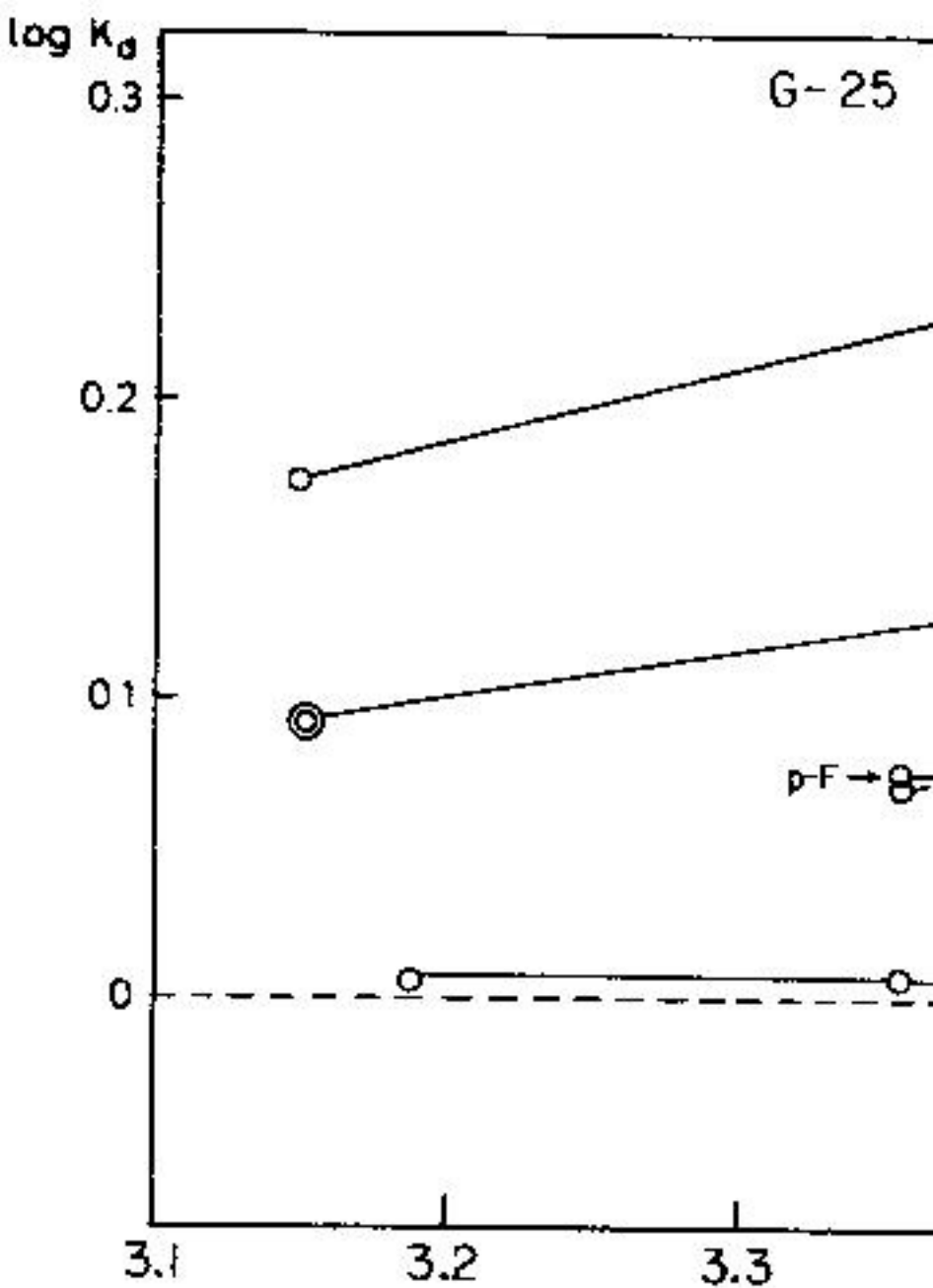


FIGURE 4. Gel G-25. The variation in $\log K_d$ with concentration for para-hydroxyl and fluorobenzoate end th

The *o*-hydroxybenzoate appears than its isomers and the fact that internal hydrogen bonding is resp

It is difficult, however, to speculate all isomers showed a strong pH reversed at about pH 5.

The same explanation, however, *o*-fluorobenzoate since in the ionic hydrogen bond because the only pro in the ionization process.

The pH value used here refers, outside the gel particles. Even if regarded as essentially similar to position and hence internal pH may water space since the K_d values of It may therefore not be valid to is not responsible for the divergent because at the value of the external evidence from experiments with is of the external solution (Marsden interest to note that in paper chromat exhibit deviations of R_F value in o

Marsden: Solut

behaviour of these gels and in particular should be useful adjuncts for structur

It seems that the dextran gels share neutral gels, in exchange resins and so on, it is perhaps pertinent to point out the product. There was similarity, for example, sugars in dextran gels and in starch, in regards such nonelectrolytes as the number is also similar in some ion-exchange resins.

Perhaps more interesting is the comparison with that in living systems. LeFevre⁶⁴ has instability classification of the pentosans into red blood cells.

For the distribution between the cell and sartorius muscle⁶⁵ the order of the solvents < methanol ~ propanol < n-butanol < ... precisely the same order as with the gel.

While the equilibrium behaviour of the solvents in the gel was similar to that in the muscle, this was not true for the diffusional properties. In water at 86 per cent water the order of diffusion coefficients (methanol < alcohols < amides < thioureas) but was

Tenally has studied the behaviour of

4. The K_{d} of the n-alcohols in ethanol) with molecular size. This which increases with decreasing increased with temperature (endotherm due to gain in entropy was discussed iceberg model.

5. The pattern among the alkanes

6. Urea and thiourea have high temperature (exothermic). It is suggested that the interaction in these energetically favourable confor-

7. The monosubstituted benzoates arise from the internal hydrogen bond.

8. The similarity of the properties of living systems is briefly discussed.

ACKNOWLEDGEMENTS

I am very grateful to Professor J. Gelotte, Dr. K. Granath, Dr. S. H. Östling and Dr. M. Zade-Oppen for discussion. I would also like to thank Miss Å. Andersson for valuable technical assistance. This work was received from U. S. Air Force Research Institute, Wright-Patterson Air Force Base, Ohio.

Marsden: Solut

12. TAYLOR, N. W., H. F. ZOBEL, M. WHIT
change in starches and amylose. *J.*
13. MARSHALL, L. M. & D. MAGEE. 1964. C
 ^{14}C . *J. Chromatog.* 15: 97-99.
14. MARSHALL, L. M. & R. E. COOK. 196
tercurrent distribution of arabinos
2648.
15. MARSDEN, N. V. B. 1965. Cation sele
published.
16. MARSDEN, N. V. B. & H. R. ULFENDA
tion by gel filtration. *Acta Physiol*
17. TEORELL, T. 1961. Oscillatory electro
Arkiv f. Kemi. 18: 401-408.
18. ISHERWOOD, F. A. & M. A. JERMYN.
ture of the simple sugars and the
gram. *Biochem. J.* 48: 515-524.
19. HOROWITZ, S. B. & I. R. FENICHEL.
hydrogen-bonding systems. *J. Phys*
20. WILKE, C. R. 1949. Estimation of li
Prog. 45: 218-225.
21. GREGOR, H. P., F. C. COLLINS & M.
resins III. Diffusion of neutral m
change resin. *J. Coll. Sci.* 6: 304-322.
22. LATHE, G. H. & C. R. J. RUTHVEN. 19
estimation of their relative molecular
in water. *Biochem. J.* 62: 665-674.
23. SQUIRE, P. G. 1964. A relationship bet
molecules and their elution volume
filtration. *Arch. Biochem. Biophys*

36. GLECKAUF, E. & G. P. KITT. 1956. The effect of solvents on protein-changers. III. The hydration of proteins. *Proc. Roy. Soc. Lond. A* **228**: 322-341.
37. LAURENT, T. C. 1964. The interaction of proteins with small molecules. 9. The exclusion of proteins from aqueous solutions. *Biochem. J.* **93**: 106-112.
38. PIGMAN, W. 1957. The Carbohydrates. *Advances in Carbohydrate Chemistry*. Vol. 12. Academic Press, New York.
39. JÄGER, H., A. RAMEL & O. SCHÜTZ. 1958. Die Papierchromatographischen Verfahren. *Papierchromatographische Methoden*. Vol. 40: 1310-1319.
40. HAZEBROOK, P. & L. J. OOSTERHOFF. 1957. The effect of sodium hydroxide upon the properties of proteins. *Proc. Roy. Soc. Lond. B* **147**: 87-93.
41. REEVES, R. 1958. Chemistry of the proteins. *Advances in Protein Chemistry*. Vol. 15: 3-34.
42. BARTON, D. H. R. & R. C. COOKSON. 1957. The effect of sodium hydroxide upon the properties of proteins. *Quart. Rev.* **10**: 44-82.
43. REEVES, R. E. 1951. Cuprammonium analysis. *Analyst* **76**: 107-134.
44. REEVES, R. A. & F. A. BLOOM. 1957. The effect of sodium hydroxide upon the properties of proteins. *Proc. Roy. Soc. Lond. B* **147**: 2261-2264.
45. HASSEL, O. & B. OTTAR. 1947. The effect of sodium hydroxide upon the properties of hexose and pentose rings. *Acta Chem. Scand.* **1**: 107-116.
46. KELLY, R. B. 1957. A relationship between the properties of proteins and their physical derivatives and their physical properties. *Advances in Protein Chemistry*. Vol. 15: 35-64.
47. WHIFFEN, D. H. 1956. Optical rotatory power of proteins. *J. Polymer Sci. Ind.* **9**: 964-968.
48. CANTOR, S. M. & Q. P. PENISTON. 1957. The effect of sodium hydroxide upon the properties of proteins measured by the dropping mercury electrode. *Analyst* **82**: 107-112.

Marsden: Solut

60. DVORÁK, J., I. M. HAIS & A. TOCKS. Paper Chromatography. p. 73 in *Handbook of Paper Chromatography*, Prague and New York.
61. SIMPSON, T. H. & L. GARDEN. 1952. *Anal Chem* 24: 4644.
62. SHAW, B. L. & T. H. SIMPSON. 1952. *Anal Chem* 24: 5032.
63. ROUX, D. G. & S. R. EVELYN. 1958. The paper chromatographic behaviour of some monosaccharides. *J. Chromatogr.* 1: 537-546.
64. LEFEVRE, P. G. 1961. Sugar transport and energy relationships in substrates and acids. *Adv Biochem Eng* 1: 1-20.
65. FENICHEL, I. R. & S. B. HOROWITZ. 1961. Glucose uptake by muscle as a diffusional process in the intact animal. *J. Physiol.* Supp. 221: 1-63.

N.M.R. AND RAMAN PROPERTIES OF WATER IN COLLOIDAL SYSTEMS

J. Clifford, B. A. Pethica, W. A. Senior

*Unilever Research Laboratory, Port Sunlight,
Cheshire, England*

INTRODUCTION

There have been a number of investigations of water in biological systems by nuclear magnetic resonance methods. The line width or relaxation time of water protons have been measured. Much interesting information has been obtained which, in general, indicates that the rate of molecular motion of water protons in biological systems is less than in pure water. However, with few exceptions the systems investigated have been much too complex to allow detailed interpretation of the results.

Solutions of surface active agents serve as a convenient and simple model for the investigation of the interaction with water of part of biological systems. Below the critical micelle concentration (CMC) the surface active agents exist as single ions containing long hydrocarbon chains in contact with the water, and the results of investigations of the interaction between chains and the water are relevant to the interaction of hydrophobic parts of biological molecules with water. Above the critical micelle concentration the surface active agent form micelles, colloidal particles with highly charged surfaces, and the interaction of these surfaces with water will also be relevant to many biological situations.

We have measured the N.M.R. chemical shift of water protons, the N.M.R. spin lattice relaxation time of water protons, and the change in frequency and intensity of the Raman bands of water, in aqueous solutions of a series of sodium alkyl sulphates from C₂ to C₁₂. The chemical shift and Raman measurements provide information about hydrogen bonding in the water in these solutions, and the spin lattice relaxation time results provide information about the mobility of water protons.

EXPERIMENTAL

Materials. Sodium salts of the higher alkyl sulphates (C₂-C₁₂) were prepared by the method of Dreger¹ and purified by prolonged extraction with ether; commercial sodium ethyl sulphate was purified by recrystallization. For the measurements on solutions of alcohols, 'Analar' n-butanol and spectroscopic-grade ethanol were used without further purification. Laboratory-distilled water which had been deionized by means of an ion-exchange column was used as a solvent.

Clifford et al.: N.M.R. a

N.M.R. chemical shift measurement. The chemical shifts of water protons in solution have already been described.² A Perkin Elmer 3B spectrometer was used. The shift between the water peak measured and the position of the water peak in air was obtained by extrapolation. The proton separation between the water peak and the solvent peak in cycles per second, i.e., the results given here for the water protons are accurate to ± 0.01 cps.

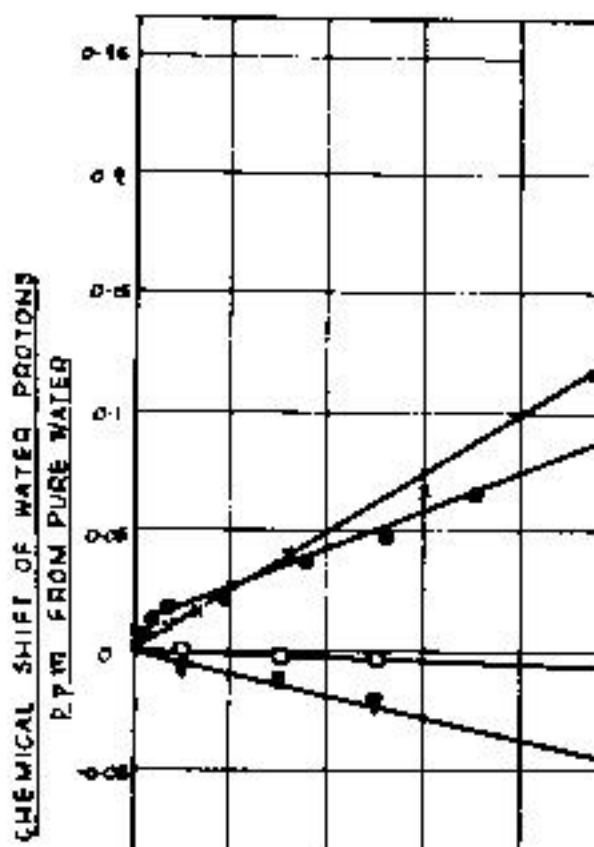
N.M.R. relaxation time measurements. The spin-lattice relaxation times of the water protons in these solutions were measured by the spin-echo or spin-pulse passage technique. As signal recovery was exponential within experimental error, each solution was characterized by a single T_1 . The overall errors in the T_1 values are estimated to be ± 2 per cent.

Raman Measurements. All Raman measurements were made with a Varian Model 81 recording Raman spectrophotometer. A 100-watt tungsten lamp was employed together with the standard 100-watt quartz-halogen lamp.

The solutions of long chain sulphates were measured on a weight per cent basis. All the intensity values have been corrected for the absorption

R

The variation of the N.M.R. chemical shift of water protons in butanol and ethanol, and in solutions of sodium sulphates with concentration is shown in Figures 1 and 2. Higher applied fields are regarded as zero. Integration of the water peak shows that within the accuracy of the measurements no water is removed from the liquid state by the solutes.



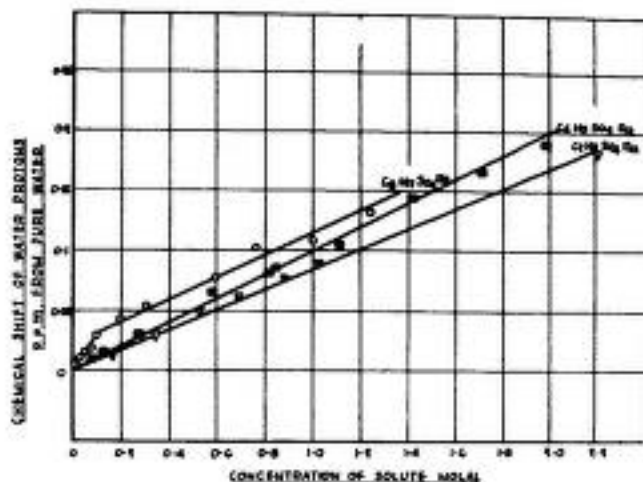


FIGURE 2. The chemical shifts of water protons in solutions of $C_2H_5SO_4Na$ ▽; $C_4H_9SO_4Na$ ■; $C_6H_{13}SO_4Na$ ○; all relative to pure water. Reproduced by permission of the Faraday Society.

of the nonmicellised alkyl sulphate and sodium ions on the water. Above the CMC the concentration of single ions is assumed to be that at the CMC so that all the excess concentration of alkyl sulphate above the CMC is in the form of micelles. Consequently the slope of the chemical shift-concentration curve above the CMC is a measure of the effect of the micelles on the water. Thus TABLE 1 is obtained (see FIGURE 3 also).

Similarly, from the curves in FIGURE 1 the molal shifts for ethyl and n-butyl are -0.047 and -0.005 p.p.m. It is clear that both for the longer sodium alkyl sulphates and for the alcohols, the addition of CH_2 groups to the chain results in an increased positive shift.

TABLE 1
EFFECT OF ALKYL SULPHATES ON THE CHEMICAL
SHIFT OF WATER PROTONS

Form of alkyl sulphate in solution	Molal chemical shift (ppm/mol/1000 g. water) for the alkyl sulphate				
	C_2	C_4	C_6	C_8	C_{12}
Single ions	0.09	0.10	0.13	0.20	0.34 (approx.)
Micelles	-	-	0.05	0.09	0.09

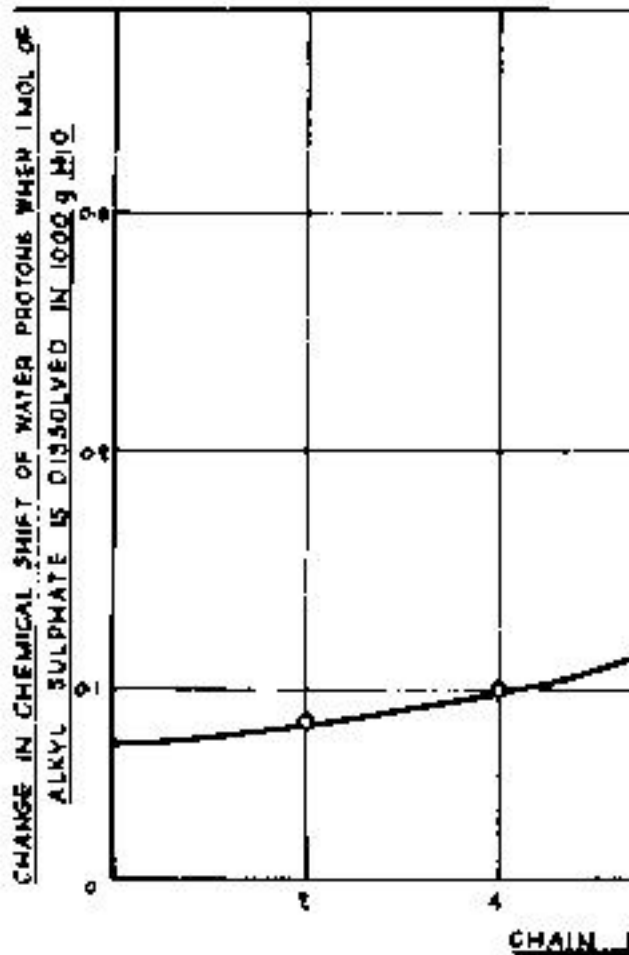


FIGURE 3. The effect of chain length on the change in chemical shift of water protons in solutions of sodium alkyl sulphates.

C_7 SULPHATE

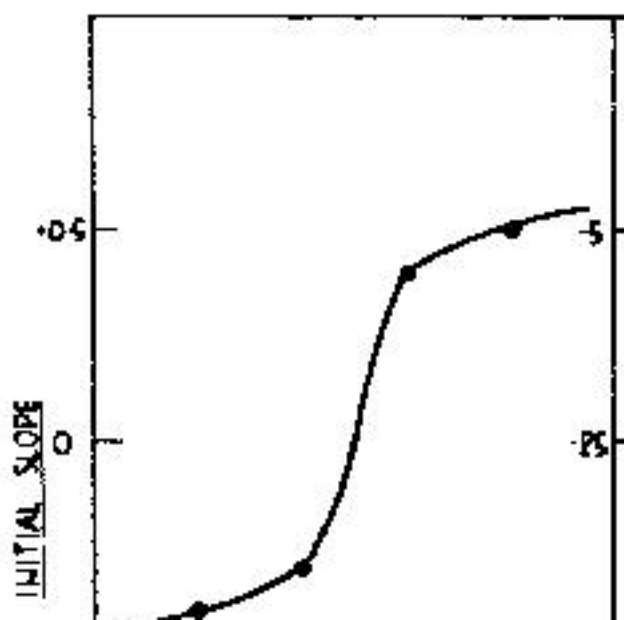
-0.8

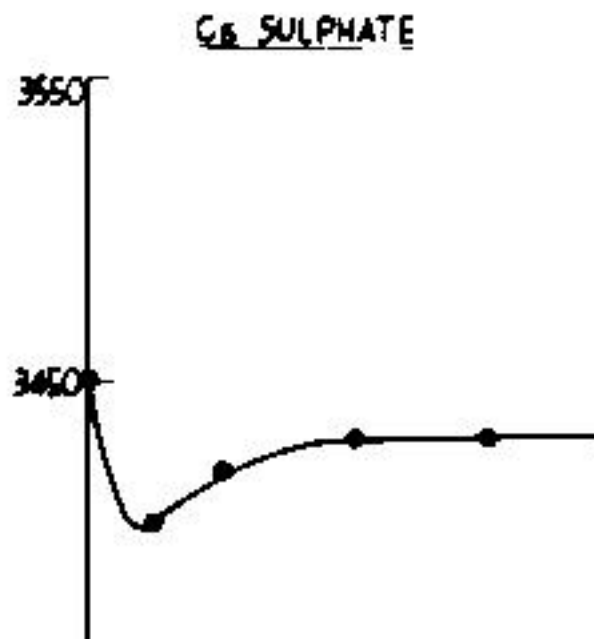
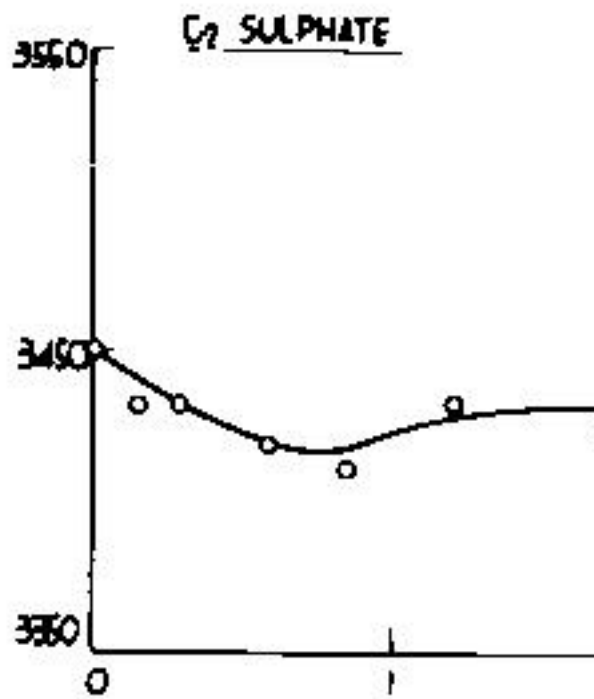
Clifford *et al.*: N.M.R. a

The Raman measurements can be divided into those related to intensity measurements and those related to frequency measurements.

Raman intensities are related to the vibrational energy of the molecule when it undergoes a vibrational mode. The intensities are very susceptible to changes in the environment and can thus be used to study the interaction of the molecule.

The results (FIGURE 4) show that for some modes a reduction in intensity occurs whereas for others an increase (up to ~40 per cent) is found.





Clifford *et al.*: N.M.R. and

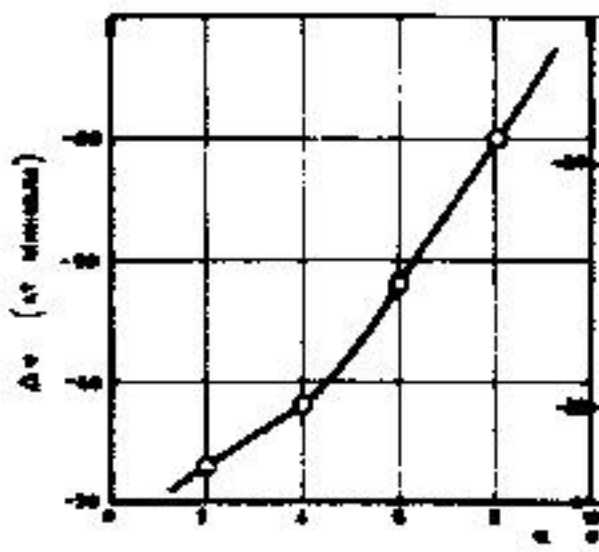
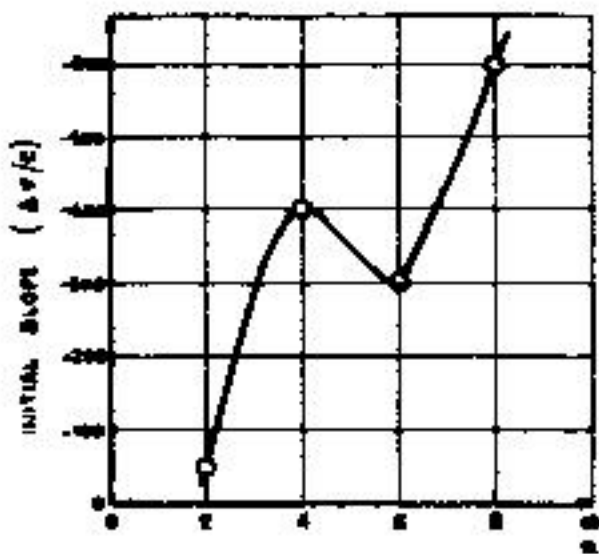


FIGURE 7. The effect of chain length on sulphate solutions.

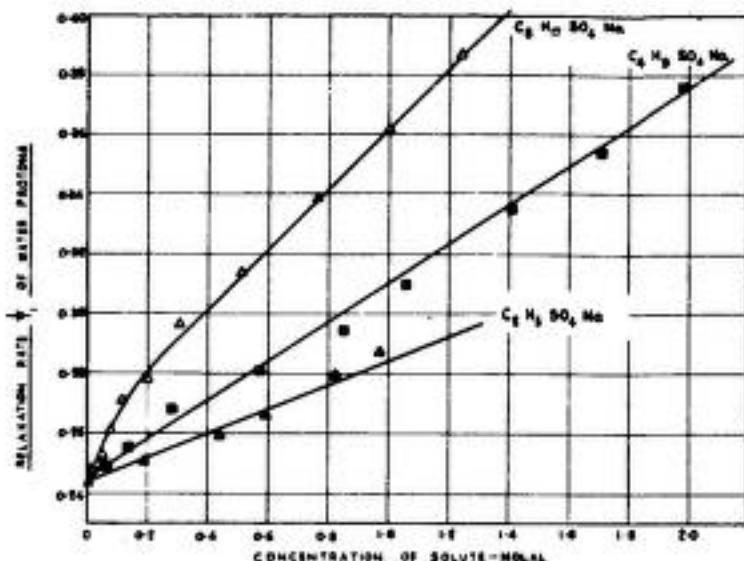


FIGURE 9. The relaxation rates of water protons in solutions of $\text{C}_2\text{H}_5\text{SO}_4\text{Na}$ ▲; $\text{C}_4\text{H}_9\text{SO}_4\text{Na}$ ■; and $\text{C}_8\text{H}_{17}\text{SO}_4\text{Na}$ Δ. Reproduced by permission of the Faraday Society.

protons of one mole of solute per 1000 grams of water is calculated and given in TABLE 2.

In FIGURE 10 the increase in relaxation rate caused by the solution of one mol of alkyl sulphate as single ions in 1000 gm. of water is plotted against the length of the alkyl chain. The CMC for the C_{12} salt is too low for an

TABLE 2
EFFECT OF ALKYL SULPHATES ON THE SPIN LATTICE
RELAXATION TIME OF WATER PROTONS

Sodium alkyl sulphate Chain Length	Effect on the relaxation rate of water protons at $32^\circ\text{C. sec.}^{-1}$ per mol. per 1000 gm. of water	
	As single ions	As micelles
C_2	0.04	—
C_4	0.07	—
C_6	0.10	0.09
C_8	0.14	0.11
C_{10}	—	0.16

Clifford *et al.*: N.M.R. a

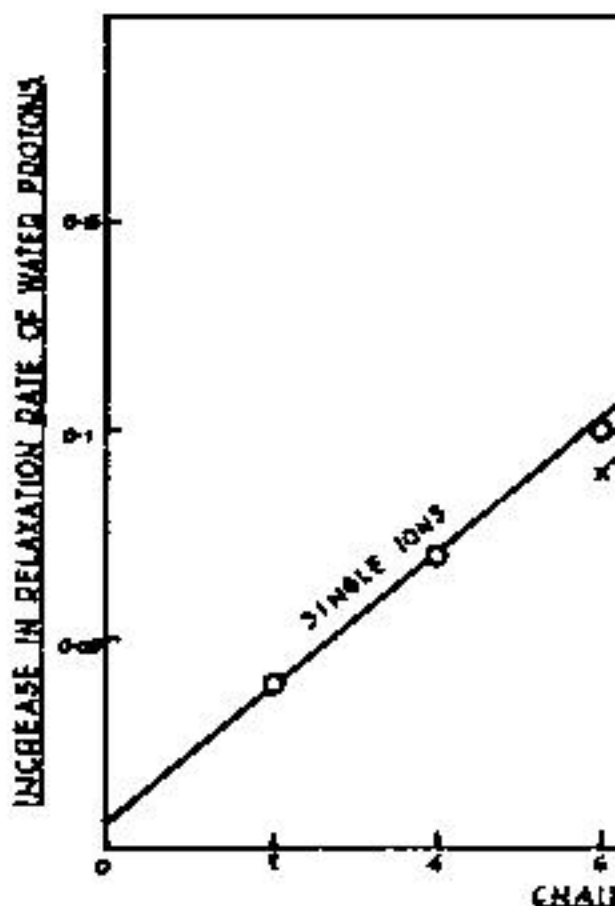


FIGURE 10. The effect of chain length on the increase in relaxation rate of water protons in solutions of sodium alkyl sulphates, micelles. Reproduced by permission of the Royal Society of Chemistry.

accurate evaluation of the effect of single ions on the $1/T_1$ concentration curves for the systems given in TABLE 1 are estimated from simple calculations based on eqn. (1).

smaller than the electrostatic effect to lower field.

The experimental N.M.R. result positive chemical shifts on adding shift becomes more positive as the c moves to higher applied field. In t sult can be interpreted in two wa pulsion or an increase in the cov From chemical shift evidence alone the two mechanisms, but when the measurements are considered, it a the more important.

The Raman intensity measurement. For the C₂ and C₄ sulphates a whereas for the C₆ and C₈ comp Measurements on the simple system decreases which can be attributed to for the C₂ and C₄ sulphates the d head group. For the C₆ and C₈ sul factor, and by comparison with the tone (to be reported later) the con the water is increased.

Clifford *et al.*: N.M.R. and

water protons will be caused largely by protons and the relaxation rate $1/T_1$ will depend on the time τ describing the motion of the water molecule. It has been shown¹ that $1/T_1$ for water protons is increased

Part of this effect, can be explained by interactions between water protons and alkyl sulphate ions. If the ion has a tetrahedrally coordinated structure this would mean that the nearest H H distance between H-H is $\sim 2.8 \text{ \AA}$, whereas the H H-C di-

However, more evidence to clear up this question has been obtained by investigating the variation of T_1 with temperature. In a 0.1 molal solution of C₆ sulphate over the temperature range 20–100°C the activation energies for the relaxation process were found to be 1.55 and 4.65 K cals./mole respectively. This indicates that in the presence of a hydrocarbon chain the forces on the water protons are increased in agreement with the chemical shift and Raman data.

It is particularly interesting that many of the curves shown in Fig. 2 here show discontinuities at a chain length of C₆. It is known¹⁰ that the alkyl sulphates first form micelles. It is also known¹¹ that for chain lengths less than C₅ the solubility of the solute on water. However, when the chain length is increased to C₆ the solubility increases again.

areas of the C₁₂, C₈ and C₆ micelle molecule of micellised sulphate. If one layer of water around each micelle by the micelle then about 13 molecules required and the relaxation rate for solutions of all the alkyl sulphates are bound for long periods in a regular can be rejected. In such a model the motions would be determined by the motion of the micelle. Assuming a medium with a viscosity of 0.01 dl/g. calculated and from it an intramolecular magnitude greater than the observed be said that the water on the micelle of any molecule on the micelle is much more than one or two order of magnitude between jumps in any one position in

REF.

1. DREGER, E. E. 1944. Ind. Eng. Chem. 36, 100.
2. CLIFFORD, J. & B. A. PETHICA. 1953. J. Polym. Sci. 10, 101.
3. CLIFFORD, J. & B. A. PETHICA. To be published.
4. MARSHALL, J. & J. A. POPLE. 1958. J. Polym. Sci. 22, 101.
5. TARTAK, H. V. 1959. J. Coll. Sci. 14, 101.

THE EFFECTS ON BIOLOGIC SYSTEMS OF HIGHER-ORDER PHASE TRANSITIONS IN WATER*

Walter Drost-Hansen

Institute of Marine Science, University of Miami, Miami, Fla.

The purpose of this conference is to discuss "Forms of Water in Biologic Systems." This undertaking is very ambitious and most likely our achievements at the present time will be limited. The principal difficulty before us is simply that we do not as yet possess a picture of the structure of water or aqueous solutions that has any degree of finality about it. Hence, it is indeed somewhat presumptuous for us to try to discuss various forms of water in biologic systems as long as we are without any appreciable understanding or agreement about the structure of bulk water or aqueous solutions. We might well add to this regrettable state of affairs our lack of knowledge of the structure of water near such simple interfaces as the air-water interface, water-immiscible liquid interface, or the structure of water near any simple solid-water interface, such as may exist near the surface of a mineral grain.

Theories of Water Structure

A few years ago, Henry Frank (1963) gave a brief but eloquent survey of the current status with respect to theories of liquid water and more recently Kavanau (1964) has reviewed the current theories of water structure in some detail. From these reviews, one sees the great range of physical models that have been invoked over the past 30 years to account for the properties of water. These theories range from the "purists'", "average" models of liquids — due primarily to physicists and other strictly "theoretical" liquid structure researchers — to the models that Henry Frank has termed the "mixture models." The mixture models embrace a variety of models from simple water-ice mixtures to water polymers and water clusters. These include Eucken's polymer model (consisting of small polymeric species of water), the more recent cluster and cage models, and the "super clusters" (the older cybotactic groups of Stewart, Frenkel and Nomoto). The current status of water structure research certainly lacks finality. Because of the present state of knowledge, any discussion of water in biologic systems must definitely be limited. Without knowing the structure of water, how can we predict or understand the influence that the multitude of solutes in biologic systems have on the structure of water, or

*Contribution No. 601 from The Marine Laboratory, Institute of Marine Science, University of Miami, Miami, Fla. Acknowledgment is given the Office of Saline Water, U. S. Department of the Interior, for support of the author's research at the Institute of Marine Science.

how can we describe the water in biological systems? The unsettled question of long-range ordering in water must surely be decided before we can understand the behavior of water in membrane systems.

Thermodynamics

The present paper is a summary of his coworkers with regard to water coming — and at the same time approach is that we do not build a model of water. Rather, our speculations are reported in the literature, of the properties of water and aqueous studied the properties of water and have become convinced that the anomalies at a number of different reflect more or less abrupt structures which for want of a better name has suggested previously by several others in his monograph points out that ability by Wills and Boecker and beyond the vicinity of 35 to 55°C., and Do-

Drost-Hansen: Phase Transitions

a general review of the evidence will be given (Drost-Hansen, 1965). In this section we show only how the diversity of conditions and parameters are observed in both pure water and aqueous solutions. A brief summary of the major conclusions that can be drawn from an examination of the data presented in the following sections *Biologic Implications* and *Discussion* of the anomalies displayed in biologic systems by the anomalies in aqueous solutions is discussed.

The kinks are manifested in both the density and viscosity of aqueous solutions. It is instructive first to consider the density anomalies from measurements on pure water. One difficulty in searching for the anomalies is the lack of a suitable thermometer at sufficiently closely spaced temperatures. There are a few cases in which parameters have been measured at temperatures (over a relatively narrow temperature range) and the analysis of the resulting data. One such case is the density determined by Chappuis at the International Conference on Weights and Measures (1907). We have previously analyzed these data (Lavergne & Drost-Hansen, 1956) and we present the results here. The data obtained by Chappuis were plotted as

Rather than work with the density itself,

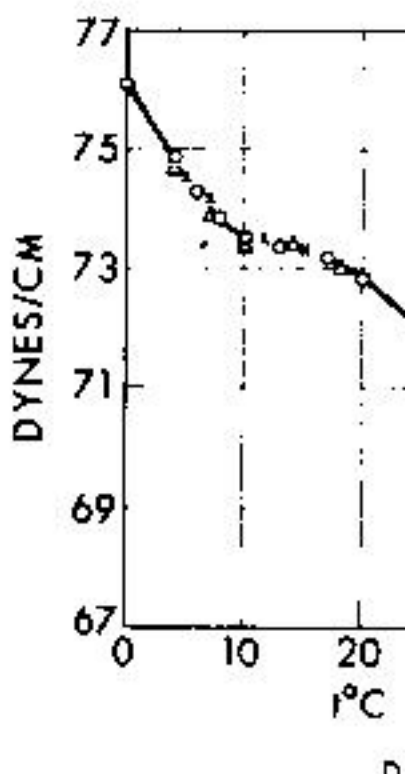


FIGURE 1. Surface tension of water (1937).

(1956) shows a minimum in the $(d\varepsilon/dt)$ near $60-65^{\circ}\text{C}$. and very poor data near $30-35^{\circ}\text{C}$. An anomaly in the properties of pure water has been observed in the temperature dependence of many surface properties. Franks and Ives (1960) have no

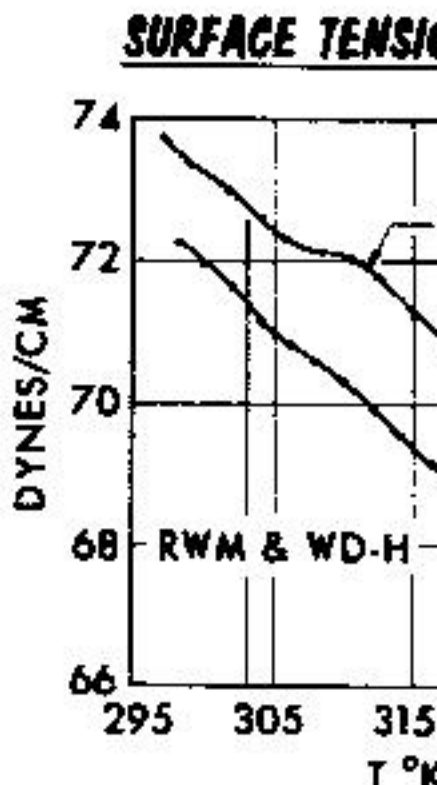


FIGURE 3. Surface tension of water. Data of Hansen and Myers.

water as determined by Timmermans and his co-workers in the thirties. FIGURE 2 shows the data for both sets of authors. It is remarkable that such a pronounced inflection points have been observed by these authors but not by the investigators of the surface tension of water. However, that inflection points are indeed present in the measurements of the surface tension of

in Italy and by the present author points are observed near 30 to 33. Finally, FIGURE 4 shows the "entropy" Drost-Hansen (1965). The three calculated surface tension data obtained and Vannel, and Drost-Hansen and exists to the extent shown in FIGURE 4 derivative of the surface tension. A directly this quantity with the entropy indicate an abrupt change of order. In discussion, the reader is referred to

Anomalies in the viscosity of water as a function of temperature have been noted by Saito (1952), Magat (1935), Neill and Parker (1944), Qurashi and Ahsanullah (1972). In a study of the viscosity and diffusion coefficient of water in the solid state that "where water is the solvent, viscosity minimum occurs at about 30°C. An exactly similar break in the curve of viscosity is observed at the same temperature when viscosity of water is plotted against vapor pressure of water."¹⁰ They also mention that "The temperature at which the change in viscosity occurs may vary somewhat with the dissolved solute."

of some of Brown's data: the ordinate is log transverse relaxation time while the abscissa is the reciprocal absolute temperature. The kink near 60°C. is fairly pronounced. An anomaly in the NMR data is also suggested by Simpson and Carr (1958) in the vicinity of 40–45°C. on basis of their NMR studies.

Spectroscopic evidence for anomalies in water has been suggested by Magat (1937) near 40°C. Other evidence for the existence of anomalies in the properties of pure water may be obtained from the data by Pinkerton on the ultrasonic amplitude absorption coefficient (1947). FIGURE 6 shows

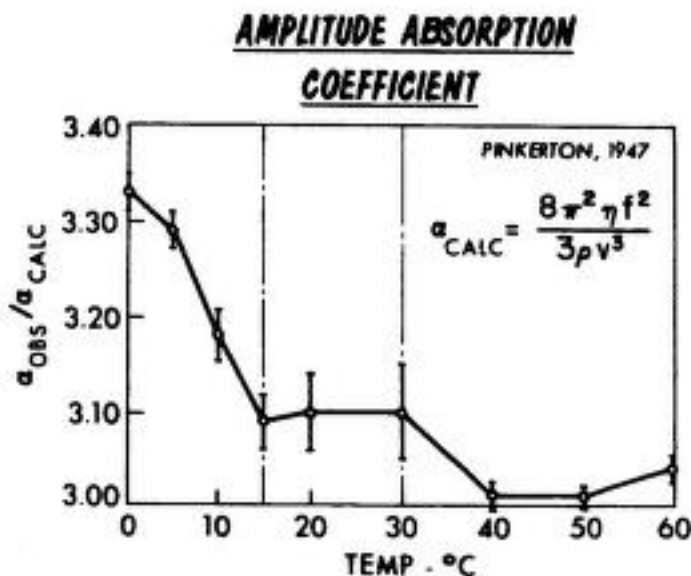


FIGURE 6. Excess ultrasonic sound absorption coefficient. Based on data by Pinkerton.

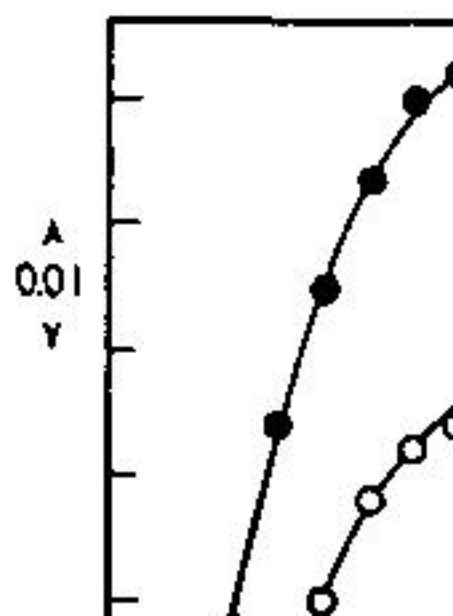
Pinkerton's data point and his estimated errors on the determinations. It should be noted that the limits of error suggested by Pinkerton appear to be unnecessarily large for the data points near 20 and 30°C., thus the apparent anomalies at 15 and near 30°C. seem very likely to be real. The thermal conductivity data obtained by Frontas'ev (1956) are also suggestive of an anomaly and Frontas'ev states: "It can be assumed that a fundamental modification in the structure of water takes place in the range of 30 to 40°C. which is reflected in the indicated anomaly in the thermal conductivity polytherm."

Much skepticism has been voiced with regard to the reality of the anomalies discussed above. One frequent criticism has been that it often appears that each investigator has his "choice" temperature or temperatures

for the anomaly (or anomalies) hardly condemn the notion that a considering the present author's exist, it is obvious that a considering on a particular range of t approximately 15, 30, 45, and 60°C and "symmetrical," evidence will transitions being at least in the

"Kinks" in Proper

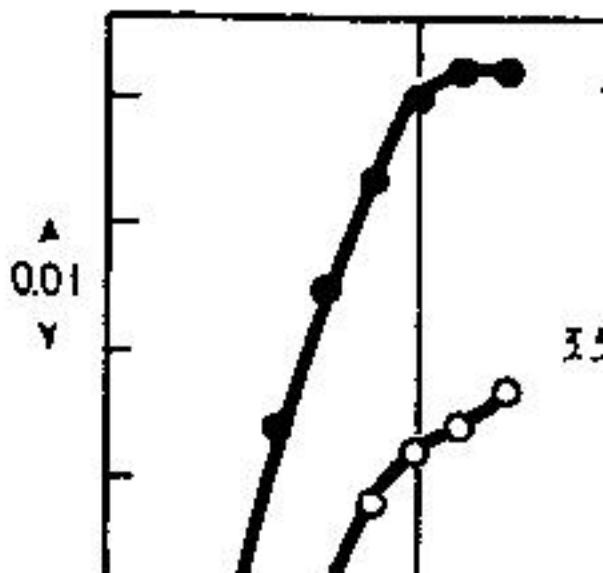
We shall briefly show a number ties of aqueous solutions. While th



Drost-Hansen: Phase Tr

to demonstrate unambiguously on any other solvent. On pure water, it is often easier to find anomalies in the properties of aqueous solutions than solubility, kinetic data for hydrolysis, and dissociations seem frequently to exhibit the kin

FIGURE 7 shows the activity coefficient as a function of temperature. This illustrates Harned and Owen's monograph (1958) of the activity coefficient for sodium chloride to fit the data. In FIGURE 8 we have shown smoothed curves; instead, we have drawn



lieve represent far more realistic activity coefficient. Unfortunately also, the data below 40°C. were measurements while the measurement boiling point elevations. While it observation were used for the diff that there are pronounced trends one can escape the conclusion that mation descreases linearly with Secondly, in all cases there is a and the data at 60°C. Furthermore curvatures may exist for the 1.5 ameter of the circles representing responding to, respectively, 0.15 m Considering the accuracy and in p may ordinarily be measured, the tic, smooth curve of FIGURE 7 — above, the *trend* in the data is ex amazingly high concentrations f up to three to four molar.

FIGURES 9 and 10 show the con tial molal volume for potassium

Drost-Hansen : Phase T

PARTIAL MOLAL

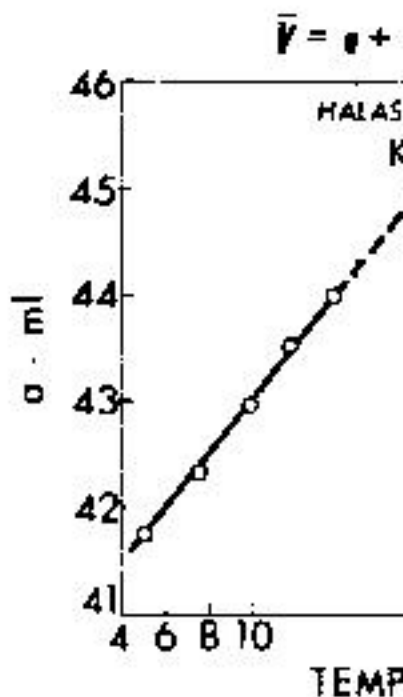


FIGURE 10. Concentration-independent total molal volume of potassium iodide.

were obtained by Sister Halasey (1941). The kinks do not occur exactly at the temperature $15^{\circ}\text{C}.$, but certainly in the vicinity of $15^{\circ}\text{C}.$ It is also to notice the opposite trends in change in the vicinity of $15^{\circ}\text{C}.$.

Solubility data often reflect the kink

smoothed curve originally suggested by the manometric method. The right side of the curve, two separate curve segments, was obviously done for the density and diffusion coefficient analysis. It is significant that two separate curve segments pass through the combined intervals. It turned out so markedly in the present case that the solubility of two quite similar gases is different. The difference in the solubility of these gases to the same pressure is due to the fact that the two gases form Type I hydrates and both of them decompose at the same temperature (Boscher Heem, 1964), hence, it is partially due to specificity; it should be noted, however, that the solubility of methane in the hydrates at 0°C. is only 95 atm.

Many other solubility studies such as this are unfortunately quite rare to find the solubility of water studied at sufficiently closely spaced temperatures to enable one to look for all four kinks. However, in the solubility of lanthanides in water as shown in FIGURE 12 where the kinks are clearly visible, although apparently displaced a few degrees by the presence of the solutes, the temperatures for the kinks in pure water are 10.5, 13.5, 16.5, and 19.5°C.

Drost-Hansen: Phase T

15°, 25 to 30° and in the vicinity of 60°. The molar ratio of solute to solvent is approximately 1:4. Similarly, like *r*- and *l*- mandelic acid also shows the same molar ratios of solute to solvent. Among the substances mentioned, mention the solubility of thiourea (Jäger, 1938), nitrate, thallium hydroxide, silver iodate, ether and benzoic acid (Seidell, 1940).

General Observations

A large number of other examples can be adduced to illustrate the reality of the anomalies in water and aqueous solutions. Owing to the limited time we refer to the following literature. We present in greater detail the total evidence available and then summarize the main conclusions which may be drawn concerning thermal anomalies in water based on all available data (Drost-Hansen, Sept. 1963).

A. The temperatures of the kinks observed in the DSC curves are 60°C. within $\pm 1^\circ - 2^\circ$ of these temperatures. The kinks may be centered, for instance, near 40°C. or they may occur at 44°C. Hence, the glarification of the kinks which may be implied is not necessarily real, although the multiples may serve conveniently and adequately as a reference.

ever, remain but the temperature values for pure water and dilute solutions. D. The kinks are present in both port phenomena.

E. The kinks show up in surface in bulk properties. For surface probably different temperatures than

Biologic Implications:

It has been claimed that there exist transitions in biological systems which are manifested in the temperature dependence of various properties. It has also been claimed that these transitions are not due to the presence of solutes in the solutions and have inferred that the transitions in biological systems must reflect the persistence of the water in the system. It has been unaffected by the presence of the solutes. It has been claimed that the water in biologic systems is in a more ordered state than in pure water.

Over the years, many authors have reported the presence of more or less abrupt anomalous changes in the properties of biological systems as a function of temperature. FIGURE 13 shows some of the data obtained by

Drost-Hansen: Phase T

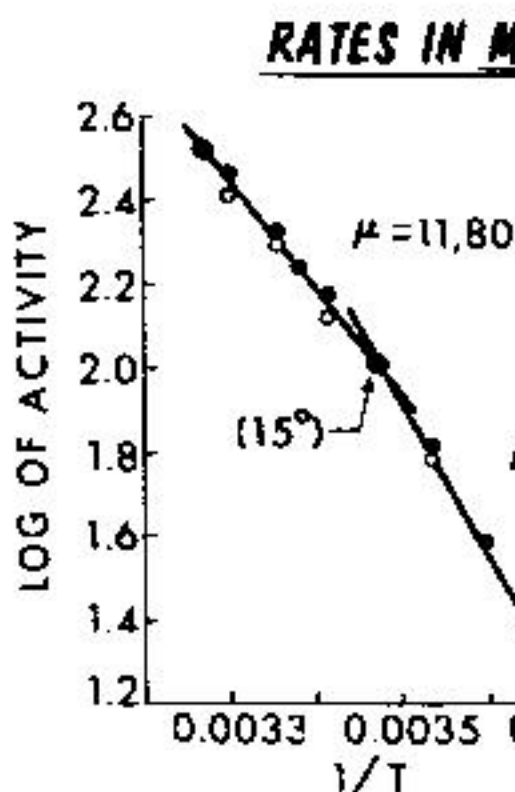
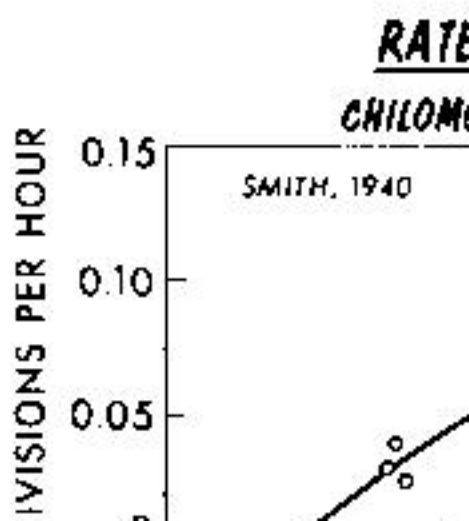


FIGURE 14. Rate of ciliary activity and epithelium in the clam, *Mytilus*.

of two other phenomena, namely, cilia which is shown as solid circles, and epithelium of the same clam, shown Gray, worked up by Crozier in the m show a kink; again the previous autho which they believed the kink occurs, a

viscosity in *Cumingia* eggs as determined by the viscosity method. It is evident that marked changes occur in the viscosity of the egg at temperatures of 2, 15 or 16°C., and again near 30°C. It is difficult to say just what the significance of these changes is above any criticism concerning "frozen-in" viscosity. The two curves, line segments deviating only slightly from a smooth curve, are not very puzzling by the anomaly near 2°C.; they appear to coincide very nicely with the anomalous behavior of the viscosity. Not all examples are as dramatic as this one, but the available evidence indicates that the temperature changes are in general consistent with the marked changes in biological activity.

FIGURE 16 shows the relation between the rate of division and the temperature of division in *Chilomonas paramecium*.



Drost-Hansen: Phase Transitions

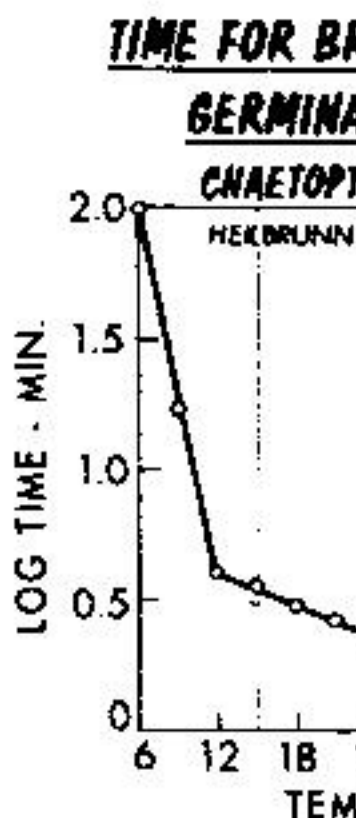


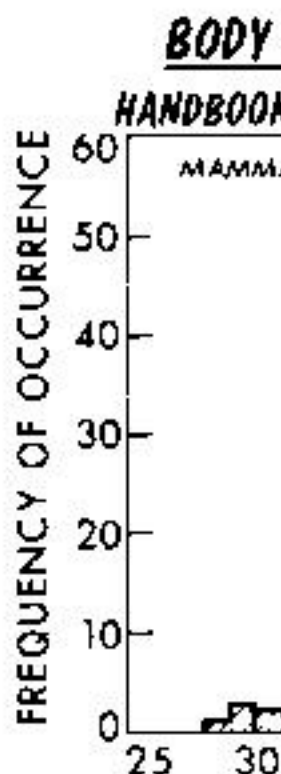
FIGURE 17. Time for breakdown of germination as a function of temperature.

considers a reasonably good fit to the data near 15 and 30°C.

Complex Physiological Processes: Phase Transitions

As shown above, a number of "simple" systems show the occurrence of more complex processes.

temperatures. Consider, for instance, temperature the properties and behavior processes may undergo rapid and seems "safer" to operate the biological words, as far removed as possible from the environment. I propose that in the course of evolution have been favored by mammals as the best way to do this. FIGURE 19 shows a graph of body temperature.



Drost-Hansen: Phase T

cause for the displacement from 37 or to venture the guess that this is a com highest possible energy production (s Arrhenius type of activation mechanism ture and properties of water. In other may facilitate the production of energ same time sacrificing "thermal latitud diseases (by minimizing the temperat hyperthermia). It is interesting in this birds that do not fly, such as the ostr "normal" body temperatures namely be

It is well known that in both man a temperature of considerable physiol man there is loss of consciousness below ability to regulate body temperature changes occur in the oxygen consump one of the reasons why cardiovascular under hypothermia, often at temperatu

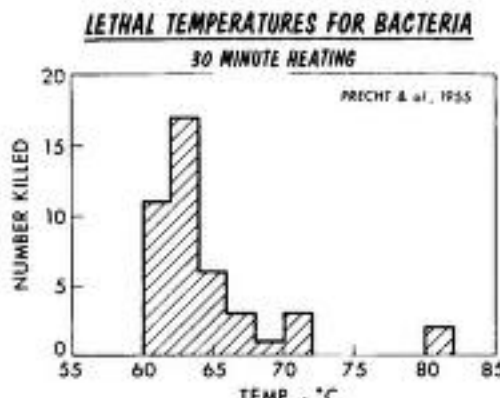


FIGURE 21. Lethal temperatures for a number of bacteria under various conditions (heating time: 30 minutes).

53–55°C., pasteurization temperatures usually tend to be approximately 60 to 62°C. FIGURE 21 shows the lethal effects of heating above 60°C. for a compilation of 20 different bacteria under a variety of different conditions, mostly different media. The data shown are all those cases for which heating times of 30 minutes have been used; this histogram has been drawn from data compiled by Precht, Christophersen and Hensel (1955).

The same type of argument as presented above can be applied to the interval between 15 and 30°C. Here we find optimum activity near 22 to 25°C. for a large number of vastly different types of animals: many insects (though not all), many fishes, and many soil bacteria seem to have optima in the vicinity of 23 to 25°C. Also, 30°C. is known to be an important temperature physiologically for both fishes and insects. We shall illustrate this shortly with a number of specific examples. Furthermore, it is known that 15°C. often is a controlling factor in ecology: for example, in the distribution of fishes in the South Pacific (Jones, 1947) where the density of fishes of commercial interest drops precipitously at temperatures below 15°C. Another example of ecologic interest is shown in FIGURE 22 where the ordinate is the rate of egg deposition of the gastropod *Urosalpinx cinerea* and the abscissa is the temperature. This illustration, which is redrawn from the data by Moore (1958) shows that 15°C. is indeed a critical temperature below which no deposition of eggs take place.

Some Kinetic Aspects and Examples

As outlined above, there exist in water more or less abrupt structural changes that give rise to changes in the properties of pure water and in aqueous solutions. I believe that these changes significantly influence the behavior of biologic systems. Obviously, it is not claimed that these changes

Drost-Hansen: Phase T

EGG DEPOSITION OF GASTRO

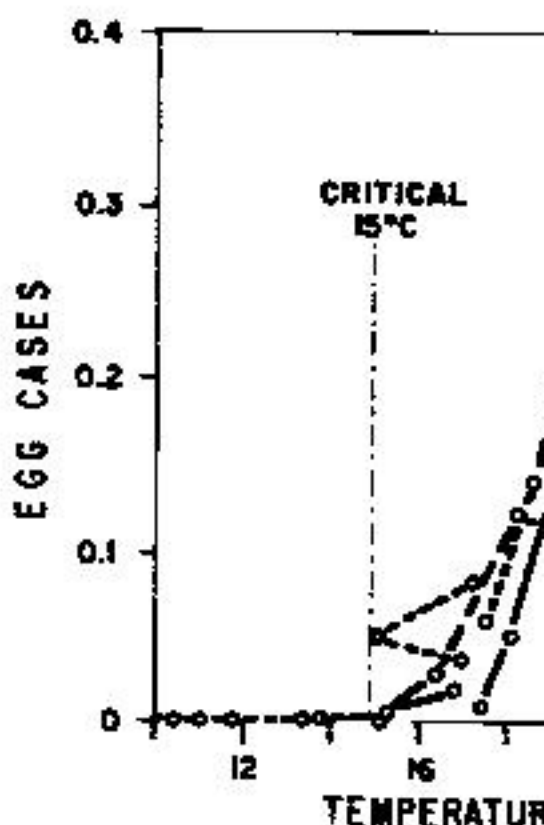
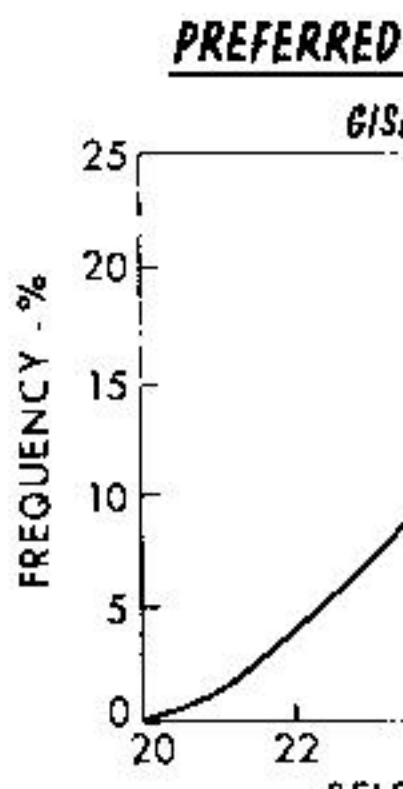


FIGURE 22. Rate of egg de-

determine all the thermal properties of biological systems. The changes in water can certainly account for many of the abrupt changes encountered. These changes may suggest reasons for temperature selections in biological systems.

Johnson, Eyring and Polissar's theory answers. One example is the observation (1954), based on an analysis by Johnson (1954) of the temperature ranges (*Crustacea, Echinodermata, Mollusca*) of them were restricted to a range between them, the range was 14°C. or less. The interval of 16° coincides very closely with kinks, optima for the activity of fish between 15 and 30°C. As an example,



Drost-Hansen: Phase T

RANGES FOR NORMAL
RANA PIPiens.

LOCALITY	LATITUDE
MEXICO	22 °N.
TEXAS	32
ENGL. FLA.	27
OCALA, FLA.	29
LOUISIANA	30
N. JERSEY	40
WISCONSIN	44
VERMONT	45
QUEBEC	46

0

FIGURE 24. Ranges of temperature for meadow frog, *Rana pipiens*.

the behavior follows closely the logistic deviations occur above 30°C. The logistic is identical in shape. This points to an obvious analogy. The properties of water are alleged to be identical with those of air. This is so. However, in studying the behavior of frogs in cold water it is important to

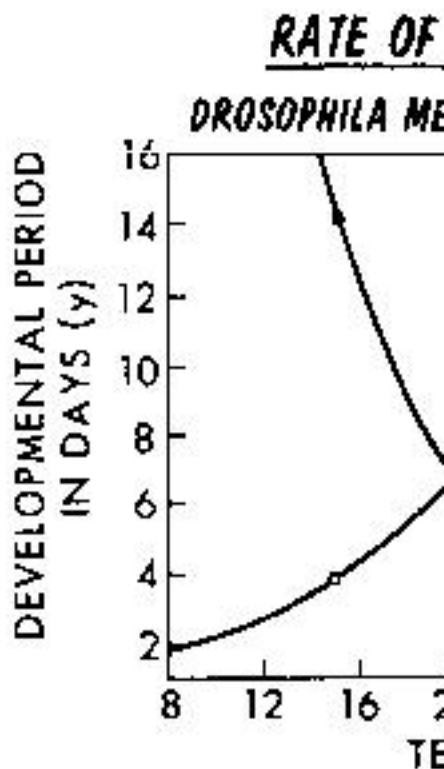


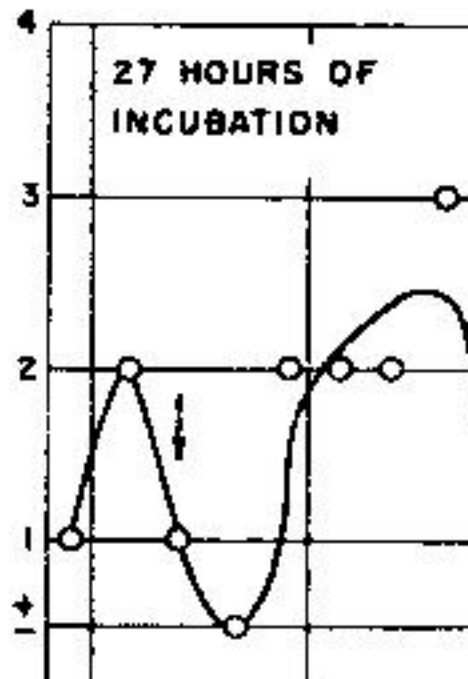
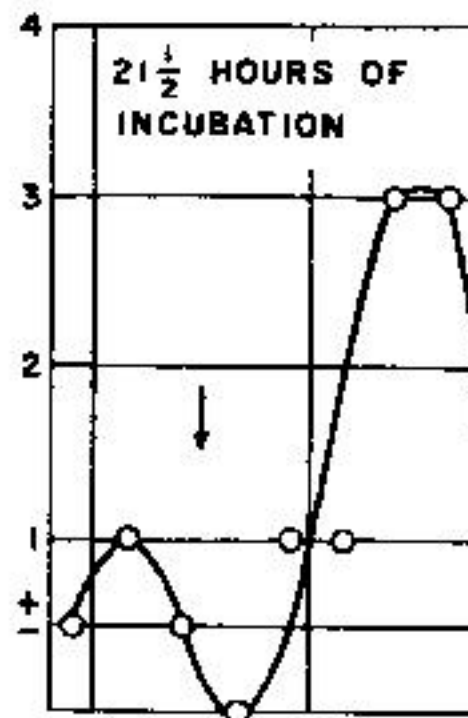
FIGURE 26. Logistics curve for development of *Drosophila melanogaster*.

be too surprised to find, as we did, that the rate of development of the insect follows very nicely a logistic curve. On the other hand, we should expect the rate to increase linearly with temperature near the kink at 30°C.

Multiple Temperature Curves

If we are correct in assessing the

Drost-Hansen: Phase T



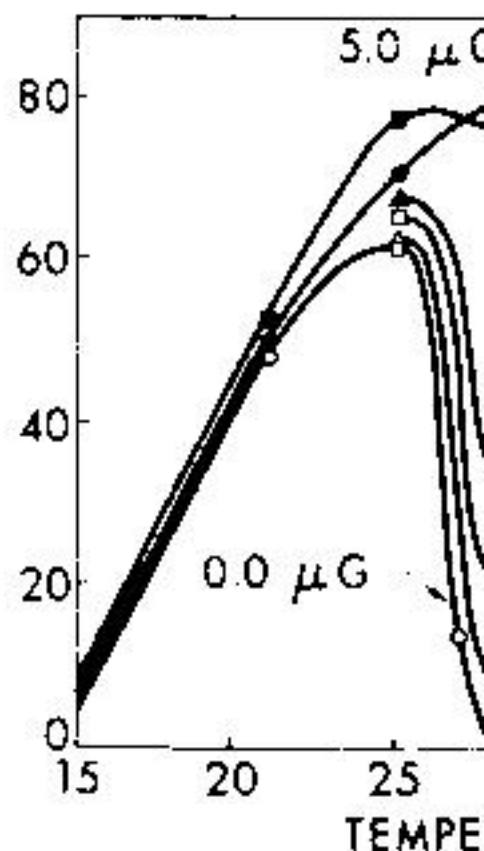
GROWTH OF NE

FIGURE 29. Growth of mold

low temperatures to determine if a minimum.

A similar type of growth curve Houlahan (1946), who studied the that was made to require lactoflavin

Drost-Hansen: Phase

would predict from our consideration the biological systems.

Further corroboration of these predictions comes from a study of the growth of *E. coli* (Schröder et al., 1962). Figure 30 shows the amount of growth, measured as optical density, at different times of growth as a function of temperature. There are again two optima for growth.

Fig. 31. pH of system shown in FIGURE 30

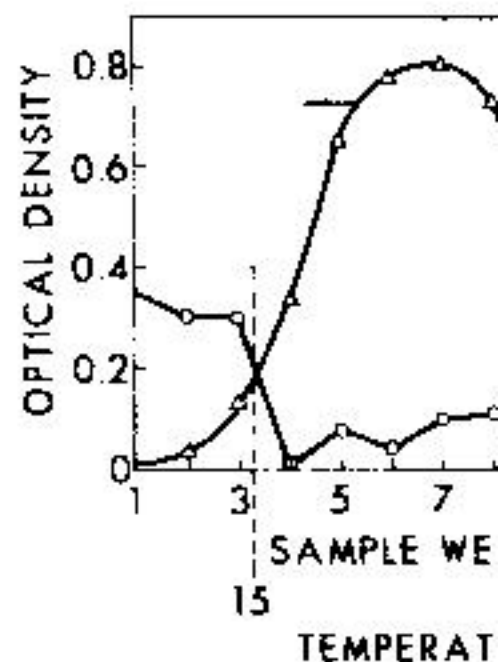


FIGURE 31. pH of system shown in FIGURE 30

suggest that the structure of water units whether they be cages or clusters operating units are between 10 to 20. Determined very roughly by the number of cooperativeness, and the upper limit of clusters much larger, they would have in optical scattering, X-ray and neutron diffraction, presumably in several other types of evidence has been reported of "clustered" water (Egelstaff, 1962). It has also been unchanged in the presence of most solutes, the persistence of structural features in the presence of solutes. Hence, it was assumed that the existence of the kinks to biologic systems with, albeit, large surface areas.

It remains to be explained how the kinks appear in biologic systems when they are present. For instance, from data on the properties of water, it may possibly be related to the fact that the kinks in water to us take place over a considerably longer time scale than over which we are able to study ordinary water with equal diligence on the part of

clusters or cages we are able to appreciate structural peculiarities of water in biologic systems without a more specific model.

In a recent paper, Davey and Miller (1965) at North Carolina State University have provided important experimental evidence for the reality of growth minima for microorganisms in the vicinities of the temperatures of the kinks in pure water. We quote their abstract: "Water in the liquid phase has been shown, by others, to undergo subtle changes in physical structure near 15, 30, 45 and 60°C. Four bacteria were used to cover the range in temperature from 5 to 70°C. in order to determine whether these temperature-dependent anomalies in the structure of water may have biological implications. In all cases growth was suppressed at the predicted temperatures. This suggests a strong interaction between the structure of water and biological activity." Davey and Miller also noted that anomalies at temperatures other than the four predicted ones were not observed (between 5 and 70°C.) and that the observed temperature-related anomalies in the growth of the four bacteria seemed to be greater in magnitude than in most, if not all, of the published physical data, indicating the highly sensitive nature of biologic systems to subtle alterations in their micro-environment.

Conclusions

There appear to exist in water and aqueous solutions thermal anomalies reflecting cooperative order-disorder phenomena in the water structure. It is suggested that these structural anomalies significantly influence the behavior of biologic systems, specifically that they may account for the existence of more or less abrupt changes with temperature in many biologic phenomena and that they delineate optimum and minimum temperatures for biologic activity.

References

- ANDREWARTHA, H. G. & L. C. BIRCH. 1954. The Distribution And Abundance Of Animals. Univ. of Chicago Press. Chicago, Ill.
- ANTONOFF, G. 1950. Colloid Chemistry. A. E. Alexander, Ed. 8: 83. Oxford Press, London, England.
- BORDI, S. & F. VANNEL. 1962. Proprietà superficiali e variazioni strutturali dell'acqua. Ann. Chim. 52: 80.
- BROWN, M. G. & C. V. TAYLOR. 1938. The kinetics of excretion in *Colpoda Duodenaria*. J. Gen. Physiol. 21: 475.
- BROWN, R. J. S. 1958. Private communication. See also Bull. Am. Phys. Soc. 2(3): 166.
- BRUNNER, C. 1847. Untersuchung über die cohäsion der flüssigkeiten. Ann. der Physik und Chemie (Poggendorff's Ann.) 70: 481.
- CAMPBELL, A. N. & M. L. BOYD. 1943. The system: Silver-nitrate-water. Can. J. Res. B21: 163.
- CHAPPUIS, M. P. 1907. Dilation de l'eau. Trav. Mem. Internat. Poids et Mesures. 13: D1-D40.
- DAVIDSON, J. 1944. On relationship between temperature and rate of development of insects at constant temperatures. J. Anim. Ecol. 13: 26-38.

- DAVEY, C. B. & RAYMOND J. MILLER. 1940. The Growth of Microorganisms; America, Proceedings.
- DECARVALHO, H. G. 1944. Contributions to the properties of water (transl). *Anais. Assoc. Brasil. Química* 16: 1-12.
- DORSEY, N. E. 1940. Properties of Ordinary Water. New York: #81 Reinhold Publishing Corp. No. 1000.
- DROST-HANSEN, W. 1956. Temperature optima in the process of evolution.
- DROST-HANSEN, W. 1963. The evidence for liquid water and some structural properties. Paper presented at the ACS Meeting (Sept.) New York, Vol. 10.
- DROST-HANSEN, W. 1964. Aqueous structures and their relation to the properties of interfaces. Indust. & Eng. Chem. Res. 3: 100-104.
- DROST-HANSEN, W. 1965. Monograph on the properties of aqueous systems. Copenhagen.
- DROST-HANSEN, W. & R. W. MYERS. 1966. The effect of temperature on the interfacial tension between water and organic solvents. Paper presented at the International ACS Meeting in Los Angeles, Calif., Sept. 1966.
- EGELSTAFF, P. A. 1962. Neutron scattering from water. *Advances in Physics* 11: 203.
- FEATES, F. S. & D. J. G. IVES. 1956. The structure of water and its properties in relation to the structure of water. *J. Chem. Soc. (London)* : 2798.
- FORSLIND, E. 1952. A Theory Of Water. Stockholm: Förlaget för Cement och Betong vid Tekniska Högskolan. Stockholm. p. 16.
- FRANKS, F. & D. J. G. IVES. 1960. The structure of water and its properties at water interfaces. *J. Chem. Soc. (London)* : 2798.

Drost-Hansen: Phase T

- MAGAT, M. 1935. Sur un changement de phase à 40°C. *J. Physique* 6: 179.
- MAGAT, MICHEL. 1937. Raman spectra and phase diagrams. *Faraday Society* 33: 114-120.
- MALMBERG, C. G. & A. A. MARYOTT. 1956. The effect of temperature on the viscosity from 0° to 100°C. *J. Res. Nat. Bur. Std.* 56: 1.
- MITCHELL, H. K. & M. B. HOULAHAN. 1957. The effect of temperature on the viscosity of a sensitive riboflavinless mutant. *Am. J. Physiol.* 193: 100.
- MOORE, H. B. 1958. *Marine Ecology*. John Wiley & Sons, New York.
- MOSER, H. 1927. Der absolutwert der osmotic pressure of dilute aqueous solutions nach der bügelmethode und seine abhängigkeit von der temperatur. *Z. Physik*, 82: 993.
- NEILL, H. W. & W. DROST-HANSEN. 1955. The effect of temperature on the viscosity of water. Unpublished.
- OPPENHEIMER, C. H. & W. DROST-HANSEN. 1956. The effect of temperature on the temperature optima for biological systems. *Bacteriol. Rev.* 30: 21.
- OTHMER, D. F. & M. S. THAKAR. 1953. Correlation of viscosity with temperature. *J. Indust. Eng. Chem.* 45: 589.
- PINKERTON, J. M. M. 1947. A pulse method for measuring absorption in liquids: results for water. *Trans. Faraday Soc.* 43: 100.
- PRECHT, H., J. CHRISTOPHERSEN & H. H. HANSEN. 1956. *Phase Transitions in Biological Systems*. Springer Verlag, Berlin, Germany.
- QURASHI, M. M. & A. K. M. AHSANULLAH. 1960. The effect of temperature on the viscosity and continuities in the mutual potential energy of polyhydric alcohols. *Brit. J. Appl. Phys.* 11: 100.
- SCHMIDT, M. G. & W. DROST-HANSEN. 1960. The effect of temperature on the viscosity and the temperature optima for the growth of *E. coli*. *Abstracts of the 11th International Congress of Pure and Applied Chemistry*, p. 100.
- SCHMIDT, M. G. & W. DROST-HANSEN. 1961. The effect of temperature on the viscosity and the temperature optima for the growth of *E. coli*. *Abstracts of the 11th International Congress of Pure and Applied Chemistry*, p. 100.

PHASE TRANSITIONS RAPID FREEZING OF

B.

American Foundation for Bas

The findings of the last few years on the problem of the phase transitions which occur during the rapid freezing and the rewarming of aqueous solutions. In this problem, I shall, after a short history of the development of our knowledge, present some newly established facts and some conclusions.

HISTORICAL

Early Developments: The Vitrification of Water

The German physicist Tammann,¹ in 1903, found that when water is cooled very rapidly, the transition to the solid state is suppressed, and the liquid may solidify without crystallization. He reported experiments in which "vitrification," was verified in some cases, and he also described how his vitrified material would remain in the glassy state during being rewarmed. The answer to one

Luyet: Phase Transitions

vitrification and devitrification by combining high solute concentration and high cooling rates. Luyet (1937) found that rapidly cooled aqueous solutions of dilute gelatin at rates of several hundred degrees per second.

Barnes (1939), studying by x-ray diffraction patterns of rapidly cooled aqueous solutions of Luyet's method, found them to be amorphous.

Thus, according to the findings reported by Barnes, even pure water, like the organic liquids, can vitrify upon being rapidly frozen and devitrify upon rewarming. From the point of view of the phase transitions, this would seem to be as outlined above: no transition upon cooling, but one upon rewarming.

Later Developments: of Rapidly Cooled Amorphous Substances

Zachariasen (1932), Randall (1934) and others, by x-ray analysis, came to the conclusion that substances which appear to be vitreous contain crystallites and consist of both ordered and partly disordered, materials. They suggested that the substances in question had undergone partial crystallization. (For more detailed information see the references.)

Then Luyet and Rapatz (1957 & 1958) studied the properties of aqueous solutions thought to be amorphous after rapid cooling.

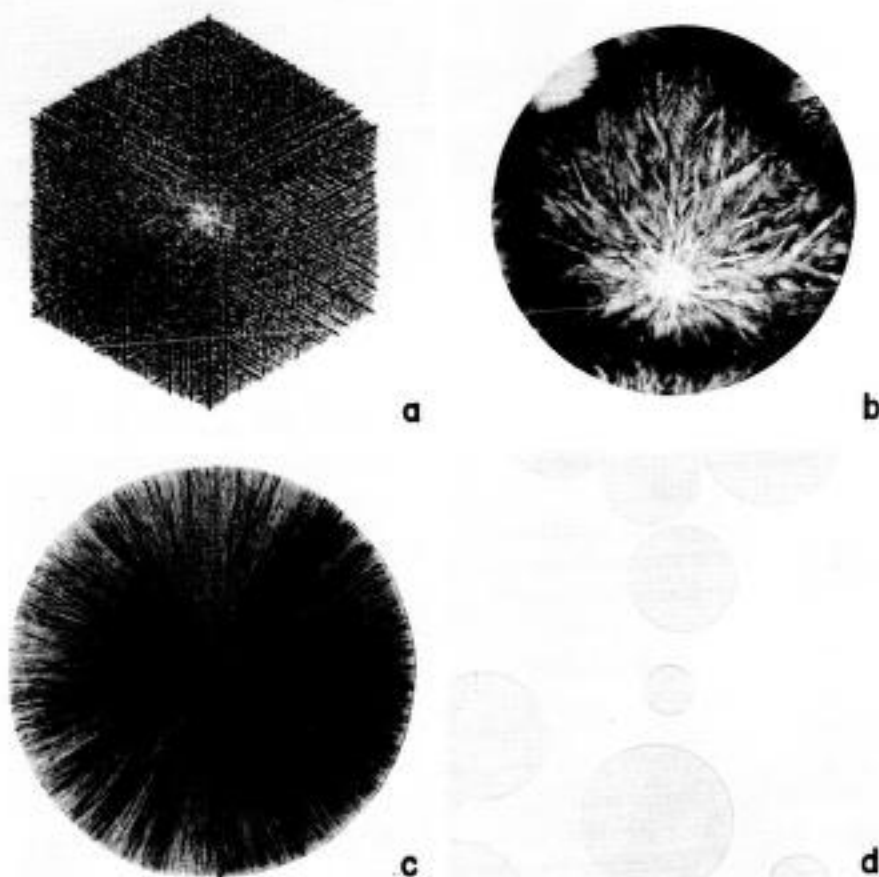


FIGURE 1. The three principal types of ice formations encountered in aqueous solutions. (a) Regular dendrite (hexagonal crystal); (b) irregular dendrite; (c and d) spherulites; (c) coarse spherulite; (d) "evanescent" spherulite. $\times 86$. (Reproduced from Luyet & Rapatz, 1958, by permission of *Biodynamica*.)

which indicated a gradual hindrance to crystallization at increasing rates, but which did not furnish evidence of complete inhibition.

According to the latter authors, the situation, in regard to the phase transitions encountered in the rapid freezing of aqueous solutions, would then be that the highest cooling rates obtainable with the method of immersion of specimens in liquid baths are still insufficient to prevent the transition of water into the crystalline state; rapid cooling would only *hinder* and *limit* that transition. Rewarming would merely permit a *resumption* and *completion* of the hindered, interrupted crystallization.

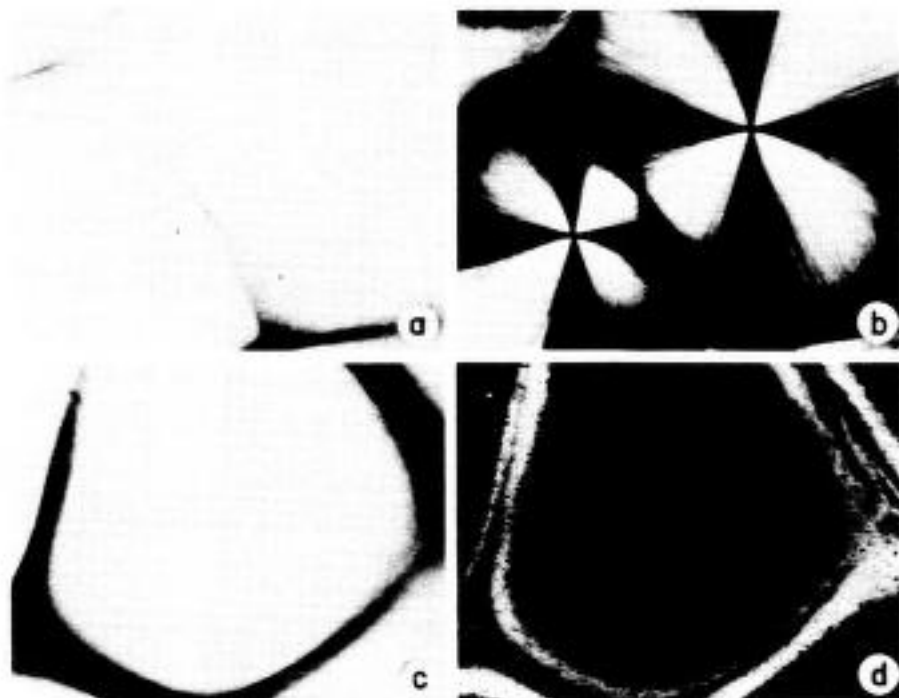


FIGURE 2. "Evanescing spherulites" formed in thin layers of 30% gelatin solutions rapidly frozen. (a and c) Spherulites seen in ordinary light; they are optically empty, except for their borderlines. (b) Same field as in a, in polarized light; the spherulitic structure is evidenced by the Maltese crosses. (d) Same field as in c, after the temperature had been raised to -10° ; the spherulite has become opaque, as a result of recrystallization. $\times 62$. (Reproduced from Luyet & Rapatz, 1958; Rapatz & Luyet, 1959, by permission of *Biodynamica*.)

The second part of this paper will consist in a presentation and a discussion of the factual evidence about this situation.

THE PRESENT STATUS OF OUR KNOWLEDGE FACTUAL DATA AND PROPOSED INTERPRETATIONS

The material to be discussed will be presented under three headings: Crystallization, Recrystallization, Overall Picture of the Phase-Transitions Complex.

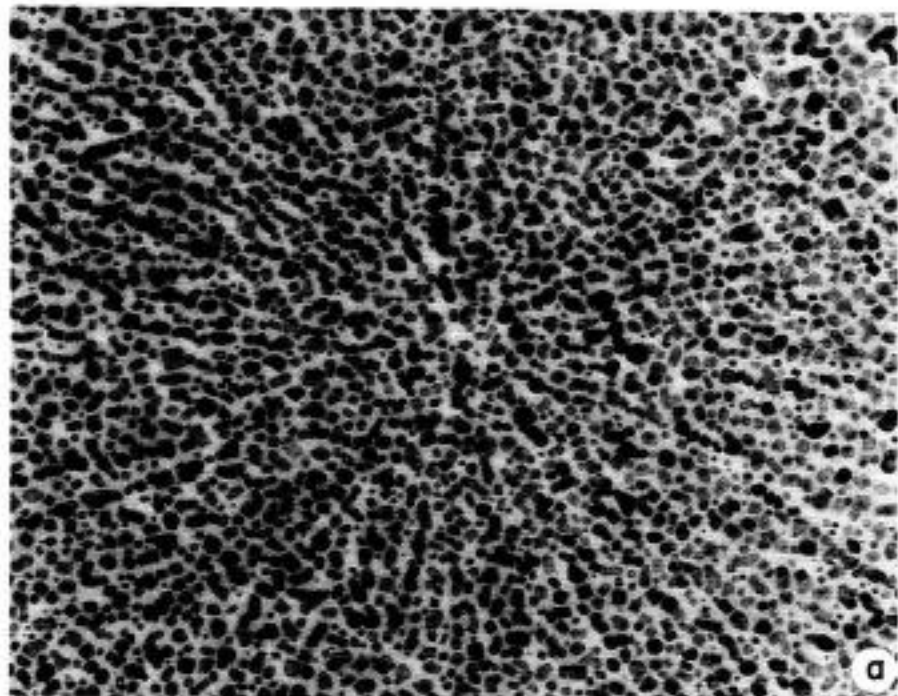
(A) *Crystallization*

Effect of rapid cooling on the pattern of ice formation. (a) Types of crystalline structures encountered. In a systematic study of the patterns of ice formation obtained with solutions of some 15 solutes, crystalloids and colloids, of various concentrations, frozen at various cooling velocities, Luyet and Rapatz (1958) described three basic types: (1) regular den-

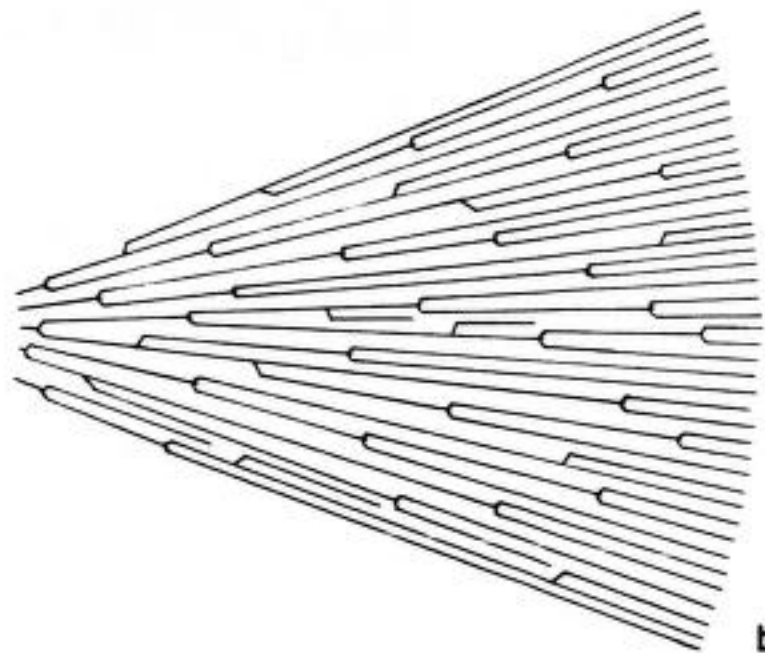
drites, which are well formed structures (Photo. 1), (2) irregular dendrites and arrangement of branches is spherulites, which appear to consist around the center of crystallization can conveniently be divided into dimensions of the radial fibers (Photos. 3 and 4, respectively). The those units of which the radial fibers in ordinary light; polarized light of the two types, the radii become increasing rates.

The evanescent spherulites are effects of rapid freezing that they

(b) The type "evanescent spherulites" under the electron microscope reveal fibers growing radially around crystalline structures, the branches of which increase in size with increasing cooling rates. In electroprecipitation of proteins from blood plasma, MacKenzie and Luyt have observed spherulitic formations of solid material (left after centrifugation) which consist of radial branches of diameters of the order of 10 microns and larger, and which



a



b

angles to the parent branch, but has direction, for the simple reason that, due to the crowded condition is, of course, an idealized representation of the spherulitic structures, as spherulites, have nothing of the reg

These observations and consider the three forms of crystalline structures, regular dendrites and spherulites, dendrites. The main distinctive characteristics of the branches and the frequent differences in cooling rates.

Effect of rapid cooling on nucleation. It is an established fact that, when a prepared solution, is immersed abruptly into a liquid of lower temperature, nucleation units that reach observable size decrease rapidly, reaching observable size decrease rapidly. Curves representing the number of nuclei in terms of decreasing temperature show such a drop. But such a drop is apparently due, to the presence of nuclei at lower temperatures.